

Insights into Nitrogen and Particle Cycling in Marine

Oxygen Minimum Zones

Dissertation

zur Erlangung des Doktorgrades der Naturwissenschaften im Fachbereich
Geowissenschaften der Universität Hamburg

Vorgelegt von

Birgit Nagel

aus Esslingen am Neckar

Hamburg 2014

Als Dissertation angenommen

vom Fachbereich Geowissenschaften der Universität Hamburg
auf Grund der Gutachten von

Prof. Dr. Kay-Christian Emeis

und

Dr. Birgit Gaye

Hamburg, den 11. April 2014

Prof. Dr. Christian Betzler

(Leiter des Fachbereichs Geowissenschaften)

Zusammenfassung

Aufgrund seines limitierenden Einflusses als Nährstoff ist reaktiver Stickstoff von großer Bedeutung für die biologische Produktivität. Reaktiver Stickstoff kommt hauptsächlich in oxidierte Form (Nitrat und Nitrit) oder reduzierter Form (Ammonium) vor. Die Oxidationsstufen des Stickstoffs und die Umsatzprozesse hängen stark vom Redoxzustand des aquatischen Milieus und damit vom Sauerstoffgehalt ab. 30 bis 50% des Verlusts an reaktivem Stickstoff erfolgen in den Sauerstoffminimumzonen der Ozeane. Alle biotischen Stickstoffumsätze, die nicht vollständig ablaufen, sind mit einer Isotopenfraktionierung verbunden und die $^{15}\text{N}/^{14}\text{N}$ -Isotopenverhältnisse der gelösten anorganischen Stickstoffverbindungen oder des partikulären Materials tragen wichtige Informationen über die Stickstoffquellen und -senken sowie über die Umsatzprozesse selbst.

Diese Dissertation befasst sich hauptsächlich mit dem Stickstoffkreislauf in den Sauerstoffminimumzonen des Arabischen Meeres und des Benguela-Auftriebsgebiets vor der Küste Namibias. Die große Sauerstoffminimumzone des offenen Arabischen Meers ist räumlich getrennt von der hochproduktiven Auftriebszone vor Oman. Die Sauerstoffminimumzone des Benguela Auftriebsgebiets ist dagegen um einiges kleiner und auf dem ebenfalls hochproduktiven Schelf gelegen. Gemeinsam haben beide, dass alle Stickstoff-Umsatzprozesse, die mit sauerstoffarmen Bedingungen einhergehen, auftreten – wenngleich in unterschiedlicher Gewichtung. Das Hauptaugenmerk dieser Dissertation liegt auf der Identifikation der innerhalb des Stickstoffkreislaufs stattfindenden Prozesse in beiden Arbeitsgebieten. Dazu nutze ich Daten zu den Verhältnissen der stabilen Stickstoffisotopen in gelöstem und partikulärem Stickstoff sowie Nährstoffdaten. Im Arabischen Meer liegt der Fokus auf der räumlichen Verteilung des Stickstoffdefizits und der Quantifizierung der Nitratreduktion und Nitritoxidation. Im Benguela-Auftriebsgebiet liegt das Augenmerk auf der Generierung und dem Ausgleich des Stickstoffdefizits. Ein weiterer Aspekt meiner Dissertation befasst sich mit der Frage, ob sich die in der Wassersäule identifizierten Prozesse und Mechanismen in den stabilen Stickstoffisotopenverhältnissen der Sedimente des Benguela-Auftriebsgebiets widerspiegeln. Deshalb wurden Aminosäurezusammensetzungen der Suspensionsfracht und der Oberflächensedimente analysiert, um die Herkunft sowie die Auswirkungen des Abbaus von organischem Material auf die stabilen Stickstoffisotopenverhältnisse zu untersuchen.

Im Arabischen Meer werden ungewöhnlich hohe N-Isotopenverhältnisse in partikulärem Stickstoff und im Nitrat der Nitratreduktion und Denitrifikation zugeschrieben, die in einer

ausgedehnten Sauerstoffminimumzone (200-1500 m Wassertiefe) stattfinden. Dabei wird frisches absinkendes organisches Material durch heterotrophe denitrifizierende Bakterien besiedelt, die aus Mangel an gelöstem Sauerstoff Nitrat verwenden, um das organische Material zu oxidieren. Wie unsere Untersuchungen an stabilen Nitrat- und Nitritisotopen zeigen, finden Denitrifikation und Nitritoxidation ($\text{NO}_2^- \rightarrow \text{NO}_3^-$) hauptsächlich zwischen 100 und 400 m Wassertiefe statt, wo sich das Nitrit bis zu einer Konzentration von 6 $\mu\text{M/l}$ als Zwischenprodukt der Denitrifizierung anreichert. Etwa 50% der Ausgangsmenge des Nitrats wird in der Denitrifikationszone bis 400 m Wassertiefe reduziert. Nitritoxidation findet am oberen und unteren Rand der Denitrifikationszone statt, da sich dort die Stickstoff- und Sauerstoffisotopenverhältnisse des Nitrats und Nitrits nicht parallel verändern. Basierend auf Isotopen- und Stoffbilanzrechnungen schätzen wir, dass 25% des als Zwischenprodukt der Denitrifikation akkumulierten Nitrits zu Nitrat rückoxidiert werden, während etwa 40% des akkumulierten Nitrits weiter zu N_2 denitrifiziert werden. Obwohl anoxische Bedingungen auch unterhalb von 400 m Wassertiefe vorherrschen, finden wir dort nur räumlich sehr begrenzte Anzeichen für Denitrifikation – möglicherweise aufgrund von mangelnder Verfügbarkeit von geeignetem organischem Material.

Die stabilen Stickstoffisotopenverhältnisse des Nitrats aus dem Benguela-Auftriebssystem zeigen, dass der jährliche Stickstoffverlust aufgrund der Denitrifikation etwa 150 Mal niedriger ist als im Arabischen Meer. Denitrifikation, anaerobe Ammoniumoxidation und Phosphatfreisetzung aus den Sedimenten in der Sauerstoffminimumzone erzeugen jedoch ein erhebliches Stickstoffdefizit relativ zu Phosphat in der Küstenauftriebszone. Sowie das Oberflächenwasser mit dem windinduzierten Ekman-Transport von der Küste wegtreibt, verringert sich das Stickstoffdefizit, obwohl wir nur ambivalente Anzeichen für N_2 -Fixierung aus der Atmosphäre finden und die entsprechende Stickstoffzufuhr durch N_2 -Fixierung sechs Mal niedriger ist als der Stickstoffverlust durch Denitrifikation. Schelfkantenauftrieb und turbulente Mischung über die Thermokline hinweg gleichen das Stickstoffdefizit hauptsächlich aus. Das Brechen interner Wellen und Tiden an den Schelfkanten mischt Wasser mit Stickstoffüberschuss ein, das bis hinauf an die Basis des durchmischten Oberflächenwassers gelangt und somit als Stickstoffquelle fungiert.

Ein weiteres Kapitel meiner Dissertation befasst sich mit den Wechselwirkungen zwischen Suspensionsfracht und Sedimenten sowie dem Abbau von organischem Material und dessen Auswirkungen auf die stabilen Stickstoffisotopenverhältnisse im Sediment. Im

Benguela-Auftriebsgebiet werden hohe Stickstoffisotopenverhältnisse in den küstennahen Sedimenten der Nitratreduktion und der Anammox-Reaktion innerhalb der Sauerstoffminimumzone zugeschrieben. Durch den Einfluss interner Wellen und Tiden werden Sedimentpartikel stellenweise umgelagert und dabei diagenetisch umgewandelt. Die Aminosäurezusammensetzungen der Sedimente zeigen, dass das organische Material innerhalb der Sauerstoffminimumzone besser erhalten ist als außerhalb. Entsprechend werden die hohen Stickstoffisotopenverhältnisse entlang der Küste nicht durch verstärkten Abbau organischen Material verursacht, sondern sind Ausdruck der in der Sauerstoffminimumzone stattfindenden Prozesse im Stickstoffkreislauf. Eine Hauptkomponentenanalyse mit den Aminosäuredaten zielte darauf ab, die Herkunft und Wechselwirkungen von Suspensionsfracht und Sedimenten zu erfassen. Dabei stellte sich heraus, dass die Suspensionsfracht nicht wie erwartet aus einer Mischung von frischen planktonischen Partikel und resuspendierten Sedimenten besteht, sondern einen eigenständigen Partikeltyp darstellt, der nur untergeordnet im Austausch mit den Sedimenten steht.

Summary

Reactive nitrogen plays a key role in biogeochemical cycling, because it is a limiting nutrient for biological productivity. Reactive nitrogen mainly occurs in forms of oxidized N (nitrate and nitrite) or reduced form (ammonium). The redox state and oxygen level of the aquatic environment are crucial for the oxidation state of nitrogen and thus for nitrogen cycling processes. 30 to 50% of the oceanic reactive nitrogen loss is estimated to occur within oxygen minimum zones. All incomplete biotic nitrogen turnover processes are associated with an isotope fractionation and the $^{15}\text{N}/^{14}\text{N}$ isotope ratios of the dissolved inorganic nitrogen forms or the particulate matter carry important information about nitrogen sinks and sources.

The dissertation mainly focusses on nitrogen cycling in the oxygen minimum zones of the Arabian Sea and the Benguela upwelling system off Namibia. The Arabian Sea hosts a large-volume oxygen minimum zone that is spatially decoupled from the highly productive upwelling zone off Oman. The oxygen minimum zone in the Benguela upwelling system is much smaller and situated on the shelf. Both have in common that all N turnover processes that are associated with oxygen depleted conditions occur – albeit in different proportions. Here, I use nutrient data and data sets of dissolved and particulate stable N isotopes to elucidate nitrogen turnover processes in both study areas. In the Arabian Sea, I focus on the spatial distribution of the N-deficit as well as on the quantification of nitrate reduction and nitrite oxidation. One main focus of my work in the Benguela upwelling system lies on the formation and balancing of the generated N-deficit. Another key aspect of the thesis deals with the question whether the N-cycling processes identified in the water column are reflected in the stable N isotope ratios of surface sediments. Thus, amino acid compositions of suspended matter and surface sediments were analysed to investigate the origin and cycling of particles and the effects of organic matter degradation on stable N isotope ratios.

In the Arabian Sea, unusually high particulate N and nitrate isotope ratios were attributed to nitrate reduction and denitrification that occur in the comprehensive oxygen minimum zone (200 to 1500 m water depth). Sinking organic matter is populated by heterotrophic denitrifying bacteria that use nitrate to oxidize organic matter due to the lack of molecular O_2 . As our investigations on stable nitrate and nitrite isotopes show, denitrification and nitrite oxidation ($\text{NO}_2^- \rightarrow \text{NO}_3^-$) mainly occur between 100 and 400 m water depth, where nitrite accumulates up to $<6 \mu\text{M}$ as an intermediate product of denitrification. About 50% of the initial nitrate is being reduced in the denitrification zone down to 400 m water depth. We identify nitrite oxidation at the upper and lower margin of the denitrification zone by a

decoupling of nitrogen and oxygen isotopes in nitrate and nitrite. Based on mass balance calculations, we estimate that 25% of the nitrite accumulated as an intermediate of denitrification is reoxidized to nitrate while about 40% of the accumulated nitrite is denitrified to N_2 . Although anoxic conditions prevail below 400 m water depth, we find only spatial indications for denitrification there - probably due to the paucity of suitable organic matter availability.

Stable N isotope ratios of nitrate from the Benguela upwelling system reveal that the annual N-loss due to denitrification is about 150 times less than in the Arabian Sea. Denitrification and phosphate release from sediments in the oxygen minimum zone create a significant N-deficit over phosphate in the coastal upwelling zone. The N-deficit diminishes as surface water moves offshore with the Ekman transport although indications for N_2 -fixation are ambiguous and the corresponding N supply by fixation is six times less than the estimated N-loss due to denitrification. Shelf break upwelling and turbulent mixing across the thermocline mainly balance the N-deficit offshore the inner shelf break. The breaking of internal waves and tides at the shelf breaks entrains water with N-excess to the base of the mixed layer and thus acts as an N-source.

Another chapter of this thesis deals with the interaction between suspended matter and surface sediments and with the degradation of organic matter and its impact on sedimentary stable N isotope ratios. High sedimentary N isotope ratios near the coast off Namibia are commonly attributed to nitrate reduction and anammox within the oxygen minimum zone. Organic matter is degraded during the resuspension of sediments which is caused by the effects of internal waves and tides. The amino acid compositions of surface sediments shows that organic matter is better preserved within the oxygen minimum zone than outside. Thus, high stable N isotope ratios in surface sediments along the coast are not caused by enhanced degradation. In fact, they are induced by N turnover processes within the oxygen minimum zone. A principal component analysis carried out with the amino acid data aimed to identify the origin and cycling of suspended matter and surface sediments. Contrary to my expectations, suspended matter was not a mixture of fresh phytoplankton and resuspended surface sediments. The results reveal that suspended matter is a discrete type of particulate matter which is hardly in exchange with surface sediments.

Table of Contents

1	Introduction.....	1
2	Evidence of parallel denitrification and nitrite oxidation in the ODZ of the Arabian Sea from paired stable isotopes of nitrate and nitrite.....	19
3	N-cycling and balancing of the N-deficit generated in the oxygen-minimum zone over the Namibian shelf – an isotope based approach.....	55
4	Effects of current regimes and oxygen deficiency on particulate organic matter preservation on the Namibian shelf.....	81
5	Conclusion and Outlook.....	97
	Figure captions.....	103
	Table captions.....	108
	List of abbreviations.....	109
	References.....	111
	Author contributions.....	126
	Curriculum vitae	127
	List of publications.....	128
	Acknowledgements/Danksagung.....	129
	Eidesstattliche Erklärung.....	131

1. Introduction

1.1. Oxygen minimum zones

Oxygen minimum zones (OMZs) or oxygen depleted zones (ODZs) are often found in wind-driven upwelling systems where aged oxygen-deficient and nutrient-rich water masses fuel primary production in the euphotic zone. The combination of high organic matter export and subsequent oxic decomposition together with poor ventilated mid-depth water masses leads to permanently oxygen-depleted or anoxic conditions in subsurface waters (Wyrki, 1962).

Oxygen depleted conditions in the water column are frequently caused by a combination of low O₂ supply from oxygen-deficient deep- or intermediate water masses, and high productivity in surface water in combination with oxygen-requiring respiration processes (Deutsch *et al.*, 2001). Upper oxygen thresholds to define OMZs depend on the context of the study and range from <2 μM to ~90 μM (Karstensen *et al.*, 2008; Lam and Kuypers, 2011; Paulmier and Ruiz-Pino, 2009). In ~1% of the global ocean volume, oxygen concentrations drop below 20 μM (Fig. 1.1.) and microorganisms exploit alternative electron acceptors than oxygen for the respiration of organic matter and carbon fixation (Lam and Kuypers, 2011; Smethie, 1987). Oxygen concentrations in the oceans have varied widely in the geological past and oceanic anoxic events caused ocean-wide black shale deposition and extinction events for instance in the Jurassic and Cretaceous (Jones and Jenkyns, 2001) and at the end of the Permian (Benton and Twitchett, 2003). Models and observations indicate recently decreasing O₂ concentrations in subsurface waters including an expansion of the major oceanic OMZs (Oschlies *et al.*, 2008; Shaffer *et al.*, 2009; Stramma *et al.*, 2008).

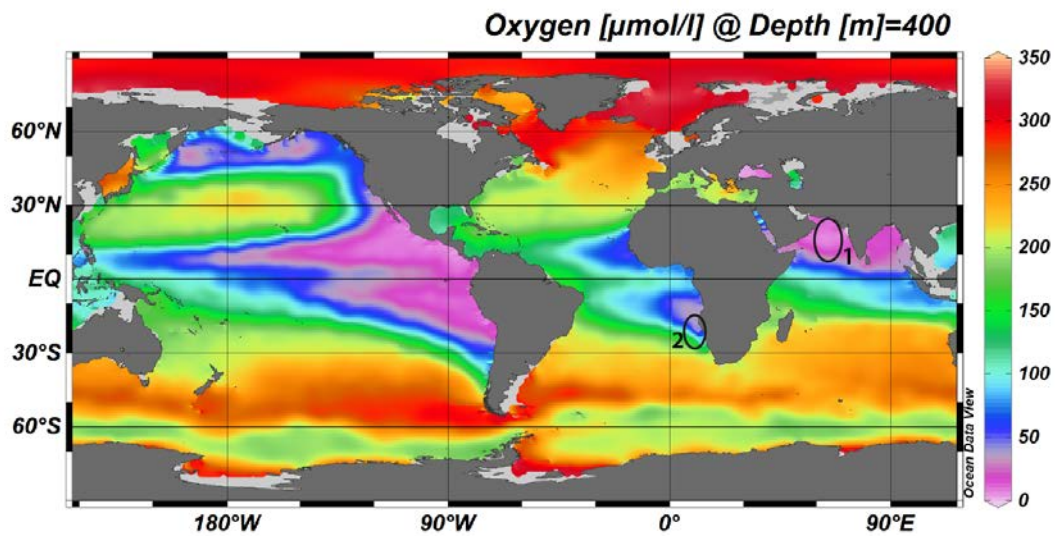


Fig. 1.1: Mean annual dissolved O_2 concentrations at 400 m water depth (World Ocean Atlas, 2009). Oxygen minimum zones that are discussed in this thesis are marked on the map (1, Arabian Sea oxygen minimum zone; 2, Benguela Upwelling System off SW-Africa). Note that the cores of different OMZs are located in different water depths and that the core of the Namibian OMZ is situated on the shelf (<300 m).

1.2. Nitrogen deficits in oxygen minimum zones

Nitrogen is a key nutrient of life on Earth and is thought to limit primary production in much of the world's oceans (McCarthy and Carpenter, 1983). Nitrogen has a direct influence on the radiative properties of the atmosphere, because nitrous oxide (N_2O), an intermediate gaseous component of nitrogen cycling, is a greenhouse gas and increases in the atmosphere (Kahlil and Rasmussen, 1992). However, more important with respect to climate change is the impact of nitrogen as a nutrient to fix carbon and sequester atmospheric CO_2 due to the tight coupling between the oceanic N and C cycles (Gruber and Galloway, 2008).

Primary producers require reactive nitrogen (reduced and oxidized forms of nitrogen) in stoichiometric proportions to carbon and phosphorus for growth. The so-called Redfield Ratio of 106C:16N:1P on a mol:mol basis characterizes marine phytoplankton grown under optimal nutrient conditions as well as dissolved nutrients in seawater, and the expression of long-term regulation by assimilation and remineralisation. Removal of reactive nitrogen from the oceanic pool mainly occurs in OMZs due to heterotrophic denitrification and anammox. Both reactions convert reactive nitrogen into N_2 that escapes to the atmosphere, and thus produce an N-deficit over phosphorus. Redfield ratios decrease to below 16 and reactive nitrogen

becomes a limiting nutrient in the OMZ, and in upwelling systems, where these waters reach the euphotic zone.

The nutrient-derived tracer N^* (Fig. 1.2; Gruber and Sarmiento, 1997) represents a method to analyze the impact of N-loss (denitrification and anammox) and N-excess (N_2 fixation; Fig 1.3) on the oceanic NO_3^- distribution by focussing on deviations from the overall Redfield stoichiometry. N^* is defined by the linear relation of nitrate and phosphate, where $2.9 \mu\text{mol/kg}$ were added to obtain a global mean of zero (Gruber, 2008; Gruber and Sarmiento, 1997).

$$N^* = NO_3^- - 16PO_4^{3-} + 2.9\mu\text{mol/kg} \quad (1)$$

Negative values indicate an N-deficit over phosphate and are caused by either N-loss processes like heterotrophic denitrification and anammox in the OMZs or in sediments, or by efflux of phosphate from sediments. The N-deficit is more pronounced in the Arabian Sea than in the Benguela Upwelling System (Fig. 1.2). Positive N^* values are caused by diazotrophic N_2 fixation in surface waters from atmospheric dinitrogen and mostly occur in the subtropical gyres.

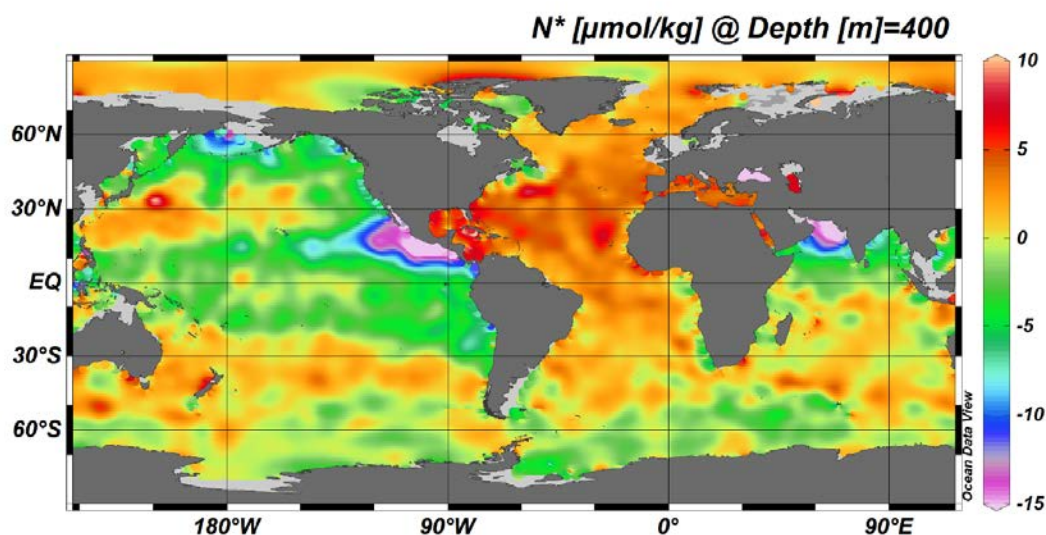


Fig. 1.2: N^* in 400 m water depth (World Ocean Atlas, 2009). Major oceanic OMZs can be identified by N-deficits (negative N^* values) that are again situated in different water depths. Excess N relative to phosphate (positive values of N^*) is found in areas where particulate N from diazotrophic N_2 -fixation is remineralised and adds to the dissolved nitrate pools.

1.3. Nitrogen cycling in oxygen minimum zones and adjacent ocean regions

The oceanic N-cycle (Fig. 1.3) is highly dependent on redox conditions since nitrogen can be easily oxidized and reduced by marine organisms, and the prevailing form of nitrogen is mainly controlled by oxygen concentrations. Nitrate (NO_3^-) is the most oxidized form of nitrogen and the first preferred alternative electron acceptor for respiration of organic matter within the electrochemical series. It yields almost as much energy as oxic respiration of organic matter (Froelich *et al.*, 1979) and thus occurs in sediments and water column OMZs.

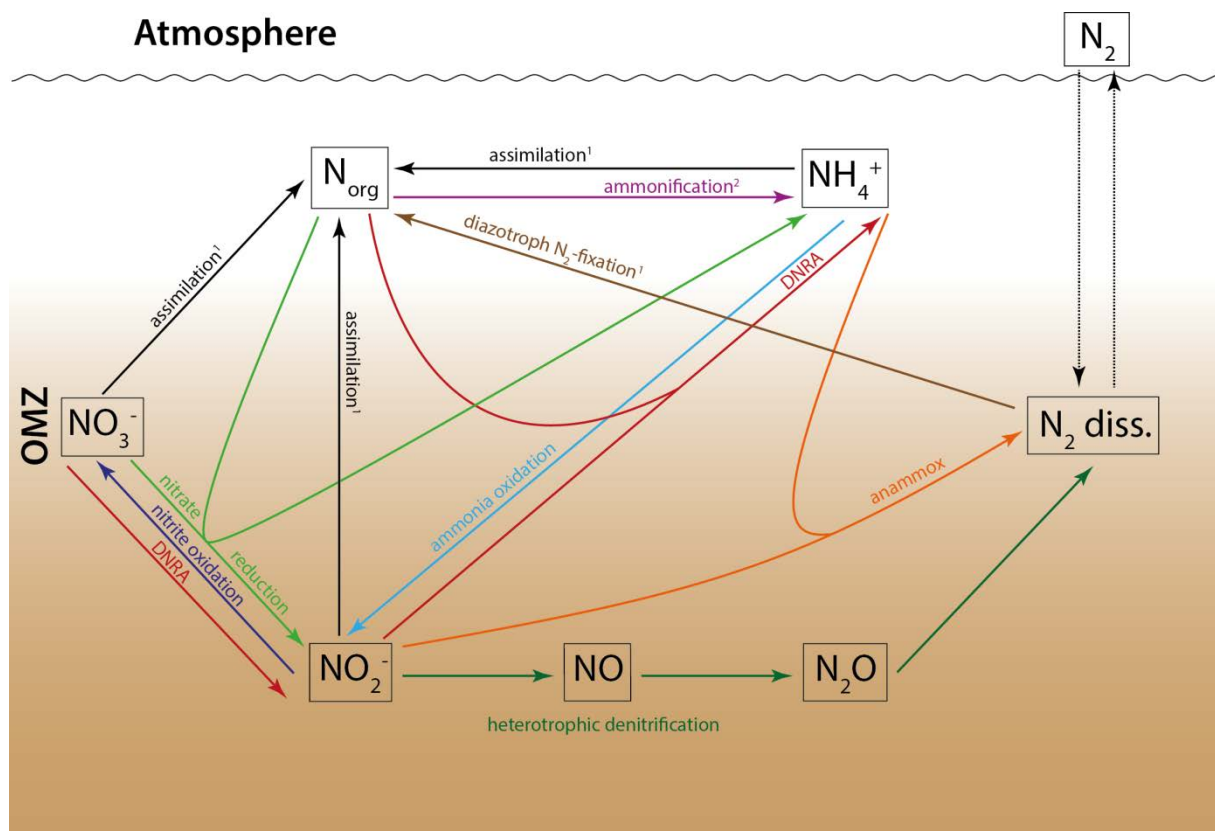


Fig. 1.3: The oceanic N-cycle in OMZs and the adjacent ocean. Decreasing O_2 concentrations are indicated by intensifying colour shading. Anammox and heterotrophic denitrification produce N_2 and cause an N-deficit over phosphorus. Nitrate reduction and DNRA are remineralisation processes that produce NO_2^- and NH_4^+ . Nitrification consists of two individual steps: ammonia oxidation seems less tolerant towards low O_2 concentrations than nitrite oxidation.

¹ these assimilatory processes as well as diazotrophic N_2 fixation are mostly carried out by photoautotrophs that are restricted to the euphotic zone.

² Ammonification is not restricted to certain O_2 concentrations. Adapted from Lam and Kuypers (2011).

1.3.1 Heterotrophic denitrification

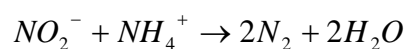
During heterotrophic denitrification (Fig. 1.3) organic matter is respired with NO_3^- that is reduced to N_2 via several intermediate products (NO_2^- , NO and N_2O). The complete reaction is considered as (Richards, 1965):



where $(\text{CH}_2\text{O})_{106}(\text{NH}_3)_{16}\text{H}_3\text{PO}_4$ represents the average composition of organic matter. Nitrate reduction (Fig. 1.3) – the first step of heterotrophic denitrification – releases nitrite (NO_2^-) and ammonium (NH_4^+), which accounts for roughly 10% of the produced nitrite (Lam *et al.*, 2009). Nitrite often accumulates in oceanic OMZs within the secondary nitrite maximum (Fiadeiro and Strickland, 1968; Naqvi, 1991) because nitrate reduction is carried out more commonly and by more bacterial species than the reduction of nitrite to N_2 (Zumft, 1997). Heterotrophic denitrification is reported to occur between O_2 concentrations of $<2 \mu\text{M}$ and $25 \mu\text{M}$ (Devol, 1978; Kalvelage *et al.*, 2011; Smethie, 1987). But as being facultative anaerobes, denitrifying bacteria are able to survive higher oxygen concentrations in dormant stages and thus play an important role in structuring the microbial diversity in the OMZs (Jones and Lennon, 2010; Lam and Kuypers, 2011).

1.3.2 Anammox

During the chemoautotrophic anammox reaction, ammonium is oxidized with nitrite to N_2 (Fig. 1.3):



Anammox is more oxygen-tolerant than denitrification and is not fully inhibited in seawater up to oxygen concentrations of $\sim 20 \mu\text{M}$ (Jensen *et al.*, 2008; Kalvelage *et al.*, 2011). Anammox occurs in OMZs at zones where NO_3^- concentrations decrease and NO_2^- accumulates. Interestingly, anammox is found over a wide range of NH_4^+ concentrations from micromolar levels to below the detection limit (Kuypers *et al.*, 2005; Lam and Kuypers, 2011; Thamdrup *et al.*, 2006). Ammonium availability is the major limiting factor for anammox since low ammonium concentrations induce low anammox rates. Thus, anammox often is associated with ammonium producing processes, such as dissimilatory nitrate reduction to ammonium (DNRA), or nitrate reduction (Lam *et al.*, 2009).

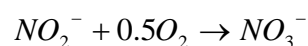
1.3.3 Dissimilative nitrate reduction to ammonium (DNRA)

DNRA is also known as nitrate/nitrite ammonification and occurs in the water column and sediments. As during nitrate reduction, organic matter is respired in the absence of oxygen for carbon fixation (Fig. 1.3). The DNRA electron potential is slightly below that of denitrification, but nitrate/nitrite ammonifiers have competitive advantages under NO_3^- -limited conditions, since denitrifying bacteria consume more NO_3^- per mole of organic substrate (Strohm *et al.*, 2007). DNRA often is linked to other nitrogen cycling processes and elemental cycles since nitrate ammonifiers are able to use alternative respiratory pathways, such as sulphate reduction.

1.3.4 Nitrification

During nitrification, nitrate is produced by the oxidation of ammonium via two independent steps: oxidation of ammonium to nitrite and nitrite oxidation to nitrate (Fig. 1.3). During the first step of nitrification, NH_4^+ has to be converted into NH_3 for further enzyme-catalyzed reactions in order to form NO_2^- . Therefore, this step is called ammonia oxidation. Most ammonia-oxidizing bacteria (AOB) are lithoautotrophs that require molecular oxygen, ammonia as an electron acceptor, and CO_2 as a carbon source (Ward, 2008). But AOB have developed several pathways to grow under oxygen-deficient conditions, for instance by using the nitrifier denitrification reaction, where organic compounds are used to reduce NO_2^- to N_2 or N_2O under anoxic conditions to oxidize ammonia (Bock *et al.*, 1995). Apparently, ammonia oxidizers are well-adapted to oxygen-deficient conditions, probably because of higher ammonium availability in suboxic environments (Lam and Kuypers, 2011). ^{15}N tracer studies carried out in the eastern tropical south and north Pacific OMZs observed significant ammonia oxidation rates (Lam *et al.*, 2009; Lipschultz *et al.*, 1990; Ward *et al.*, 1989; Ward and Zafiriou, 1988) that can account for 6-33% of the total NO_2^- production in the Peruvian OMZ (Lam *et al.*, 2009). Ammonia oxidation also contributes significantly to the secondary nitrite maximum in the upper boundary of the Arabian Sea OMZ (Lam *et al.*, 2011) that was formerly thought to be a result of nitrate reduction alone (Naqvi, 1991).

Nitrite oxidation is the second step of nitrification and is mainly a chemolithoautotrophic process that produces NO_3^- (Fig. 1.3):

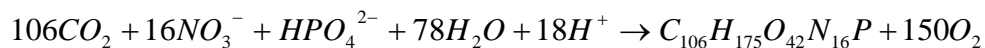


To a lesser extent also chemo-organotrophic and mixotrophic organisms occur that use simple organic compounds (Bock, 1976; Daims *et al.*, 2001; Freitag *et al.*, 1987) or they are

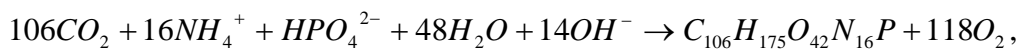
able to respire NO_3^- in the absence of oxygen (Bock *et al.*, 1988; Freitag *et al.*, 1987). Nitrite oxidation is apparently less sensitive to low oxygen concentrations compared to ammonia oxidation (Lam and Kuypers, 2011) and penetrates deeper into OMZs. Nitrite oxidation is even found under anoxic conditions (Füssel *et al.*, 2011) in the Namibian OMZ. Studies from the Pacific OMZs and the Namibian OMZ report that nitrite oxidation rates exceed ammonia oxidation rates due to an additional NO_2^- source from nitrate reduction (Füssel *et al.*, 2011; Lipschultz *et al.*, 1990; Ward *et al.*, 1989). Thus, re-oxidation of NO_2^- seems an effective process in OMZs to dampen the N-loss caused by heterotrophic denitrification or anammox.

1.3.5 Assimilation

During assimilation, nitrate, nitrite and ammonium are utilized mostly by photoautotrophs in conjunction with photosynthetic carbon assimilation (Fig. 1.3). Carbon, nitrate or ammonium and phosphate are taken up in Redfield stoichiometry as indicated by the stoichiometric ratios (Andersen, 1995):



or



where $\text{C}_{106}\text{H}_{175}\text{O}_{42}\text{N}_{16}\text{P}$ is the average composition of organic matter. NH_4^+ is the energetically most preferred source of reactive nitrogen for phytoplankton (Zehr and Ward, 2002). The assimilation of NO_3^- and NO_2^- involves the reduction to NH_4^+ by assimilatory NO_3^- and NO_2^- reductase before it can be converted into biomass (Falkowski, 1983). Thus, it is not surprising that more phytoplankton species assimilate NH_4^+ instead of more oxidized forms of nitrogen.

1.3.6 Ammonification

Ammonification is the release of NH_4^+ from organic matter (Herbert, 1999) during remineralisation (Fig. 1.3) and is mostly carried out by bacteria in sediments and in the water-column. Thus, microorganisms responsible for DNRA and nitrate reducers are considered as ammonifiers. Ammonification rates depend on the quality of organic matter, e.g. whether it is labile or highly refractory (Buchsbaum *et al.*, 1991). Thus the reaction can either be a simple deamination or a complex series of metabolic steps involving several hydrolytic enzymes. The overall reaction can be summarized as (Herbert, 1999):

Protein proteinases Peptides peptidases Amino acids deamination Organic acid + NH₄⁺

Recycling and ammonification of organic matter accounts for 20 to 80% of the N-requirements of phytoplankton in shallow coastal waters (<50 m; Hansen and Blackburn, 1992; Jensen *et al.*, 1990).

1.3.7 Diazotrophic N₂-Fixation

Diazotrophs can grow without sources of reactive nitrogen due to their ability to fix atmospheric dinitrogen (Fig. 1.3). Most research on pelagic N₂ fixation has focused on the filamentous cyanobacterium *Trichodesmium* since it is the most common pelagic bloom-forming species. But also unicellular coccoid cyanobacteria and cyanobacterial endosymbionts in diatom and flagellates exist, as well as diazotrophic bacteria and archaea. N₂ fixation mainly occurs in subtropical and tropical latitudes. Maximum growth rates and N₂ fixation rates in surface waters were measured between 24°C and 30°C (Breitbarth *et al.*, 2007), but low activity has been observed down to water temperatures of 18.3°C (McCarthy and Carpenter, 1979). Co-limiting factors on growth rates and N₂ fixation rates are iron and phosphorus availability (Rueter, 1988; Sanudo-Wilhelmy *et al.*, 2001). Low N:P ratios of available nutrients - like in surface waters adjacent to OMZs - promote N₂ fixation (Niemi, 1979). Based on geochemical estimates, observations and field studies, N:P ratios of diazotrophs are between 125 and 40 and are thus much higher than the Redfield ratio (Karl *et al.*, 1992; Letelier and Karl, 1996, 1998). Once a bloom of N₂-fixing organisms is established, the N:P ratio of the ambient dissolved and particulate matter pools increases dramatically (Karl *et al.*, 2002). N₂ fixation is the only natural biological source to balance N-deficits and to sustain the net oceanic productivity by supplying reactive nitrogen to the oceanic N-pool via ammonification and nitrification.

1.4. Stable nitrogen and oxygen isotopes in marine environments

1.4.1. Basics and background information

Isotopes of an element share the same number of protons, but have different numbers of neutrons. ^{14}N and ^{15}N are the only stable nitrogen isotopes containing 7 and 8 neutrons in their nucleus, respectively. ^{15}N is the less abundant stable nitrogen isotope constituting only 0.365% of the global nitrogen pool (Nier, 1950). Oxygen has three stable isotopes: ^{16}O , ^{17}O and ^{18}O containing 8, 9 and 10 neutrons in their nucleus, respectively. Stable oxygen isotopes naturally occur in relative atom abundances of 99.759%, 0.0374% and 0.2039% for ^{16}O , ^{17}O and ^{18}O , respectively (Nier, 1950). Since absolute isotope abundance quantities of different samples are confusing, it is more practical to quantify the isotope ratio (e.g. $^{15}\text{N}/^{14}\text{N}$ or $^{18}\text{O}/^{16}\text{O}$) between the sample and an international reference standard. The δ -notation gives the natural isotope abundances in a sample in per mil relative to the isotopic composition of a standard reference material:

$$\delta^{15}\text{N}[\text{‰}] = \left(\frac{R_{\text{sample}}}{R_{\text{standard}}} - 1 \right) \times 1000 \quad (2),$$

with $R = \frac{^{15}\text{N}}{^{14}\text{N}}$ for stable nitrogen isotopes and $R = \frac{^{18}\text{O}}{^{16}\text{O}}$ for stable oxygen isotopes.

$\delta^{15}\text{N}$ values represent the “per mil”-difference between the isotope ratio of a sample and that of atmospheric N_2 which is zero by definition (Montoya, 2008). For oxygen isotopes, standard reference material is VSMOW (Vienna Standard Mean Ocean Water) with $\delta^{18}\text{O} = 0\text{‰}$.

1.4.2. Isotope fractionation

Biologically mediated reactions of the nitrogen cycle that are incomplete (e.g. water-column denitrification and nitrification) are associated with a kinetic fractionation of stable isotopes. In most cases, the lighter ^{14}N preferentially reacts to the product and the heavier ^{15}N isotope is enriched in the residual nitrogen pool. The fractionation factor ε (also called discrimination factor or isotope effect) is expressed as the difference between the $\delta^{15}\text{N}$ of the substrate and the product:

$$\varepsilon \approx \delta^{15}\text{N}_{\text{substrate}} - \delta^{15}\text{N}_{\text{product}} \quad (3)$$

The variability in fractionation factors of different N-cycling processes derives from physical parameters like diffusivity and exchange rates and from enzymatic effects during biological uptake. Preferential removal of the lighter isotope from the substrate (normal fractionation) yields positive fractionation factors. But note, that also the inverse expression is used by Mariotti *et al.* (1981) that give negative fractionation factors for normal fractionation. During the less common negative or inverse fractionation, the heavier isotope preferentially reacts to the product and the lighter isotope accumulates in the residue.

An example for fractionation during progressing assimilation is illustrated in Fig. 1.4. During progressing nitrate assimilation of a nitrate pool with initial $\delta^{15}\text{N}_{\text{NO}_3} = 6.0\text{‰}$ in a closed system, ^{14}N is preferentially removed from nitrate with a fractionation factor of 5‰ and incorporated into the phytoplankton biomass. This leads to a progressive increase in $\delta^{15}\text{N}$ of the residual nitrate pool, of the accumulated and instantaneously produced phytoplankton biomass. But the mean $\delta^{15}\text{N}$ of nitrate and phytoplankton biomass must remain constant for reasons of mass and isotope conservation in a closed system. Thus, when nitrate is completely consumed, the accumulated phytoplankton biomass has a $\delta^{15}\text{N}$ of the initial nitrate pool.

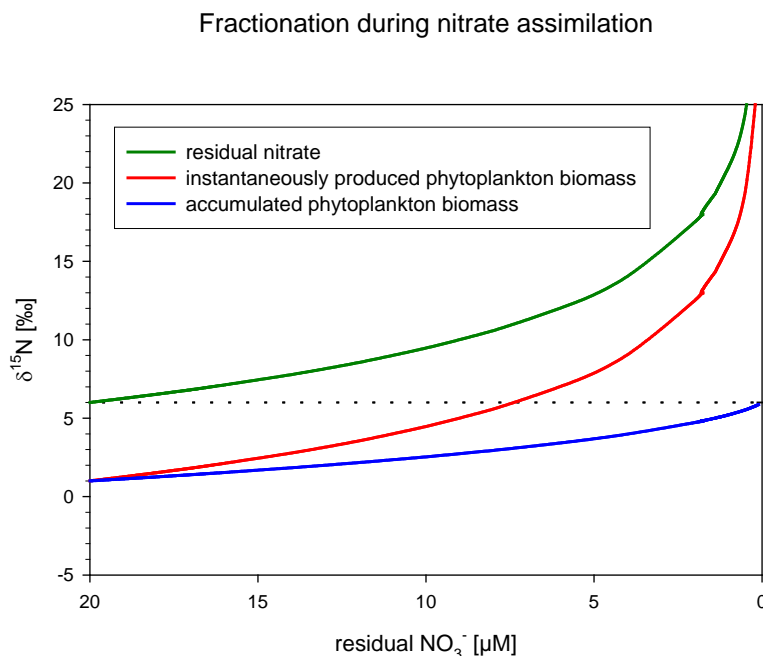


Fig. 1.4: Changes in $\delta^{15}\text{N}$ of nitrate and phytoplankton biomass during phytoplankton growth in a closed system – the so-called Rayleigh fractionation. Initial nitrate concentration was $20 \mu\text{M}$ with a $\delta^{15}\text{N}_{\text{NO}_3}$ of 6‰ . Nitrate consumption occurs with a fractionation factor of $^{15}\epsilon = 5\text{‰}$. The dashed line gives the initial nitrate isotope signature that the accumulated phytoplankton biomass reaches, when nitrate is completely consumed. The example is calculated after Mariotti *et al.* (1981) and Montoya, (2008).

1.4.3. The use of stable N and O isotopes as a proxy for N turnover processes

Nutrient-derived tracers like N^* have been established to indicate N-sources and sinks by the deviation from the classical Redfield stoichiometry (Deutsch *et al.*, 2007; Gruber and Sarmiento, 1997). However, signals from N_2 fixation that balance the N-deficit in the vicinity of denitrification zones are masked by the dominance of heterotrophic denitrification and anammox. N^* cannot distinguish between physical mixing and biological processes balancing the N-deficit at the edges of an OMZ, nor can it identify or quantify complex interactions in N-cycling. Therefore, paired measurements of N and O isotopes in nitrate ($\delta^{15}N_{NO_3}$ and $\delta^{18}O_{NO_3}$), nitrite and particulate matter ($\delta^{15}N_{PN}$) have been established to differentiate between the reactions of the nitrogen cycle (Bourbonnais *et al.*, 2009; Casciotti and McIlvin, 2007; Casciotti *et al.*, 2008; Knapp *et al.*, 2008; Sigman *et al.*, 2005; Sigman *et al.*, 2009a). Isotope fractionation during N-cycling modifies the isotope ratio of the dissolved inorganic N-source (Fig. 1.4). But since more and more is known about fractionation (Table 1.1), measurements of N (and O) isotopes in nitrate and in particulate matter can be used to identify and quantify different N-sinks and sources.

Process	$^{15}\epsilon$ [‰]	References	$^{18}\epsilon$ [‰]	References
Nitrate reduction	+13 to +30	Barford et al. (1999), Delwiche and Steyn (1970), Granger et al. (2008)		
Heterotrophic denitrification	+22 to +30	Brandes et al. (1998), Granger et al. (2008)	+5 to +23	Granger et al. (2008)
N ₂ fixation	-2 to +2	Delwiche and Steyn (1970), Hoering and Ford (1960), Meador et al. (2007)		
Ammonification	1 to +10	Prokopenko et al., 2006 ¹⁾ , Sigman et al. (2009b), Möbius (2013)		
Ammonium assimilation	+6 to +27	Hoch et al. (1992), Waser et al. (1998a), Wankel et al. (2007)		
Nitrate assimilation	+5 to +10	Granger et al. (2004), Needoba and Harrison (2004), Waser et al. (1989a)	+21 to +5	Granger et al. (2004)
Ammonia oxidation	+14 to +38	Casciotti et al. (2003), Mariotti et al. (1981), Yoshida (1988), Delwiche and Steyn (1970)	+18 to +38	Casciotti et al. (2010) ²⁾
Nitrite oxidation	-12.8	Casciotti (2009)	-10 to -1	Buchwald and Casciotti (2010)

¹⁾ Fractionation factors for ammonification depend on the metabolic pathway. If DNRA is involved, $^{15}\epsilon$ can be as high as +10‰, otherwise $^{15}\epsilon$ is considered to be 2‰ to 3‰.

²⁾ combined isotope effect for incorporation of oxygen from H₂O and dissolved O₂

Table 1.1: List of fractionation factors $^{15}\epsilon$ and $^{18}\epsilon$ for major N-cycling processes. Normal fractionation is expressed as positive values and inverse fractionation as negative values.

N-cycling not only comprises turnover processes of dissolved inorganic nitrogen forms but also the build-up and fate of particulate organic matter. Living primary producers from upwelling systems that are situated above OMZs thus carry the heavy N isotope signal from mid-water denitrification (Altabet *et al.*, 1999b; Naqvi *et al.*, 1998; Voss *et al.*, 2001). Recycling and remineralisation in the euphotic zone are relevant for the maintenance of primary productivity and only 5 to 10% of the phytoplankton produced in the surface water sink out of the euphotic zone (Wakeham and Lee, 1989). During the fate of particulate organic matter, reactive carbohydrates and proteins are preferentially consumed so that

recalcitrant components remain on the residual sinking particles. Lam *et al.* (2011) and Kalvelage *et al.* (2013) emphasized the importance of adequately preserved OM for the occurrence of heterotrophic N-cycling processes in OMZs. But to date, this aspect is mainly neglected in investigations about N-cycling activity.

1.5. Particle cycling and amino acids as indicators of organic matter sources and preservation states

1.5.1 Amino acids as indicators of organic matter (OM) sources

Amino acids (AA) are building blocks of protein molecules and are found in all living organisms. The bulk AA compositions of bacteria, phytoplankton and vascular plants are quite similar (Cowie and Hedges, 1992; Lee and Wakeham, 1988) with some minor differences in AA compositions of bacteria and frustule-bearing organisms. Peptidoglycan from bacterial cell walls is enriched in Gly compared to phytoplankton OM (Bidle and Azam, 1999; Keil *et al.*, 2000). Diatoms cell walls are enriched in Gly, Ser and Thr whereas calcifying plankton is associated with an enrichment in Asp and to a lower extent in Glu (Hecky *et al.*, 1973; Ingalls *et al.*, 2003; King, 1977). The AA composition of frustule-bearing detritus pretends to be less degraded since frustules protect OM from degradation (Ingalls *et al.*, 2003). Diatom frustules additionally act as ballast and provide excess density for fast sinking particles by excreting transparent exopolymer particles that enable the formation of large aggregates (Alldredge and Gotschalk, 1989).

1.5.2 Particle cycling and its impact on protein degradation

Particulate matter comprises several types of particles that are mainly characterized by their particle diameter. For this dissertation, I concentrate on suspended particles with a diameter $<10^2$ μm and on sinking particles (10^2 to 10^4 μm ; Fowler and Knauer, 1986; Wakeham and Lee, 1989). Suspended particles are sampled by Niskin bottles and mainly consist of free-living microbes, phytoplankton detritus and their degradation products (Sheridan *et al.*, 2002). Horizontal transport of suspended matter (SPM) dominates over vertical transport in the water column (McCave, 1984). Sinking particles are caught with sediment traps and are formed by physical aggregation and biological repackaging mainly in the euphotic zone (Knauer *et al.*, 1979; Lee and Wakeham, 1988). 90 to 95% of the OM produced in surface water is remineralised and consumed in the euphotic zone (Wakeham and

Lee, 1989). Further OM degradation of sinking particles is characterised by a decrease of reactive AA proportions with increasing water depth (Gaye-Haake *et al.*, 2005; Wakeham *et al.*, 1984). Proteins are preferentially decomposed compared to bulk organic carbon during the remineralisation of OM and the residual OM gets enriched in recalcitrant AA monomers. Several degradation indices have been developed to evaluate the degradation state of sinking particles and sediments in different environments (e.g. Dauwe and Middelburg, 1998; Jennerjahn and Ittekkot, 1997; Menzel *et al.*, 2013). They rely on the decrease of reactive AAs like Leu, Tyr, Ala, Val, Ile and Phe as well as the increase of recalcitrant AAs (β -Ala, γ -Aba, Gly, Ser) during OM degradation. The degradation indices do not distinguish between the respective influence of sources and degradation that differ depending on the sampling environment (Ingalls *et al.*, 2003). Qualitative differences in OM preservation can be observed during degradation under different oxygenation levels: Oxygen deficiency reduces degradation rates so that AA compositions of sediments beneath OMZs contain more reactive AAs (e.g. Menzel *et al.*, 2013; Nguyen and Harvey, 1997). Accumulation rates additionally affect the preservation state of OM in sediments, because fast particle burial reduces the O₂ exposure time with the (generally more oxygenated) water column. Thus, high-accumulative sediments are generally less degraded (Müller and Suess, 1979).

Surface sediment and sinking particles are distinct in their OM composition from suspended particles that are collected at comparable water depths (Repeta and Gagosian, 1984; Sheridan *et al.*, 2002; Wakeham and Canuel, 1988). The degradation state of suspended matter is not depth-dependent (Gaye *et al.*, 2013) and investigations about OM preservation of suspended matter show contradictory results (Abramson *et al.*, 2010; Gaye *et al.*, 2013; Goutx *et al.*, 2007; Rontani *et al.*, 2011; Sheridan *et al.*, 2002).

1.6. Thesis outline

The main focus of this thesis lies on the complex interactions in water-column N-cycling of the Arabian Sea OMZ and of the OMZ on the Namibian shelf. Both systems exhibit all N-cycling processes that are known to occur within OMZs (Fig. 1.3), although they are caused by completely different hydrodynamic regimes, have different thicknesses and spatial extents, and differ in their variability through time. OMZs are the main sites of N-loss in water-columns of the world's oceans, and the Arabian Sea alone is responsible for 30 to 50% of the N-loss in the oceanic water-column. Upwelling and strong diapycnical mixing were

considered to be the only important sources of NO_3^- in surface water. Recently, evidence increases that recycled NO_3^- from nitrification considerably contributes to the NO_3^- pool in surface water – even in nutrient-replete regions like upwelling systems.

A second focus is set on particle cycling within the Namibian OMZ because the breaking of internal waves and tides complicates the sedimentation on the shelf and upper slope due to resuspension of surface sediments. The aim of tracing particle cycling in the Benguela upwelling system was to find out which N turnover processes or particle cycling mechanisms are preserved in the $\delta^{15}\text{N}$ ratios of surface sediments. Initially, this study was designed to investigate the influence of OM degradation on the $\delta^{15}\text{N}$ ratios of surface sediments and to evaluate sedimentary $\delta^{15}\text{N}$ ratios as a proxy for N turnover processes in the Benguela upwelling system. The results show that besides from the determination of the degradation state of OM, amino acid data can be used to trace the origin and cycling history of different particle types.

Acknowledgements:

Financial support for the Arabian Sea study came from the Deutsche Forschungsgemeinschaft (DFG Grant No. GA 755/4-1). All investigations on the Namibian shelf were carried out in the course of the GENUS project (Geochemistry and Ecology in the Namibian Upwelling System) which is financed by the German Federal Ministry of Education and Research. Financial support by the Helmholtz-Zentrum Geesthacht is gratefully acknowledged.

The following chapters derive from three articles that are to be submitted to or are published in peer-reviewed journals:

Chapter 2

Evidence of parallel denitrification and nitrite oxidation in the ODZ of the Arabian Sea from paired stable isotopes of nitrate and nitrite

Birgit Gaye, Birgit Nagel, Kirstin Dähnke, Tim Rixen and Kay-Christian Emeis

Published in December 2013 in: GLOBAL BIOGEOCHEMICAL CYCLES

Stable N and O isotope ratios in nitrate and nitrite as well as in nitrate alone were used to trace N-transformation processes. Isotope ratios increase significantly in the upper OMZ from 100 to 400 m water depth due to nitrate reduction, heterotrophic denitrification, and to a lesser extent probably due to anammox. Isotope data and a box model show in agreement that

significant amounts of accumulated nitrite from nitrate reduction are reoxidized under suboxic conditions in the upper part of the OMZ. The data further indicate that nitrate reduction in the northwestern Arabian Sea is as effective as in the rest of the OMZ. Nitrite does not accumulate in the western Arabian Sea because of enhanced activity of nitrite oxidation possibly due to better ventilation of the western part of the basin under the influence of Persian Gulf Water and Red Sea Water – and possibly due to enhanced anammox activity.

My contribution to this chapter was:

- Most analysis of $\delta^{15}\text{N}$ and $\delta^{18}\text{O}$ of nitrate and nitrite, and interpretation of nitrate and nitrite isotope data especially in context of the hydrography of the Arabian Sea
- Co-work in manuscript preparation and discussion.

N-cycling and balancing of the N-deficit generated in the oxygen-minimum zone over the Namibian shelf – an isotope-based approach

Birgit Nagel, Kay-Christian Emeis, Anita Flohr, Tim Rixen, Tim Schlarbaum, Volker Mohrholz and Anja van der Plas

Published in March 2013 in: JOURNAL OF GEOPHYSICAL RESEARCH - BIOGEOCHEMISTRY

Variations in nutrient and oxygen concentrations, stable N and O isotopes of nitrate and stable N isotopes of particulate matter were used to describe N-cycling processes on the Namibian shelf. Dissolved N:P ratios in the water column decrease in the OMZ on the inner shelf due to denitrification, anammox and phosphate release from sediments. Thus, N-deficit hosting water masses well up at the coast and propagate offshore with the Ekman transport. On its way offshore, the N-deficit diminishes to usual Redfield stoichiometry most likely due to external sources like shelf break mixing that transfers subsurface waters with N excess into surface water. Isotope data give indications for a contribution of N_2 fixation offshore the shelf break. Data from different seasons reveal that the Benguela Upwelling system is highly dynamic since seasonal changing water mass distributions determine the N:P ratios and oxygenation on the shelf and thus influence N transformation processes.

My contribution to this chapter was:

- Complete analysis of $\delta^{15}\text{N}_{\text{PN}}$ and particulate organic carbon content as well as most analyses of $\delta^{15}\text{N}_{\text{NO}_3}$
- Conceptual design came from Birgit Nagel and Prof. Emeis
- Elaboration of the manuscript

Chapter 4

Effects of current regimes and oxygen deficiency on particulate matter preservation on the Namibian shelf: insights from amino acid biogeochemistry

Birgit Nagel, Birgit Gaye, Niko Lahajnar, Ulrich Struck and Kay-Christian Emeis

Submitted to: LIMNOLOGY AND OCEANOGRAPHY

Amino acid compositions of suspended matter from the water column and the underlying sediment were compared to elucidate the impact of organic matter degradation on stable N isotope ratios of surface sediments on the Namibian shelf. The data reveal that sedimentary organic matter from the inner shelf has a higher protein preservation state due to direct particle sedimentation from the water column under oxygen-depleted conditions. Thus, degradation of organic matter accounts for minor N isotope shifts within the OMZ and high $\delta^{15}\text{N}$ ratios of surface sediments from the inner shelf are an expression of N turnover processes that occur in the OMZ. Distinctly different amino acid compositions in suspended matter and sediments indicate only subordinate exchange between both sample types. The interaction between internal waves and tides with the shelf break is of great importance for particle cycling. It causes an uplift of suspended matter from <600 m water depth to the base of the mixed layer. Resuspension and transport within the benthic boundary layer increases the degradation state of sedimentary organic matter on the outer shelf break.

My contribution to this chapter was:

- Analyses of particulate organic carbon content from suspended matter samples and surface sediments retrieved during M76-2.
- Analyses of $\delta^{15}\text{N}$ ratios in surface sediments retrieved during M76-2 and MSM17-3
- Elaboration of the manuscript except the performance of the principal component analysis that was done by Birgit Gaye
- Conceptual design came from Birgit Nagel and Prof. Emeis

2 Evidence of parallel denitrification and nitrite oxidation in the ODZ of the Arabian Sea from paired stable isotopes of nitrate and nitrite

Birgit Gaye, Birgit Nagel, Kirstin Dähnke, Tim Rixen and Kay-Christian Emeis

Published in December 2013 in: GLOBAL BIOGEOCHEMICAL CYCLES

Keywords: Nitrogen Cycle, $\delta^{15}\text{N}$, $\delta^{18}\text{O}$, Arabian Sea, nitrification, denitrification, anammox

ABSTRACT

The Arabian Sea is a major oceanic nitrogen sink and its oxygen deficient zone extends from 150 m to 1200 m water depth. To identify the dominant transformation processes of reactive nitrogen and to quantify the amounts of nitrogen turned over in the different reactions of the nitrogen cycle, we use paired data on stable isotope ratios of nitrogen and oxygen in nitrate and nitrite measured at four near coastal and five open ocean stations in the Arabian Sea. We find significant nitrate reduction and denitrification between 100 m and 400 m in the open Arabian Sea, which are most intense in the eastern and northern part of the basin, and estimate that about 50% of initial nitrate is being reduced either to dinitrogen gas (denitrification) or to nitrite (nitrate reduction) in the core zone of denitrification. Nitrite accumulates in concentrations above 4 μM in the water column of the eastern and northern Arabian Sea. Large differences in isotopic ratios of nitrate and nitrite and a decoupling of their stable nitrogen and oxygen isotopes can be explained by the re-oxidation of nitrite. The observed decoupling of the paired isotopes may be due to the exchange of oxygen of nitrite with oxygen from ambient water. In agreement with model estimates from the literature,

about 25 % of the nitrate initially reduced to nitrite is returned to the nitrate pool by nitrification in the upper and lower denitrification layer while 40 % is denitrified.

2.1. INTRODUCTION

The main reactive nitrogen source to the ocean is diazotrophic N_2 fixation and the major sink was thought to be heterotrophic denitrification (Brandes and Devol, 2002). During the last years, nitrogen transformation processes known to occur in the sediments were detected in oxygen depleted zones (ODZs, Fig. 2.1) such as dissimilatory nitrate reduction to ammonium (DNRA; Lam *et al.*, 2009) or anaerobic ammonium oxidation (anammox), which produces dinitrogen gas from nitrite and ammonium (Kuypers *et al.*, 2003).

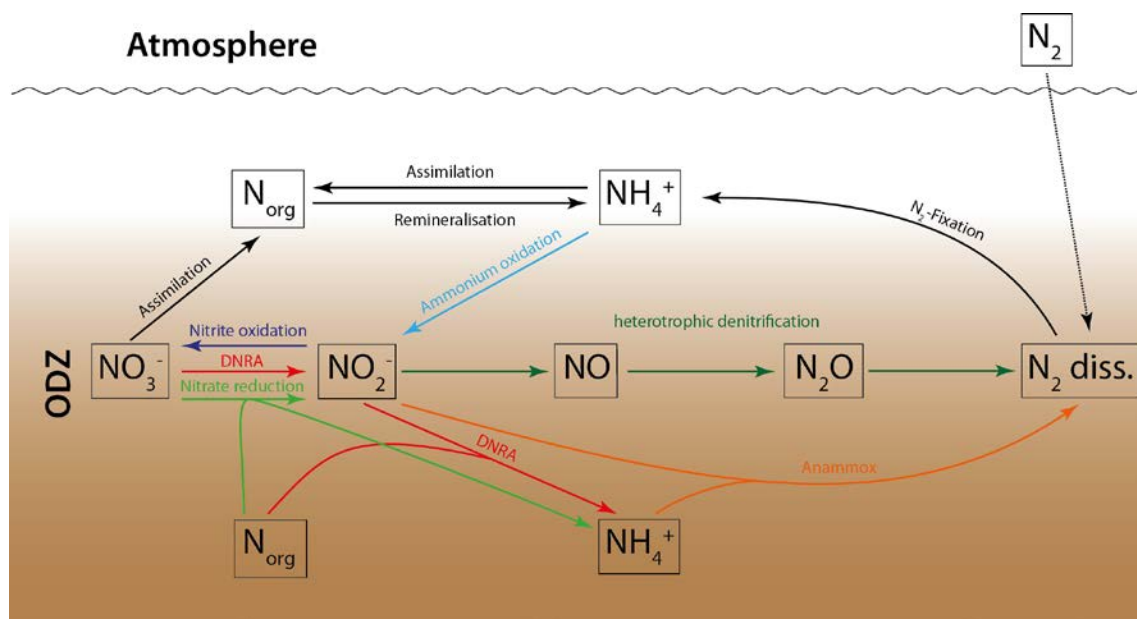


Fig. 2.1: Processes of nitrogen cycling in the ocean showing oxic and suboxic transformation processes. Nitrate and ammonium assimilation are restricted to photic zones. Ammonia and nitrite oxidation occur in oxic to even anoxic environments. Suboxic processes taking place in oxygen depleted zones (ODZs) are nitrate reduction (the first step of heterotrophic denitrification), denitrification and dissimilatory nitrate reduction to ammonium (DNRA). Chemolithotrophic bacteria use anaerobic ammonium oxidation (anammox) as an energy source and remove nitrite and ammonium as N_2 in the suboxic environment. The figure is adapted from Lam and Kuypers (2011).

Until recently it was assumed that the combined oceanic nitrogen losses were larger than the total reactive nitrogen gained by the global ocean from N₂ fixation and other external sources (Codispoti, 2007). This may, however, be due to an underestimation of diazotrophic dinitrogen-fixation by the method used previously. New results with a modified methodology supply much higher nitrogen fixation rates and suggest that the nitrogen budget has been balanced for the last 3.000 years (Großkopf *et al.*, 2012). ODZs at mid-water depths in the oceans are prominent sinks, where an estimated 1/3 of the loss occurs; the remainder is eliminated in sediments (Brandes and Devol, 2002). Evidently, most ODZs expanded and deepened in the world's oceans during the last decades (Stramma *et al.*, 2008).

Whereas anammox appears to be the dominant process of nitrogen loss in the Peru upwelling system (Lam *et al.*, 2009; Thamdrup *et al.*, 2006), the main nitrogen sink in the Arabian Sea is heterotrophic denitrification (Bulow *et al.*, 2010; Ward *et al.*, 2009). Anammox may be significant in the Oman upwelling region, if coupled with DNRA to supply sufficient amounts of ammonium (Jensen *et al.*, 2011). Nitrite accumulates in the so called secondary nitrite maximum (SNM) between 150 m and 400 m water depth in the central to northeastern Arabian Sea to concentrations >5 µM (Naqvi, 1991). This accumulation may be due to the fact that nitrate reduction is more common and carried out by more bacterial species than the reduction of nitrite to dinitrogen gas (Naqvi *et al.*, 2008; Zumft, 1997). The temporally accumulating nitrite can further be completely denitrified to dinitrogen gas (Fig. 2.1; Ward *et al.*, 2009). Alternatively, it is used in the anammox reaction to oxidize ammonium or is reduced to ammonium by DNRA (Jensen *et al.*, 2011). Nitrite may also become re-oxidized to nitrate at the upper or lower fringe of the ODZ at appropriate oxygen concentrations (Anderson *et al.*, 1982). Other ODZ studies from the eastern tropical South Pacific (ETSP) and the Benguela upwelling system detected nitrite oxidation even at low oxygen concentrations (<2.5 µM; Füssel *et al.*, 2011; Lipschultz *et al.*, 1990). Dominant processes and rates of N-elimination in the ODZ of the Arabian Sea appear to vary on short temporal and spatial scales as ¹⁵N incubation techniques suggest (Jensen *et al.*, 2011; Ward *et al.*, 2009), and the regulating environmental influences on dominance of either denitrification or anammox are unresolved.

Most incomplete reactions in the nitrogen cycle, such as water-column denitrification, and probably also anammox, are associated with a kinetic fractionation of stable isotopes ¹⁴N and ¹⁵N, so that the lighter ¹⁴N is preferentially found in the reaction product and the heavy isotope is enriched in the residual substrate pool (Cline and Kaplan, 1975; Mariotti *et al.*, 1981). The degree of fractionation is expressed by the isotopic effect (ε) as the difference

between the δ -values of the source and the product (Mariotti *et al.*, 1981). Nitrate reduction to nitrite has an isotopic effect of $^{15}\epsilon = 20\text{-}30\text{‰}$ (Altabet *et al.*, 1999a; Brandes *et al.*, 1998; Cline and Kaplan, 1975). Laboratory experiments show that during assimilation of nitrate ($^{15}\epsilon = \sim 5\text{‰}$) as well as during heterotrophic denitrification the ratio of N and O enrichment factors $^{15}\epsilon/^{18}\epsilon$ is ~ 1 (Granger *et al.*, 2008; Granger *et al.*, 2004). It can thus be assumed that if only these two processes were responsible for any change in nitrate concentrations the preformed offset in the original water mass between $\delta^{15}\text{N}_{\text{NO}_3}$ and $\delta^{18}\text{O}_{\text{NO}_3}$ would be maintained. Deep water nitrate has an average $\delta^{15}\text{N}_{\text{NO}_3}$ value of $\sim 5\text{‰}$ (Sigman *et al.*, 2005) whereas its $\delta^{18}\text{O}_{\text{NO}_3}$ should be close to 0‰ . Both values can deviate locally and studies have reported average values between 4.8 to 5‰ for $\delta^{15}\text{N}_{\text{NO}_3}$ and, respectively, 1.8 to 2.4‰ for $\delta^{18}\text{O}_{\text{NO}_3}$ (Bourbonnais *et al.*, 2009; Sigman *et al.*, 2005).

Several processes can lead to a decoupling of $\delta^{15}\text{N}_{\text{NO}_3}$ and $\delta^{18}\text{O}_{\text{NO}_3}$. Remineralisation and nitrification of organic matter from N_2 fixation for instance produce nitrate with low $\delta^{15}\text{N}_{\text{NO}_3}$ compared to $\delta^{18}\text{O}_{\text{NO}_3}$ (Sigman *et al.*, 2005). A second process decoupling $\delta^{15}\text{N}_{\text{NO}_3}$ and $\delta^{18}\text{O}_{\text{NO}_3}$ is the nitrification of ammonium or nitrite in ODZs as it is associated with the uptake of oxygen from either the dissolved oxygen pool or ambient water (Casciotti and McIlvin, 2007; Sigman *et al.*, 2005). The isotopic effect $^{15}\epsilon_{\text{NH}_4}$ associated with ammonia oxidation to nitrite (Fig. 2.1) is between 14 and 19‰ for common oceanic nitrifiers and can be much higher for some species (Casciotti *et al.*, 2003). Theoretically, half of the oxygen used for ammonia oxidation stems from ambient water and half is taken from dissolved oxygen, which has a $\delta^{18}\text{O}$ value of up to 40‰ in ODZs (Bender, 1990; Levine *et al.*, 2009). The second step of nitrification (nitrite oxidation to nitrate, Fig. 2.1) was found to be associated with a negative kinetic effect on stable nitrogen and oxygen isotopes of, respectively, about -13‰ and about -7‰ (Buchwald and Casciotti, 2010; Casciotti, 2009). The reason is that nitrite takes up water and forms an intermediate with a bound water molecule. The heavier isotope preferably reacts to nitrate, whereas the lighter isotope is more likely to again lose the water molecule (Casciotti, 2009). According to stoichiometry, $1/3$ of the oxygen taken up during ammonia oxidation to nitrate should stem from dissolved oxygen whereas $2/3$ are taken up from ambient water. However, in reality the exchange of oxygen with water may result in a dissolved oxygen contribution of less than $1/6$ (Sigman *et al.*, 2005). Moreover, any uptake of oxygen from water or the dissolved molecular oxygen pool is associated with considerable positive isotopic effects difficult to distinguish even experimentally (Buchwald and Casciotti, 2010; Casciotti, 2009).

In addition to the decoupling of $\delta^{15}\text{N}_{\text{NO}_3}$ and $\delta^{18}\text{O}_{\text{NO}_3}$ (Sigman *et al.*, 2005) a strong depletion of nitrite in ^{15}N (Casciotti *et al.*, 2007) suggests that denitrification is not the only significant process in ODZs. This highlights the importance to analytically differentiate between nitrate and nitrite in regions of nitrite accumulation (Casciotti *et al.*, 2007).

In this work we use water column data on oxygen and nutrient concentrations as well as paired isotope measurements of nitrate and nitrite in vertical profiles from the Arabian Sea to identify the predominant processes of nitrogen transformation in the ODZ. Using the fractionation factors, the difference between isotopic ratios of nitrate and nitrite and paired isotope measurements we attempt to quantitatively estimate the relevance of the various processes of the nitrogen cycle.

2.2. STUDY AREA

The Arabian Sea is one of three major sinks of reactive nitrogen in the world's ocean due to widespread reduction of nitrate in its mid-water ODZ; the two other are the eastern tropical north and south Pacific. High sinking fluxes of organic matter result from monsoonal upwelling of nutrients and conspire with poor ventilation of intermediate waters to cause low oxygen concentrations in the water depth interval from 150 m to >1000 m. Most intense upwelling and primary production occur along the Arabian Peninsula during the SW monsoon (Banzon *et al.*, 2004; Marra and Barber, 2005). The oxygen deficit is stronger in the NE basin due to poorer ventilation and is spatially decoupled from the western Arabian Sea upwelling area (Naqvi, 1991). The main water mass in the ODZ is the Indian Central Water (ICW; $\sigma_\theta = 26.7 \text{ kg m}^{-3}$) that combines Subantarctic Mode Water (SAMW), Antarctic Intermediate Water (AAIW), and Indonesian Intermediate Water (IIW) (Böning and Bard, 2009; Morrison, 1997; Morrison *et al.*, 1998). Already depleted in oxygen, the ICW enters the Arabian Sea in its western part at a core depth of 300 m and continues to lose oxygen while accumulating nutrients from mineralisation of sinking organic matter on its way to the northern and eastern parts of the basin. Effective nitrate loss occurs mostly between 150 m and 400 m (Naqvi *et al.*, 2008).

The inflows of intermediate water masses from the Persian Gulf (PGW) and Red Sea (RSW; Shailaja *et al.*, 2006) locally modify the water mass structure of the western Arabian Sea. These water masses are surface-derived and thus oxygen-rich and nutrient-poor (Morrison *et al.*, 1998). Their admixture contributes to the nitrate deficit at depth intervals situated at 200-400 m (PGW; $\sigma_\theta = 26.2\text{-}26.8 \text{ kg m}^{-3}$) and 500-800 m (RSW; $\sigma_\theta = 27.0\text{-}27.4 \text{ kg m}^{-3}$)

m^{-3}), respectively, and cause better ventilation of the western part of the basin (Mantoura *et al.*, 1993; Prasad *et al.*, 2001).

O_2 concentrations below $\sim 5 \mu\text{M}$ in the mid-water ODZ trigger denitrification (Cline and Richards, 1972; Devol, 1978) which creates a nitrate minimum and high $\delta^{15}\text{N}_{\text{NO}_3}$ values of the residual nitrate (Naqvi *et al.*, 1998). Upwelling and assimilation of that enriched nitrate transfers the high $\delta^{15}\text{N}_{\text{NO}_3}$ values into biomass, sinking particles of export production and eventually to the sediment record, which evidences large changes in regional denitrification intensity on glacial/interglacial time scales (Altabet *et al.*, 2002; Möbius *et al.*, 2011; Suthhof *et al.*, 2001).

2.3. MATERIALS AND METHODS

2.3.1. Sampling

Water was sampled at nine stations during the cruise Meteor 74/1b in September/October 2007 (Fig. 2.2; Supplement ts01). The open ocean stations had been occupied repeatedly in 1995 to 1997 during the JGOFS cruises (Codispoti, 2000; Morrison *et al.*, 1998). Samples for stable nitrate and nitrite isotopes measurements were taken between 0 and 400 m water depth at four stations on the shelf and slope off Oman (#944 to #947) in coarse vertical resolution (three to four samples). At five stations in the open Arabian Sea (#949, #950, #953, #955, #957; Fig. 2.2), the denitrification zone was sampled every 25 m down to 400 m. The sampling intervals increased from 50 to 200 m between 400 m to 1200 m water depth. Ancillary water samples from the denitrification zone were taken for stable isotope analysis of only nitrate ($\delta^{15}\text{N}_{\text{NO}_3}$ and $\delta^{18}\text{O}_{\text{NO}_3}$) by removing nitrite with ascorbate treatment onboard (Granger *et al.*, 2006). Samples for stable nitrite and nitrate isotopes ($\delta^{15}\text{N}_{\text{NO}_3+\text{NO}_2}$ and $\delta^{18}\text{O}_{\text{NO}_3+\text{NO}_2}$) were kept frozen until analyses in the home laboratory. Nutrient analyses were carried out onboard for every 25 m at all of these stations.

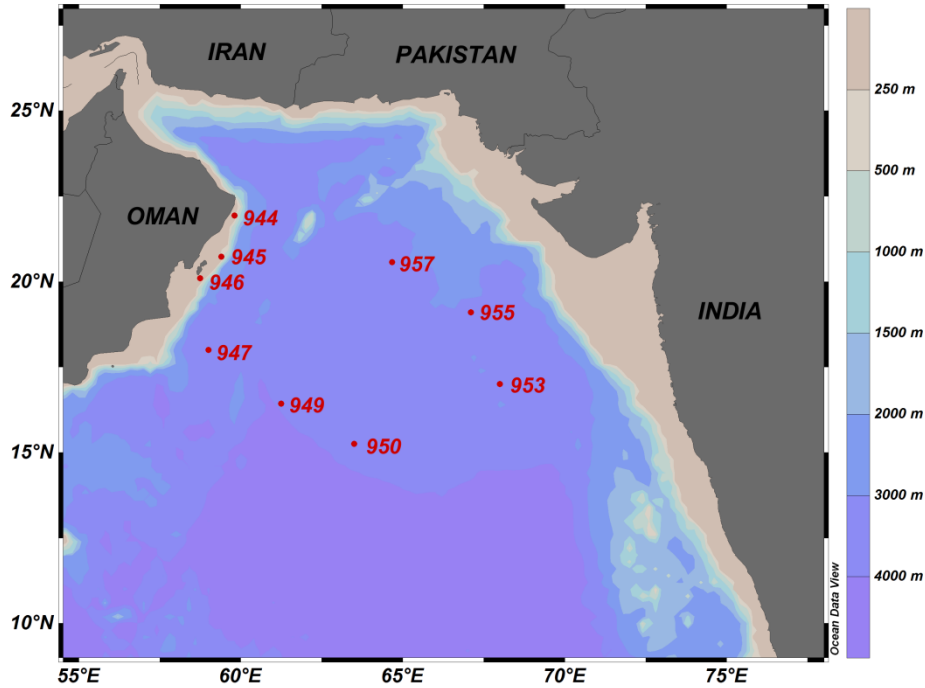


Fig. 2.2: Sampling locations in the Arabian Sea along the coast of Oman and in the open Arabian Sea.

2.3.2. Analyses

CTD, Oxygen, Nutrients

The CTD used was a SEABIRD electronic underwater unit equipped with pressure, temperature, conductivity, oxygen, and fluorescence sensors attached to an OCEANIC rosette water sampler with 18 bottles. Raw CTD data were post-processed with the SEABIRD data processing tool (data conversion, wild edit, split, window filter and bin average).

Nutrients (NO_3^- , NO_2^- , PO_4^{3-}) were measured with a SKALAR autoanalyser directly after sampling onboard RV Meteor. Oxygen concentrations in discrete samples were measured by using Winkler methods and were further used to calibrate oxygen data obtained from the CTD.

Nitrate and Nitrite Isotopes

$\delta^{15}\text{N}$ and $\delta^{18}\text{O}$ of nitrate and nitrite ($\delta^{15}\text{N}_{\text{NO}_3+\text{NO}_2}$ and $\delta^{18}\text{O}_{\text{NO}_3+\text{NO}_2}$) were determined using the “denitrifier method” (Casciotti *et al.*, 2002; Sigman *et al.*, 2001a). Based on nitrate and nitrite concentrations, sample volumes calculated to yield 10 nmol N_2O were injected into suspensions of *Pseudomonas aureofaciens* (ATCC#13985) for combined analysis of $\delta^{15}\text{N}$ and $\delta^{18}\text{O}$. The resulting N_2O gas in the headspace was purged into a GasBench II (Thermo

Finnigan), and analysed in a Delta Plus XP mass spectrometer. Isotope ratios are reported in ‰ using the delta-notation:

$$\delta^{15}\text{N}_{\text{sample}} = \left(\frac{(^{15}\text{N}/^{14}\text{N})_{\text{sample}}}{(^{15}\text{N}/^{14}\text{N})_{\text{reference}}} - 1 \right) * 1000 \quad (4)$$

$$\text{and } \delta^{18}\text{O}_{\text{sample}} = \left(\frac{(^{18}\text{O}/^{16}\text{O})_{\text{sample}}}{(^{18}\text{O}/^{16}\text{O})_{\text{reference}}} - 1 \right) * 1000 \quad (5)$$

with air N₂ and VSMOW as reference for ¹⁵N/¹⁴N and ¹⁸O/¹⁶O, respectively. The values were calibrated using IAEA-N3 ($\delta^{15}\text{N}_{\text{NO}_3} = +4.7\text{‰}$ and $\delta^{18}\text{O}_{\text{NO}_3} = +25.6\text{‰}$) and USGS-34 ($\delta^{15}\text{N}_{\text{NO}_3} = -1.8\text{‰}$ and $\delta^{18}\text{O}_{\text{NO}_3} = -27.9\text{‰}$; Böhlke *et al.*, 2003). A further internal potassium nitrate standard was measured twice within each run for quality assurance. Isotope values were corrected using the “bracketing scheme” from Sigman *et al.* (2009a) for $\delta^{18}\text{O}_{\text{NO}_3}$ and the single point correction referred to IAEA-N3 for $\delta^{15}\text{N}_{\text{NO}_3}$. The standard deviation for IAEA-N3 was 0.2‰ for $\delta^{15}\text{N}_{\text{NO}_3}$ and 0.3‰ for $\delta^{18}\text{O}_{\text{NO}_3}$ which is within the same specification for $\delta^{15}\text{N}_{\text{NO}_3}$ and $\delta^{18}\text{O}_{\text{NO}_3}$ for at least duplicate measurements of the samples.

2.4. RESULTS

2.4.1. Nutrient and oxygen concentrations

The surface mixed layer of 10-50 m is saturated with oxygen (Fig. 2.3a and 2.3b). Suboxic conditions with oxygen concentrations <5 μM were generally encountered between 100 m and 1025 m water depth, except at nearshore stations #944 and # 947 (Fig. 2.3a; Supplement fs01). The most intense ODZ was found at station #957 (Fig. 2.3b). Station #950 had the thickest oxygenated surface layer due to the influence of a mesoscale eddy that also caused enhanced mixing of nutrients into surface waters.

Ratios of nitrate to phosphate decrease in the ODZ as a consequence of denitrification or anammox. Usually, the amount of nitrate removed by denitrification in the ODZ is calculated by using an empirical relationship of nitrate to phosphate molar concentrations of 16:1 in ocean waters (Redfield, 1934). More specific, however, are regional N:P ratios. In the Arabian Sea, the nitrate deficits are best calculated from a stoichiometric relationship established from Arabian Sea JGOFS data (Codispoti *et al.*, 2001):

$$\text{NO}_{3\text{def}} = (4.89 * ([\text{PO}_4^{3-}] - 0.28) - ([\text{NO}_3^-] + [\text{NO}_2^-] + [\text{NH}_4^+])) * 0.86 \quad (6)$$

Ammonium contents are below the detection limit of 20 nM in the ODZ (Lam *et al.*, 2011) and were thus not included in the calculation. The $\text{NO}_{3\text{def}}$ is most pronounced in the core of the ODZ between 125 m and 400 m with considerable variations among the stations (Fig. 2.3b; Table 2.1) and vanishes at 1200 m water depth.

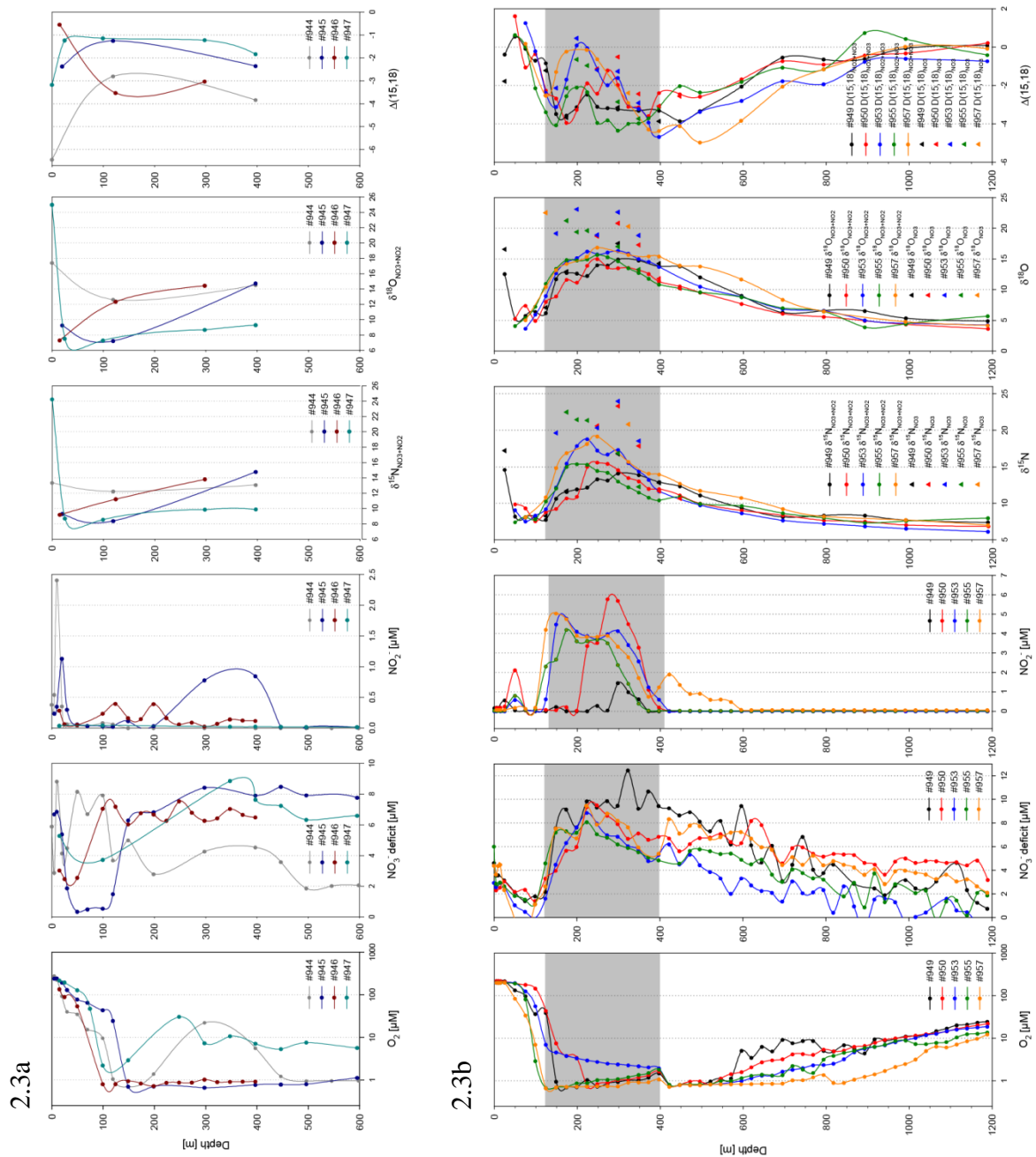


Fig. 2.3: Depth profiles of oxygen, nitrate deficit, nitrite, $\delta^{15}\text{N}$ [‰], $\delta^{18}\text{O}$ [‰], and $\Delta(15,18)$ at the near shore locations #944-#947 (2.3a), and the offshore locations #949, #950, #953, #955 and #957 (2.3b).

Station No.	Depth range of oxygen minimum and nitrate deficiency				Total from 100-1100m water depth		
	O ₂ <4.5 µM	O ₂ <1 µM	NO ₂ >0.5 µM	NO _{3def} >5 µM	NO ₂ Mol m ⁻²	NO ₃ Mol m ⁻²	NO _{3def} Mol m ⁻²
M 74-1 949	150-625m	150-425m	300-350m	150-625m	0.09	34.2	6.4
M 74-1 950	175-775m	225-525m	225-375m	175-875m	0.70	34.6	6.4
M 74-1 953	175-850m	425-600m	125-400m	150-475m	0.94	34.0	3.4
M 74-1 955	100-850m	125-575m	125-325m	125-600m	0.71	35.5	4.4
M 74-1 957	125-1025m	125-700m	125-575m	125-775m	1.13	34.3	5.6

Table 2.1: Depth ranges of oxygen concentrations <4.5 µM, <1 µM, nitrite concentrations >0.5 µM, and a nitrate deficit (NO_{3def}) >5 µM. Nitrite and nitrate concentrations, nitrogen deficit (NO_{3def}) are given in Mol m⁻²

Primary nitrite maxima (PNM) occur within the nutricline (at about 10 m at the near coastal stations and at 50 m at the offshore stations) under oxic conditions (Fig. 2.3a, 2.3b; Supplement fs01). In a global review on PNM occurrences, Lomas and Lipschultz (2006) concluded that PNM most likely originate from the release of nitrite by phytoplankton due to incomplete assimilation of nitrate under conditions of light limitation. A minor amount of nitrite in the PNM may also be an intermediate product of dissimilatory nitrification (Lomas and Lipschultz, 2006). In accordance with a general link to phytoplankton biomass, the most pronounced PNM of our study occur at those stations where plankton counts suggest the highest primary productivity (Kate Darling, personal communication). These were the near shore stations #944 and #945, both influenced by active late SW monsoon upwelling, and the offshore station #950, where a mesoscale eddy mixed nutrients into the euphotic zone (Fig. 2.3a, 2.3b).

SNM that always coincide with nitrate concentration minima were recognised at all five offshore stations. Nitrite concentrations vary between 1.5 µM (#949) and 5.8 µM (#950) in the core of the denitrification zone (Fig. 2.3a, 2.3b). The other three offshore stations had a broad nitrite layer with maximum concentrations >4 µM at the top and bottom. The SNM occurred only at two of the near coastal stations (#945 and #946) and had nitrite concentrations <1.0 µM (Fig. 2.3a)

2.4.2 δ¹⁵N ratios and δ¹⁸O ratios of nitrate and nitrite

Nitrate and nitrite are both reduced to N₂O when analysing stable N and O isotopes by the denitrifier method so that results represent the stable isotopic N and O ratios of total nitrate plus nitrite (subsequently named δ¹⁵N_{NO₃+NO₂} and δ¹⁸O_{NO₃+NO₂}). Due to different fractionation processes within the nitrogen cycle, nitrate and nitrite can have significantly different stable isotopic ratios (Casciotti, 2009; Casciotti and McIlvin, 2007). To get an

estimate of these differences, $\delta^{15}\text{N}_{\text{NO}_3}$ and $\delta^{18}\text{O}_{\text{NO}_3}$ (after treatment with ascorbate) were determined in two to five samples at each of the five offshore stations.

Maximum $\delta^{15}\text{N}_{\text{NO}_3+\text{NO}_2}$ and $\delta^{18}\text{O}_{\text{NO}_3+\text{NO}_2}$ generally correspond to the core depth of nitrite accumulation at 200-300 m water depth (Fig. 2.3b; Supplement fs01). Highest values at depths of the nitrite maximum for both $\delta^{15}\text{N}_{\text{NO}_3+\text{NO}_2}$ and $\delta^{18}\text{O}_{\text{NO}_3+\text{NO}_2}$ were found at stations #953 and #957 (19.2‰ for $\delta^{15}\text{N}_{\text{NO}_3+\text{NO}_2}$ and 16.5‰ for $\delta^{18}\text{O}_{\text{NO}_3+\text{NO}_2}$, respectively) whereas lowest values (14.1‰ and 15.0‰ for $\delta^{15}\text{N}_{\text{NO}_3+\text{NO}_2}$ and $\delta^{18}\text{O}_{\text{NO}_3+\text{NO}_2}$, respectively) occur in the western Arabian Sea at station #949.

Nitrate concentrations $<2 \mu\text{M}$ prevented accurate measurements of nitrate isotope composition in most mixed layer samples. In the subsurface layer between the ODZ and the mixed layer, we determined $\delta^{15}\text{N}_{\text{NO}_3+\text{NO}_2}$ values between 7.4 and 8.1‰ (Fig. 2.3b). Minimum $\delta^{18}\text{O}_{\text{NO}_3+\text{NO}_2}$ values of this subsurface layer range between 3.9 and 5.3‰. $\delta^{15}\text{N}_{\text{NO}_3+\text{NO}_2}$ and $\delta^{18}\text{O}_{\text{NO}_3+\text{NO}_2}$ sharply decrease above and below their maxima in the nitrite accumulation zone (Fig. 2.3b).

$\delta^{15}\text{N}_{\text{NO}_3}$ and $\delta^{18}\text{O}_{\text{NO}_3}$ are generally low in deepest samples below the ODZ (6.1 to 8.0‰ and 3.6 to 5.7‰, respectively) with average $\delta^{15}\text{N}_{\text{NO}_3}$ of 7.2 ± 0.6 ‰ and $\delta^{18}\text{O}_{\text{NO}_3}$ of 4.6 ± 0.6 ‰, respectively (nitrite was not present below 650 m water depth). We use these values as source nitrate stable isotope ratios in the ODZ (ICW) rather than the lower values from other deep oceanic areas, as intermediate water masses entering the Arabian Sea have a preformed nitrate deficit (Mantoura *et al.*, 1993) so that nitrate isotopic values may already be elevated.

Differences between $\delta^{15}\text{N}_{\text{NO}_3}$ and $\delta^{18}\text{O}_{\text{NO}_3}$ compared with $\delta^{15}\text{N}_{\text{NO}_3+\text{NO}_2}$ and $\delta^{18}\text{O}_{\text{NO}_3+\text{NO}_2}$ in samples with trace amounts of nitrite are within or very close to the error range of the $\delta^{15}\text{N}_{\text{NO}_3+\text{NO}_2}$ and $\delta^{18}\text{O}_{\text{NO}_3+\text{NO}_2}$ method. In samples with higher nitrite concentrations, $\delta^{15}\text{N}_{\text{NO}_3}$ and $\delta^{18}\text{O}_{\text{NO}_3}$ are higher by 4-9‰ compared to the $\delta^{15}\text{N}_{\text{NO}_3+\text{NO}_2}$ and $\delta^{18}\text{O}_{\text{NO}_3+\text{NO}_2}$ (Table 2.2). Maximum $\delta^{15}\text{N}_{\text{NO}_3}$ and $\delta^{18}\text{O}_{\text{NO}_3}$ values occur in the SNM corresponding to the most pronounced NO_3 deficit.

Sample	Depth	$\delta^{15}\text{N}_{\text{NO}_3+\text{NO}_2}$	$\delta^{18}\text{O}_{\text{NO}_3+\text{NO}_2}$	$\delta^{15}\text{N}_{\text{NO}_3}$	$\delta^{18}\text{O}_{\text{NO}_3}$	$\delta^{15}\text{N}_{\text{NO}_2}$	$\delta^{18}\text{O}_{\text{NO}_2}$	NO_2 (μM)	$\Delta\delta^{15}\text{N}$	$\Delta\delta^{18}\text{O}$	$\Delta(15,18)$
949	25	14.59	12.56	17.21	16.59			0.56			-0.38
	125	7.75	6.20	8.26	7.08			0			-0.84
	175	11.56	12.73	11.69	12.95			0			-3.57
	300	14.11	14.95	16.77	17.52	-23.90	-21.68	1.45	40.67	39.20	-3.24
	400	12.91	13.82	12.80	14.27			0			-3.31
950	250	15.59	15.01	20.59	18.72	-10.87	-4.63	3.52	31.46	23.34	-2.42
	300	14.55	13.52	23.31	20.82	-14.69	-10.86	5.68	38.00	31.68	-1.97
	350	13.02	13.17	17.86	17.30	-21.62	-16.45	3.28	39.48	33.75	-3.14
	400	11.96	11.34	11.71	11.78			0.19			-2.39
953	450	11.10	10.55	10.67	10.22			0.01			-2.45
	150	12.18	12.70	19.36	19.16	-19.72	-14.97	4.47	39.08	34.13	-3.12
	200	17.86	15.17	26.16	23.11	-15.14	-16.37	4.11	41.30	39.48	0.09
	248	17.25	15.77	20.33	18.92	2.35	0.56	3.71	17.98	20.05	-1.13
	298	17.32	16.33	23.98	22.64	-14.44	-13.81	4.13	38.42	24.24	-1.60
955	350	14.38	14.99	18.54	18.85	-23.11	-19.85	2.56	41.65	38.70	-3.21
	175	14.99	14.84	22.48	21.25	-16.17	-11.80	4.19	38.65	33.05	-2.55
	200	15.36	14.76	21.47	19.40	-15.93	-9.02	3.60	37.40	28.42	-2.10
	225	15.29	14.94	21.18	19.62	-16.85	-9.88	3.61	38.03	29.50	-2.35
957	300	12.99	14.64	16.92	17.03	-26.18	-9.42	2.38	43.10	26.45	-4.35
	350	11.48	12.74	12.26	13.29			0.39			-3.97
	325	15.68	15.69	20.83	20.32	-22.12	-18.33	2.78	42.95	38.65	-2.90
	375	14.06	15.45	17.40	18.08			0.74			-4.29
Σ		15.04	14.75	20.7	19.62	-17.03	-12.61		37.73	31.47	
stdev		1.69	1.65	4.2	3.53	7.09	5.67		6.58	6.23	

Table 2.2: Measured $\delta^{15}\text{N}_{\text{NO}_3+\text{NO}_2}$ and $\delta^{18}\text{O}_{\text{NO}_3+\text{NO}_2}$, $\delta^{15}\text{N}_{\text{NO}_3}$ and $\delta^{18}\text{O}_{\text{NO}_3}$, and calculated $\delta^{15}\text{N}_{\text{NO}_2}$ and $\delta^{18}\text{O}_{\text{NO}_2}$ in ‰, nitrite concentrations in μM . $\Delta\delta^{15}\text{N}$ and $\Delta\delta^{18}\text{O}$ are the differences between stable isotopic values of nitrate and nitrite. $\Delta(15,18)$ is the difference between $\delta^{15}\text{N}_{\text{NO}_3+\text{NO}_2}$ and $\delta^{18}\text{O}_{\text{NO}_3+\text{NO}_2}$ corrected for the offset between both stable isotopic ratios at 1000-1200 m water depth. $\delta^{15}\text{N}_{\text{NO}_3+\text{NO}_2}$, $\delta^{18}\text{O}_{\text{NO}_3+\text{NO}_2}$, $\delta^{15}\text{N}_{\text{NO}_3}$ and $\delta^{18}\text{O}_{\text{NO}_3}$ are shown in italics when $\delta^{15}\text{N}_{\text{NO}_2}$ and $\delta^{18}\text{O}_{\text{NO}_2}$ are not calculated in samples with nitrite $< 1 \mu\text{M}$. Numbers in italics were not included in the average values (Σ) and standard deviations (Stdev).

$\delta^{15}\text{N}$ and $\delta^{18}\text{O}$ values of nitrite ($\delta^{15}\text{N}_{\text{NO}_2}$ and $\delta^{18}\text{O}_{\text{NO}_2}$) may be calculated for samples with nitrite concentrations $> 1 \mu\text{M}$ according to equations 4 and 5:

$$\delta^{15}\text{N}_{\text{NO}_2} = (([\text{NO}_3^-] + [\text{NO}_2^-]) * \delta^{15}\text{N}_{\text{NO}_3+\text{NO}_2}) - ([\text{NO}_3^-] * \delta^{15}\text{N}_{\text{NO}_3}) / \text{NO}_2^- \quad (7)$$

and

$$\delta^{18}\text{O}_{\text{NO}_2} = (([\text{NO}_3^-] + [\text{NO}_2^-]) * \delta^{18}\text{O}_{\text{NO}_3+\text{NO}_2}) - ([\text{NO}_3^-] * \delta^{18}\text{O}_{\text{NO}_3}) / \text{NO}_2^- \quad (8).$$

With one exception, calculated $\delta^{15}\text{N}_{\text{NO}_2}$ and $\delta^{18}\text{O}_{\text{NO}_2}$ are negative and range from -11 to -26‰ and from -5 to -22‰, respectively (Table 2.2). Samples with nitrite concentrations $< 1 \mu\text{M}$ were excluded from nitrite isotope calculations because in these cases the propagating error becomes much larger than 10‰.

Nitrite can exchange up to 50% of its oxygen with ambient water in stored samples depending on pH, temperature and storage time. This exchange can lead to a strong enrichment of $\delta^{18}\text{O}_{\text{NO}_2}$ as oxygen in water has a $\delta^{18}\text{O}_{\text{H}_2\text{O}} \sim 0\text{‰}$ and the isotopic effect of this equilibration is $\sim 11\text{--}14\text{‰}$ (Casciotti *et al.*, 2007). We thus have to take into account that $\delta^{18}\text{O}_{\text{NO}_3+\text{NO}_2}$ was enriched prior to analyses so that calculated $\delta^{18}\text{O}_{\text{NO}_2}$ are too high and any decoupling between $\delta^{15}\text{N}_{\text{NO}_3+\text{NO}_2}$ and $\delta^{18}\text{O}_{\text{NO}_3+\text{NO}_2}$ is partly due to this exchange.

2.5. DISCUSSION

2.5.1 Nitrite accumulation and nitrate deficit

In essence, the entire depth interval below 100 m and extending to our deepest sample at 1200 m potentially was a sink for nitrate, nitrite, and ammonium. Based solely on oxygen concentrations, heterotrophic denitrification may occur in the interval from 100-175 m down to 625-1025 m (Table 2.1). Anammox could occur roughly from 100 m down to 1200 m at our study sites as oxygen concentrations in that interval are below the anammox threshold of $O_2 \sim 10 \mu\text{M}$ (Jensen *et al.*, 2008) and seems to be limited mainly by the availability of ammonium.

A plot of phosphate concentrations versus nitrate concentrations (Fig. 2.4) shows that our samples have excess phosphate compared to the global average (Gruber and Sarmiento, 1997) and that most samples are nitrate deficient compared with the regional Redfield ratio adjusted for the preformed nitrate deficit of the Arabian Sea (Codispoti *et al.*, 2001). The nitrate deficit of virtually all samples illustrates that denitrification has depleted nitrate relative to phosphate in the entire water column down to our deepest samples at 1200 m.

There are local deviations in the extent of the ODZ and of the nitrate deficient depth interval: Oxygen supply by the PGW entrained into the ODZ water depth interval is very likely responsible for the elevated oxygen concentrations of $>10 \mu\text{M}$ and the suppression of denitrification between 200 m and 350 m water depth at stations #944 and #947 (Fig. 2.3a). O_2 concentrations are between 30.5 and 0.7 μM in the PGW (Morrison *et al.*, 1999) and a branch of this water mass has been observed to flow along the coast of Oman and to spread eastward into the central basin (Morrison, 1997; Prasad *et al.*, 2001). Furthermore, the $\text{NO}_{3\text{def}}$ is greater at the western and northwestern stations (#949, #950, #957) than in the eastern part of the Arabian Sea (stations #953 and #955) (Table 2.1). The main reason for this difference is the larger nitrate deficit in the water masses below 300 m of the western stations, which is probably preformed (Mantoura *et al.*, 1993). Only a small amount of nitrite builds up at station #949, whereas it comprises more than 20% of the $\text{NO}_{3\text{def}}$ at station #957 (Table 2.1). Low nitrite concentrations have previously been reported from the western Arabian Sea, although oxygen concentrations are below the threshold for denitrification (Mantoura *et al.*, 1993). The virtual absence of nitrite in the western region (in which #949 is situated) may be due to either complete denitrification, which would then increase the $\text{NO}_{3\text{def}}$, or to nitrification/re-oxidation to nitrate, or else to continuous consumption of nitrite by anammox.

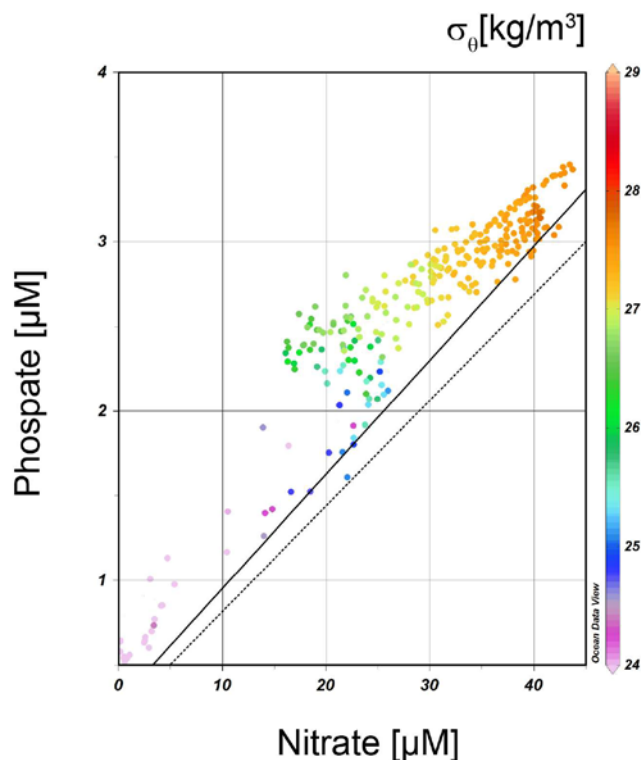


Fig. 2.4: Correlation of nitrate vs. phosphate concentrations. All samples plot above the mean oceanic ratio of $[\text{NO}_3^-] = 16 [\text{PO}_4^{3-}] + 2.9$ (dashed line; *Gruber and Sarmiento*, 1997) and most samples above the ratio of $[\text{NO}_3^-] = 14.89 ([\text{PO}_4^{3-}] - 0.28) * 0.86$ typical for the Arabian Sea (solid line; *Codispoti et al.*, 2001). Colour coding of dots indicates the potential density σ_θ [kg m^{-3}]. Strongest nitrate deficiencies are observed in PGW, ICW and part of the RSW.

2.5.2. Isotopic evidence for heterotrophic denitrification and parallel nitrite oxidation

Denitrification is indicated by nitrite accumulation and by maxima of the two stable nitrate isotope ratios between 150 m and 400 m water depth. Mid-water denitrification is a process acting on the $^{18}\text{O}/^{16}\text{O}$ and $^{15}\text{N}/^{14}\text{N}$ mixtures in source nitrate with similar fractionation factors $^{15}\epsilon$ and $^{18}\epsilon$ which are between 20 and 30‰ (*Altabet et al.*, 1999a; *Barford et al.*, 1999; *Granger et al.*, 2008; *Sigman et al.*, 2009b; *Voss et al.*, 2001). The “Rayleigh” fractionation model is often used to calculate apparent fractionation factors from $\delta^{15}\text{N}_{\text{NO}_3}$ values (*Altabet et al.*, 1999a; *Brandes et al.*, 1998). This model assumes that the nitrate pool is advected into the ODZ and is not replenishment via isopycnal mixing. The fractionation factors obtained by the Rayleigh model are generally lower than by models taking diffusive replenishment of nutrients into account (*Brandes et al.*, 1998). Highest isotopic effects are obtained by the so called “open system model” (Supplements text01, ts02, fs02). When using the Rayleigh

fractionation (described in Mariotti *et al.* (1988)) the stable isotope value of the substrate increases according to:

$$\delta^{15}\text{N}_{\text{substrate}} = \delta^{15}\text{N}_{\text{initial.substrate}} - {}^{15}\epsilon \{ \ln(f) \} \quad (9),$$

with $\delta^{15}\text{N}_{\text{initial}}$ being the stable isotope value of the initial product and f being the fraction of the original substrate remaining. The instantaneous product is calculated as:

$$\delta^{15}\text{N}_{\text{inst.product}} = \delta^{15}\text{N}_{\text{substrate}} - {}^{15}\epsilon \quad (10),$$

and the accumulated product is calculated as:

$$\delta^{15}\text{N}_{\text{acc.product}} = \delta^{15}\text{N}_{\text{initial.substrate}} + {}^{15}\epsilon \{ f/(1-f) \} \ln(f) \quad (11).$$

The same equations can be used for $\delta^{18}\text{O}_{\text{NO}_3}$ measurements, but they are not applied to $\delta^{18}\text{O}_{\text{NO}_3+\text{NO}_2}$ due to the sample storage artefact discussed above. Values for f are calculated according to:

$$f = ([\text{NO}_3] + [\text{NO}_2]) / ([\text{NO}_3] + [\text{NO}_{3\text{def}}]) \quad (12)$$

when using $\delta^{15}\text{N}_{\text{NO}_3+\text{NO}_2}$ and according to:

$$f = ([\text{NO}_3]) / ([\text{NO}_3] + [\text{NO}_{3\text{def}}]) \quad (13)$$

when using $\delta^{18}\text{O}_{\text{NO}_3}$ and $\delta^{15}\text{N}_{\text{NO}_3}$.

The ${}^{15}\epsilon$ and ${}^{18}\epsilon$ are obtained from the slope of $\ln(f)$ plotted against $\delta^{18}\text{O}_{\text{substrate}}$ or $\delta^{15}\text{N}_{\text{substrate}}$. The ϵ values obtained in our study are mostly higher than those found in incubation experiments (Barford *et al.*, 1999; Granger *et al.*, 2008; Table 3). Most differences between $\delta^{15}\text{N}_{\text{NO}_3}$ and calculated $\delta^{15}\text{N}_{\text{NO}_2}$ ($\Delta\delta^{15}\text{N}$; Table 2.2) are even higher than our calculated ${}^{15}\epsilon$ (Table 2.3). Moreover, the ${}^{15}\epsilon/{}^{18}\epsilon$ of 1.2 is higher than the expected value of 1 (Table 2.3). Nitrate and nitrite isotopic compositions in the ODZ are thus not consistent with a sole denitrification effect and imply fractionating reactions other than or additional to denitrification as well as reactions that decouple nitrogen and oxygen isotopic compositions in nitrate and nitrite. The only process known to date which could explain, both, the low nitrite N-isotope values and a decoupling of N and O isotopic fractionation in nitrate is nitrite oxidation. This process shows a rare inverse isotope fractionation, with initial products being isotopically enriched relative to their source signature, depleting the source nitrite of heavy isotope species. A decoupling of oxygen versus nitrogen isotope signatures can occur due to different isotope effects for N and O during nitrite oxidation and due to the incorporation of oxygen from external sources (Buchwald and Casciotti, 2010; Casciotti and McIlvin, 2007; Sigman *et al.*, 2005).

100- 1200m	Nitrate + Nitrite		
	¹⁵ ε	¹⁸ ε	¹⁵ ε/ ¹⁸ ε
949	17.9	-	-
950	31.1	-	-
953	34.8	-	-
955	29.3	-	-
957	26.7	-	-
949-957	25.6	-	-
		Nitrate	
949-957	34.5	28.8	1.2

Table 2.3: Fractionation factors ϵ by the Rayleigh fractionation model derived from the slope of a plot of $\ln(f)$ against $\delta^{15}\text{N}_{\text{NO}_3+\text{NO}_2}$, $\delta^{18}\text{O}_{\text{NO}_3}$ or $\delta^{15}\text{N}_{\text{NO}_3}$, respectively (see text for explanation of the Rayleigh model).

Plots of paired $\delta^{15}\text{N}_{\text{NO}_3+\text{NO}_2}$ and $\delta^{18}\text{O}_{\text{NO}_3+\text{NO}_2}$ values for depths ≥ 100 m, as well as $\delta^{15}\text{N}_{\text{NO}_3}$ and $\delta^{18}\text{O}_{\text{NO}_3}$ reveal a deviation from the expected 1:1 line at intermediate values (Fig. 2.5a and 2.5b).

A term to express this decoupling of nitrate N and O isotopes was defined by Sigman *et al.* (2005) as:

$$\Delta(15,18) = (\delta^{15}\text{N} - \delta^{15}\text{N}_{\text{deep}}) - {}^{15}\epsilon/{}^{18}\epsilon * (\delta^{18}\text{O} - \delta^{18}\text{O}_{\text{deep}}) \quad (14).$$

For the ratio ${}^{15}\epsilon/{}^{18}\epsilon$ the isotopic effects of denitrification with ${}^{15}\epsilon = {}^{18}\epsilon$ are inserted so that ${}^{15}\epsilon/{}^{18}\epsilon$ is about one and any deviation of the $\Delta(15,18)$ from 0 should reflect processes during which $\delta^{15}\text{N}$ and $\delta^{18}\text{O}$ ratios are affected differently. We used the average deep water nitrate stable isotope ratios from the individual stations, as we have no end member of source waters, and can assume that their stable isotope ratios are elevated above the oceanic average (see above). Most $\Delta(15,18)_{\text{NO}_2+\text{NO}_3}$ and $\Delta(15,18)_{\text{NO}_3}$ are negative in the interval from 100 m to 1000 m water depths, meaning that O isotope values are relatively more enriched than N isotope values. In the case of $\Delta(15,18)_{\text{NO}_2+\text{NO}_3}$ this is partly an artefact of oxygen exchange of nitrite with water during sample storage, which can lead to elevation of $\delta^{18}\text{O}_{\text{NO}_2}$ towards and above the isotope value of ambient water due to equilibrium fractionation (Casciotti *et al.*, 2007).

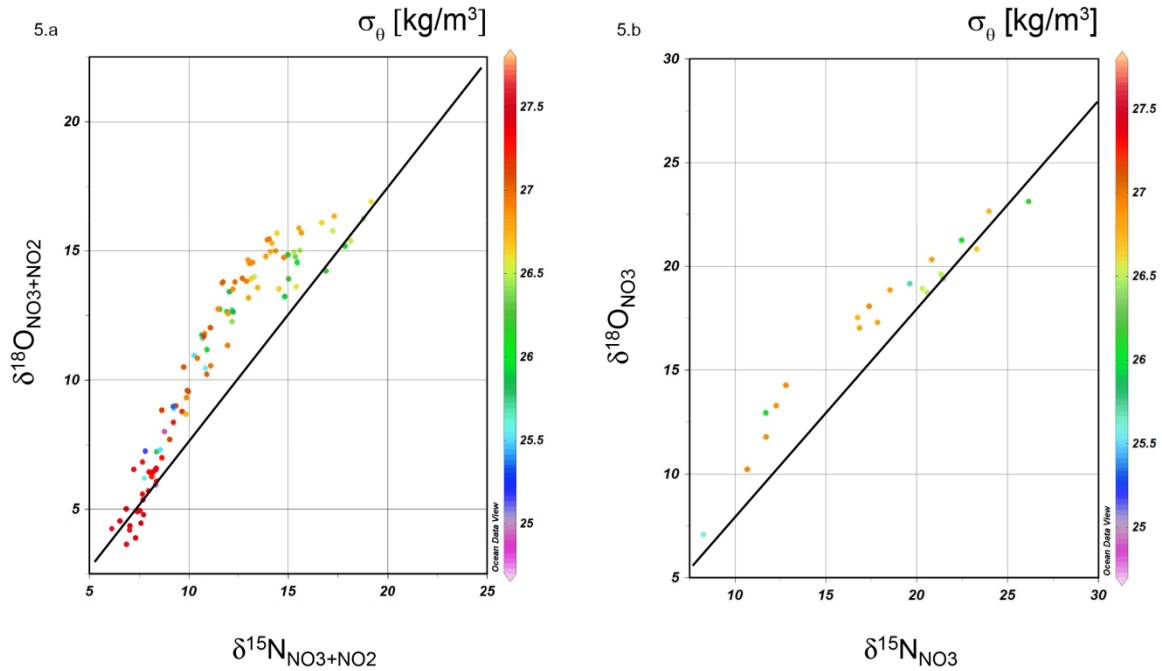


Fig. 2.5: $\delta^{15}\text{N}_{\text{NO}_3+\text{NO}_2}$ [%] plotted against $\delta^{18}\text{O}_{\text{NO}_3+\text{NO}_2}$ [%] (a) and $\delta^{15}\text{N}_{\text{NO}_3}$ [%] plotted against $\delta^{18}\text{O}_{\text{NO}_3}$ [%] (b). Colour coding of dots indicates the potential density σ_θ [kg m⁻³]. The 1:1 line corrected for the deep water offset between paired isotopes of 2 ‰ is indicated.

To attain negative $\Delta(15,18)_{\text{NO}_3}$, an external oxygen source is required. One important source of isotopically enriched oxygen is the exchange of oxygen between ¹⁸O-depleted nitrite and ambient water. This is an abiotic process depending on temperature, pH and the residence time of nitrite, and it leads to a convergence of $\delta^{18}\text{O}_{\text{NO}_2}$ with the $\delta^{18}\text{O}$ of water (Kool *et al.*, 2007; Snider *et al.*, 2010). Recent experiments indicate that oxygen equilibration with water can affect 25% of nitrite (Buchwald and Casciotti, 2010; Casciotti *et al.*, 2010). This relative enrichment of $\delta^{18}\text{O}_{\text{NO}_2}$ in relation to $\delta^{15}\text{N}_{\text{NO}_2}$ can be transferred into the nitrate pool if nitrite is reoxidised.

Differences in the negative kinetic effects on nitrogen and oxygen isotopes during nitrite oxidation, with N and O isotope effects of, respectively, $\sim -13\text{‰}$ and $\sim -7\text{‰}$ (Buchwald and Casciotti, 2010; Casciotti, 2009) would further deplete both nitrite isotopes and, additionally, increase $\delta^{18}\text{O}_{\text{NO}_2}$ relative to $\delta^{18}\text{N}_{\text{NO}_2}$.

In our setting, however, values for $\Delta(15,18)_{\text{NO}_3}$, where nitrite was removed by ascorbate treatment, are also negative and mostly close to $\Delta(15,18)_{\text{NO}_2+\text{NO}_3}$. We consequently surmise that, barring some uncertainty regarding the abiotic equilibration of nitrite oxygen with ambient water, the two isotopes are truly decoupled (Fig. 2.3b) owed to differences in biological processes. In the centre of the nitrite maximum the $\Delta(15,18)$ values are close to 0

suggesting that denitrification is the only significant process affecting $\Delta(15,18)$ and nitrification is virtually absent (Fig. 2.3b, Table 2.2).

The four stations with significant nitrite accumulation $>1 \mu\text{M}$ in the SNM (Fig. 2.3b) show minimum $\Delta(15,18)_{\text{NO}_3+\text{NO}_2}$ and $\Delta(15,18)_{\text{NO}_3}$ values at 150 m and 400 m water depth, i.e. above and below the zone with highest isotope values in the core of the denitrification maximum. We interpret this as a nitrification signal, which, as discussed above, differentially modifies nitrite oxygen and nitrogen isotopes, promoting a deviation of $\Delta(15,18)$ from zero. This observation agrees with the model of Anderson *et al.* (1982), who assumed that nitrification occurs adjacent to the zone of denitrification, i.e. between 300 m and 400 m water depth and above 150 m, producing nitrate that diffuses back into the denitrification zone and further fuels denitrification. The tight spatial coupling of nitrification and denitrification may be due to the presence of microenvironments with locally higher oxygen concentrations, or due to oxygen diffusion across the oxycline. The lower boundary of the denitrification zone coincides with a small but distinct oxygen peak at 400 m at all stations (Fig. 2.3b), which we attribute to lateral advection of a relatively more oxygenated water mass such as PGW. Furthermore, little oxygen is needed for nitrification to occur: direct measurements of nitrite oxidation rates from the ETSP and the Benguela upwelling system reveal significant nitrite oxidation at O_2 concentrations below $2.5 \mu\text{M}$ (Füssel *et al.*, 2011; Lipschultz *et al.*, 1990). Nitrite oxidation is independent of prior ammonia oxidation if nitrite is provided by nitrate reduction.

The production of low $\Delta(15,18)$ by nitrification under suboxic conditions helps to interpret the deviating nitrite concentration profiles at stations #949 and #950 (Fig. 2.3b). Nitrite concentration in the SNM at #949 is very low and the ODZ maximum values of $\delta^{15}\text{N}$ are significantly lower than at the other locations. But the $\text{NO}_{3\text{def}}$ is up to $11 \mu\text{M}$ (Supplement fs01), indicating that denitrification has been equally effective as at the other locations. The low nitrite concentrations and relatively depleted $\delta^{15}\text{N}_{\text{NO}_3}$ and $\delta^{18}\text{O}_{\text{NO}_3}$ between 150 m and 500 m water depth indicate that intense nitrification has indeed taken place as suggested by Lam *et al.* (2011), and that the complete oxidation of depleted nitrite has lowered the $\delta^{15}\text{N}_{\text{NO}_3}$ and $\delta^{18}\text{O}_{\text{NO}_3}$. This unusual pattern may be due to better ventilation of the western part of the basin by PGW or ICW (see above). At station #950, where a mesoscale eddy has eroded the thermocline and mixed oxygen down to 220 m, the layer affected by the eddy is nitrite free and has relatively low isotope values, but a pronounced $\Delta(15,18)$ minimum as a legacy of nitrification under initially suboxic conditions.

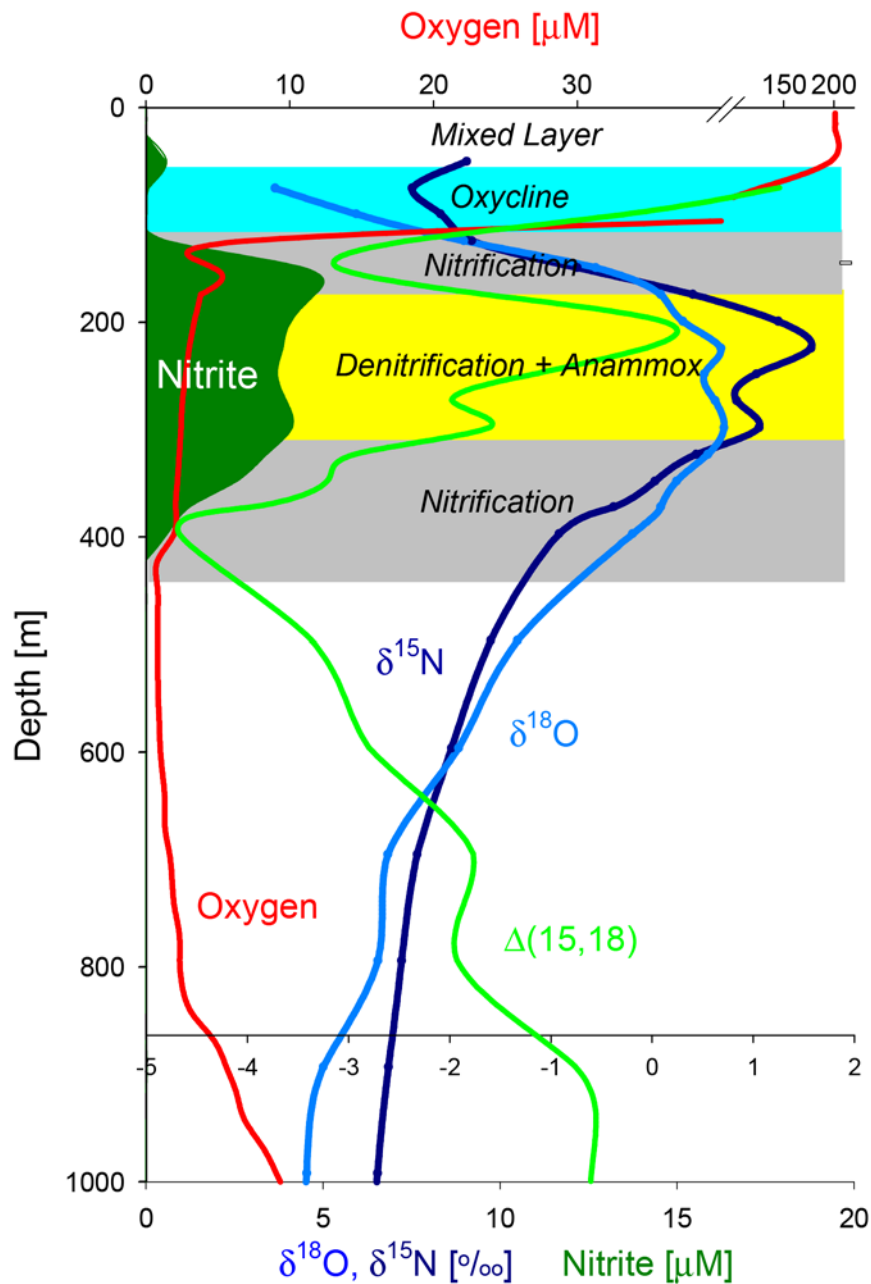


Fig. 2.6: Schematic picture of the processes in the water column using station # 953 as an example. The PNM is at the base of the mixed layer. The oxycline is the zone of sharply decreasing oxygen concentrations and of the upper $\delta^{15}\text{N}_{\text{NO}_3+\text{NO}_2}$ and $\delta^{18}\text{O}_{\text{NO}_3+\text{NO}_2}$ minimum. The zone dominated by denitrification is evident from nitrite accumulation, maxima of $\delta^{15}\text{N}_{\text{NO}_3+\text{NO}_2}$ and $\delta^{18}\text{O}_{\text{NO}_3+\text{NO}_2}$ as well as high $\Delta(15,18)$. Denitrification is coupled to anammox to remove the ammonia released during organic matter oxidation. Above and below this are zones dominated by nitrification indicated by minima of the $\Delta(15,18)$ which may co-occur with denitrification. The bimodal nitrite maxima may be a product of both nitrite accumulation during incomplete denitrification and nitrification. Removal of nitrite by anammox in the core of the denitrification zone could also explain the small nitrite minimum at 250 m.

Based on the concept that low $\Delta(15,18)$ thus mark zones of ongoing nitrification, Figure 2.6 is a schematic plot of variables and processes in the ODZ. Denitrification dominates in the zone between about 200 m and 300 m water depth, where nitrite accumulates and nitrate isotopic ratios attain maxima. This process may also be coupled to the anammox reaction, because ammonium produced by heterotrophic denitrification does not accumulate to any extent. Removal of nitrite by anammox explains the bimodal nitrite peak at locations #953-957, where we observe a relative concentration minimum in the core of nitrite accumulation and a slight isotopic enrichment of nitrate at about 250 m (Table 2.2). Nitrification is indicated by declining $\Delta(15,18)_{\text{NO}_3}$ and low $\delta^{15}\text{N}_{\text{NO}_2}$ values in the upper ODZ just below the oxycline and below the core of the denitrification zone. Nitrification probably also adds to the bimodal pattern of nitrite accumulation that has maxima on either side of the denitrification layer. Because nitrite is an intermediate of both nitrification and denitrification, it may accumulate where microenvironments and diffusion allow close coupling of the two processes. Whereas the oxygen concentrations show a steep increase above 100 m, they drop to almost 0 μM below the small oxygen peak at 400 m. We believe that nitrification occurs only in a small layer around 400 m where oxygen remains available. Mixing and diffusion lead to the linear increases of $\Delta(15,18)$ above and below the two nitrification layers.

2.5.3 Box model-derived mass balance and stable isotopic ratios in the ODZ

In order to obtain a rough estimate of the amounts of reactive nitrogen taking part in nitrate reduction, denitrification and nitrite oxidation, we produced a box model for the upper part of the ODZ (Fig. 2.7, Supplement text02). It encompasses the secondary nitrite maximum and ranges from a water depth of 125 m to 350 m. The areal extent of the secondary nitrate maximum is $1.95 \times 10^{12} \text{ m}^2$ (Naqvi, 1987,) so that the box volume becomes $4.38 \times 10^{14} \text{ m}^3$. The in- and outflow of water is calculated by dividing the volume of water by the mean residence time of water within the ODZ. As an estimate of the residence time of ODZ water, we used an estimate of 10 years (Olson *et al.*, 1993). Nitrate inputs are calculated by multiplying the total inflow with a nitrate concentration of 34 μM ; the $\delta^{15}\text{N}_{\text{NO}_3}$ is assumed to be 7‰. The second source of nitrogen is organically bound nitrogen exported from the euphotic zone. There are a variety of equations allowing a calculation of the organic carbon (OC) flux at all water depths if the primary production (Pp) is known. Based on satellite-derived data on primary production and results derived from sediment trap experiments such an equation was adapted

to the condition found in the Arabian Sea ($OC = 0.01 \text{ Pp}^2/\text{water-depth}^{0.628}$; Rixen *et al.*, 2002). The mean primary production in the Arabian Sea of $180 \text{ g C m}^2 \text{ yr}^{-1}$ is used to calculate the organic carbon flux at the top (125 m) and the bottom (350 m) of the modelled box. The difference between these fluxes is the amount of organic matter remineralised within the box. This number is converted into nitrogen by using the Redfield ratio. Two different remineralisation processes are considered (i) nitrification which is a chain of reactions in the course of which NH_4^+ is converted via NO_2^- (ammonia oxidation) to NO_3^- (nitrite oxidation) and (ii) heterotrophic denitrification which can be described by two reactions which are the NO_3^- reduction (eq. 12) followed by the NO_2^- reduction to N_2O and N_2 (eq. 13):

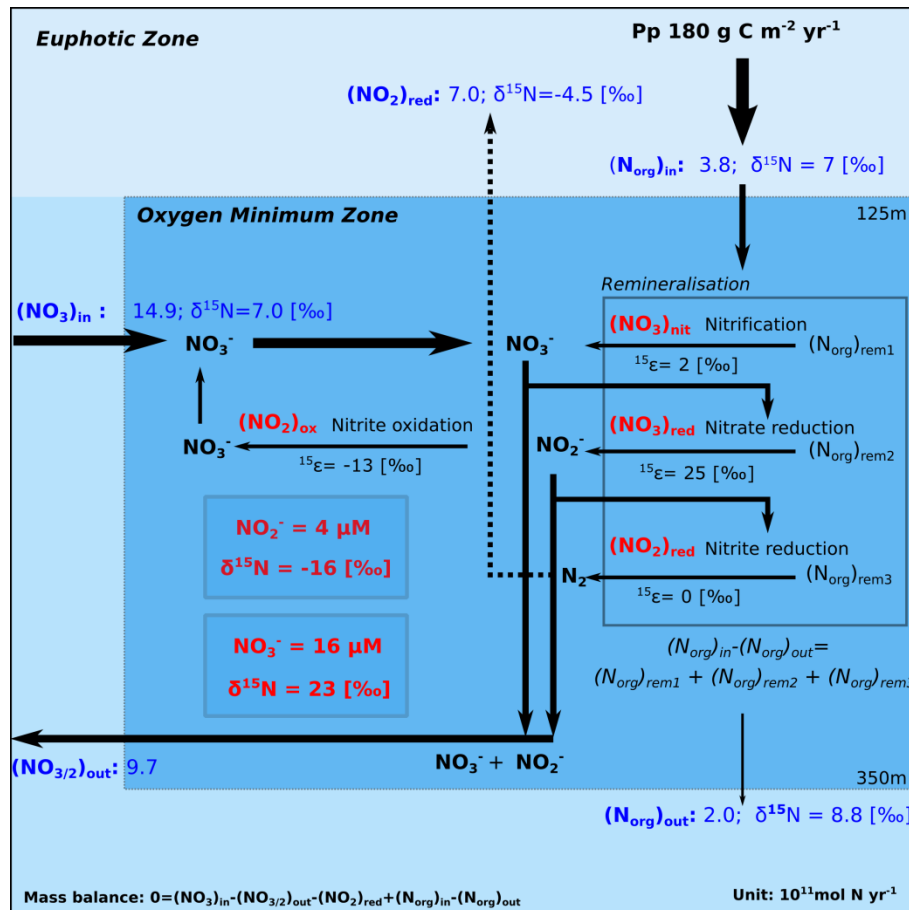
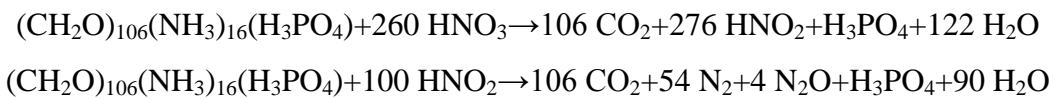


Fig. 2.7: Box model of N-cycling in the Arabian Sea ODZ (see further explanation in the text and in supplement text02). Unitless numbers are fluxes in 10^{11} moles N yr^{-1} . Nitrogen sources are advection of nitrate and sinking organically bound nitrogen. Nitrogen sinks are heterotrophic denitrification and lateral export of nitrate and nitrite (all in blue). Red colours indicate concentrations of nitrate and nitrite in the ODZ and their stable isotopic values and correspond with measurements at location #953.

The formation of N_2 as well as the outflow of reactive nitrogen, are the two sinks balancing the nitrogen inputs. The N_2O formation during denitrification is ignored because N_2O , in spite of being an important greenhouse gas, is quantitatively of low importance for the nitrogen budget in the ODZ.

All together 1000 model years were calculated to get the model into equilibrium whereby the conditions were changed in five steps after steady state was reached for the set conditions (Figure 8, Supplement text02). For the first 200 model years there was no remineralisation of organic nitrogen and the mean NO_3^- concentration attained a value of 31 μM , NO_2^- concentrations were 0 μM and $\delta^{15}N_{NO_3}$ was 7‰ as prescribed. In the second step after the model year 200 the entire organic nitrogen was decomposed and converted into NO_3^- via complete oxidation of organic nitrogen (complete nitrification). Accordingly, the NO_3^- concentration increased by approximately 4 μM and the $\delta^{15}N_{NO_3}$ was reduced slightly, as the lighter ^{14}N is preferentially decomposed. An isotopic fraction factor of $^{15}\epsilon = 2‰$ (Möbius, 2013) was used as the isotopic effect of ammonification. In a third step nitrification was reduced and the remaining organic nitrogen was remineralised by denitrification. Consequently the NO_3^- concentration decreased and the NO_2^- concentration increased. Assuming a fractionation factor of $^{15}\epsilon = 25‰$ for denitrification which is in the range of those determined experimentally and empirically (Altabet *et al.*, 1999a; Barford *et al.*, 1999; Granger *et al.*, 2008; Sigman *et al.*, 2009b; Voss *et al.*, 2001), the residual nitrate became heavier and reached values around 20‰ as measured in profile #953 (Table 2.2). Assuming furthermore that approximately 24% of the produced NO_2^- is not reduced to N_2 the accumulating NO_2^- attains concentrations of around 5 μM which also agrees quite well with measurements of profile #953. However, the resulting $\delta^{15}N_{NO_2}$ is -6‰ which is much higher than the measured $\delta^{15}N_{NO_2}$ of $\sim -16‰$. Assuming, in a fourth step that the entire available organic nitrogen was utilized by denitrification, the $\delta^{15}N_{NO_2}$ further increases. Considering in the fifth step that 60% of the produced NO_2^- is not reduced to N_2 and that 40% of the accumulated NO_2^- is reoxidized to NO_3^- with an isotopic effect of -13‰ (Buchwald and Casciotti, 2010; Casciotti, 2009), the resulting $\delta^{15}N_{NO_2}$ values are similar to the ones measured in profile #953. Thus, a reoxidation of 24% of initial nitrite appears to be the process explaining the low $\delta^{15}N_{NO_2}$ values in the upper part of the ODZ.

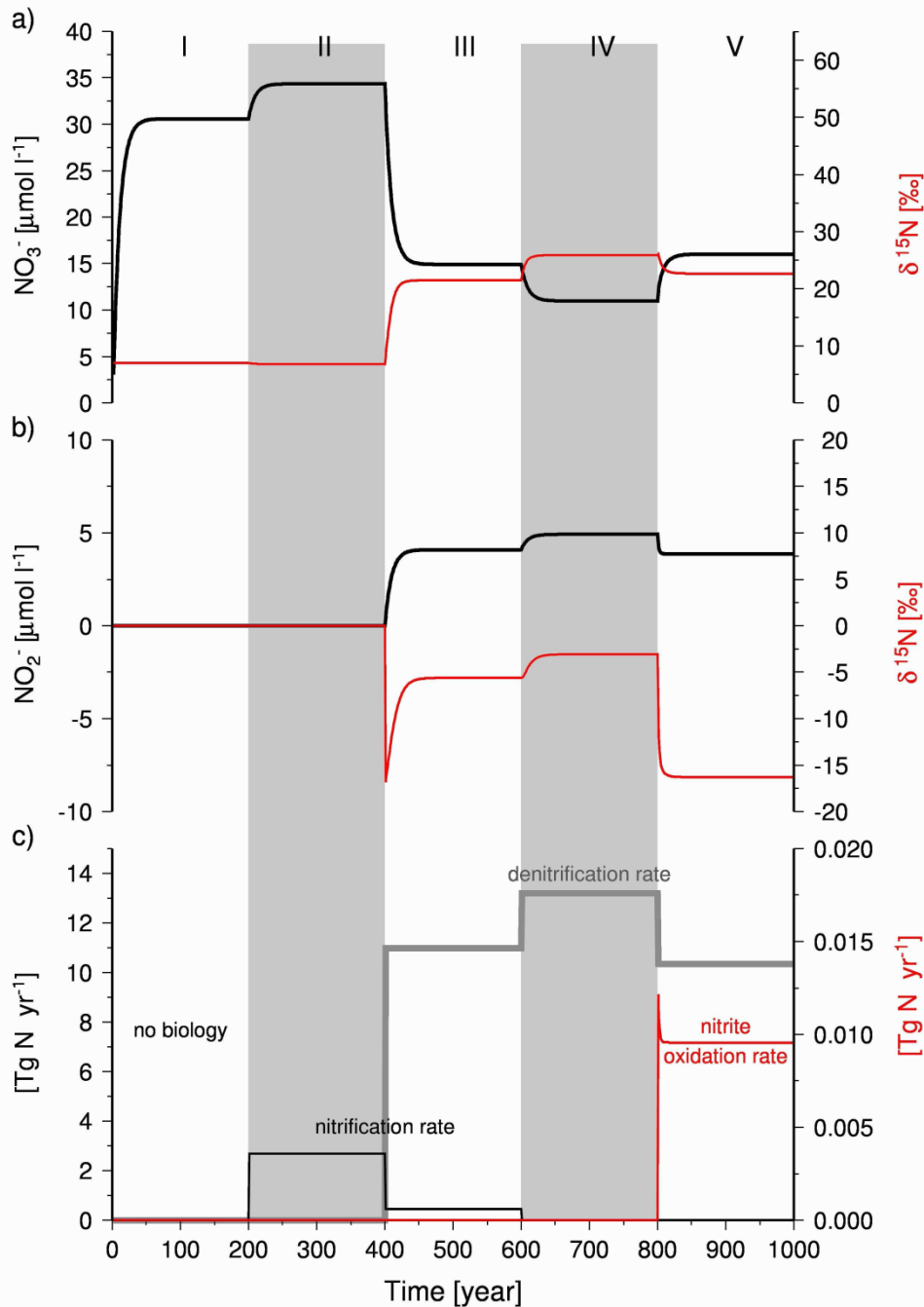


Fig. 2.8: Model run of 1000 years changing the conditions in 200 year steps:

I – accumulation of nitrate concentrations by advective inflow

II – nitrification of settling organic matter so that the remineralised organic nitrogen is added to the nitrate pool is reactive nitrogen

III – denitrification starts; part of the organic nitrogen is oxidised by nitrification and part of it is respired by denitrification; 24 % of the nitrite accumulating is not further denitrified to dinitrogen but accumulates in the water column

IV – the entire organic matter decomposition is carried out by heterotrophic denitrification; nitrite is allowed to accumulate as in step III

V – 40% of the nitrite produced during nitrate reduction is denitrified and released as dinitrogen gas and 40 % of the remaining nitrite is reoxidised to nitrate (i.e. 24 % of initially produced nitrite).

Concentrations of nitrate and nitrite (in μM) are shown in black; their respective stable isotopic ratios are shown in red. The assumed nitrification, denitrification and nitrite oxidation rates are shown in Tg N yr^{-1} .

2.5.4 Processes in the lower ODZ

There is no nitrite accumulation below 400 m at most stations except at #957, although oxygen concentrations are $<1 \mu\text{M}$ down to ~ 600 m (Fig. 2.3b; Table 2.1) and would thus promote both denitrification and anammox. Although observations suggest that denitrification occasionally and locally extends down to 600 m (Brand and Griffiths, 2008; Morrison *et al.*, 1999), we observe a gradual decrease of the $\text{NO}_{3\text{def}}$, $\delta^{15}\text{N}_{\text{NO}_3}$ and $\delta^{18}\text{O}_{\text{NO}_3}$ suggesting linear mixing of intermediate and deep water masses. The zone of iron reduction, indicated by maxima of dissolved Fe(II), is equivalent to the nitrite accumulation zone in the Arabian Sea (Moffett *et al.*, 2007). Manganese (Lewis and Luther, 2000) and iodate reduction (Farrenkopf and Luther, 2002) apparently extend to greater depths than denitrification, so that oxidation of organic matter in the lower ODZ is probably mediated by manganese and iodate reduction. Our oxygen measurements with a conventional electrode on a SEABIRD CTD are by a factor of 10 higher than oxygen concentrations simultaneously measured with the more sensitive STOX microsensor (Revsbech *et al.*, 2009) at some stations. Observed thresholds of denitrification or anammox in the oxygen profiles at our stations are thus likely too high. Denitrification is linked to very low oxygen concentrations and depends on sufficient supply of organic substrate. It is possible that denitrification ceases below approximately 400 m in the Arabian Sea, despite low but persistent oxygen concentrations. We attribute this to a limitation by organic substrate caused by rapidly sinking aggregates, reduced suspended matter concentrations, and lower quality of organic matter.

2.6 SUMMARY AND CONCLUSIONS

Oxygen, nutrients and paired stable isotope ratios of nitrate and nitrite as well as the major nitrogen transformation processes in the ODZ of the Arabian Sea were investigated during the late SW monsoon of 2007. The near coastal stations off Oman revealed little nitrite accumulation and sporadic ventilation of the upper ODZ by intrusion of oxygenated waters, probably from the Persian Gulf outflow. All five offshore stations have low oxygen

concentrations below 5 μM so that denitrification and anammox are feasible between 100 and 1200 m water depth. However, active denitrification is restricted to the upper ODZ indicated by the accumulation of nitrite and peaks of $^{15}\text{N}_{\text{NO}_3+\text{NO}_2}$ and $\delta^{18}\text{O}_{\text{NO}_3+\text{NO}_2}$. $\delta^{15}\text{N}_{\text{NO}_3}$ and $\delta^{18}\text{O}_{\text{NO}_3}$ measured in selected samples are elevated compared to $^{15}\text{N}_{\text{NO}_3+\text{NO}_2}$ and $\delta^{18}\text{O}_{\text{NO}_3+\text{NO}_2}$ so that calculated $\delta^{15}\text{N}_{\text{NO}_2}$ and $\delta^{18}\text{O}_{\text{NO}_2}$ are negative. As the apparent fractionation factors are higher than those commonly assumed for nitrate reduction and the difference between nitrate and nitrite stable isotopic values are much higher than feasible with nitrate reduction, additional transformation processes of reactive nitrogen are evidently significant in the ODZ of the Arabian Sea. The decoupling of the $\delta^{15}\text{N}_{\text{NO}_3}$ and $\delta^{18}\text{O}_{\text{NO}_3}$, furthermore, suggests that nitrification is an important process. The smaller inverse isotopic effect on oxygen compared to nitrogen during nitrite oxidation, as well as the exchange of oxygen between the strongly depleted oxygen in nitrite with the heavier oxygen of ambient water are responsible for the relative enrichment of oxygen isotopes compared to nitrogen isotopes. Negative $\Delta(15,18)$ values indicate two nitrification layers at 150 m and 400 m, i.e. at the upper and lower margin of the zone of denitrification. We propose that the core of the ODZ is dominated by denitrification, during which dinitrogen gas is released and nitrite is produced. Ammonium produced by organic matter remineralisation is most likely removed by anammox bacteria. Bimodal nitrite peaks result not only from nitrite removal, but also from coupled denitrification and nitrification at the upper and lower margins of the denitrification zone. Coupled nitrification and denitrification has been proposed by (Anderson *et al.*, 1982) with nitrate from nitrification fuelling denitrification by diffusion or mixing processes. With a simple box model the $\delta^{15}\text{N}_{\text{NO}_3}$ and $\delta^{15}\text{N}_{\text{NO}_2}$ found in the ODZ could be reproduced if 40% of the nitrite of nitrate reduction is further reduced to dinitrogen, 24% are reoxidising to nitrate and 36% accumulate as nitrite in the ODZ.

Below 400 m oxygen concentrations $<1 \mu\text{M}$ prevail, but denitrification occurs only scarcely in the Arabian Sea. The lower margin of the denitrification zone is probably determined by the paucity of organic substrate rather than by low oxygen concentrations. At the lower boundary of the ODZ other electron acceptors such as iron, manganese or iodate govern organic matter remineralisation.

ACKNOWLEDGEMENTS

We thank Udo Hübner for operating the CTD and water samplers as well as captain Uwe Pahl and crew of R/V Meteor (M 74-1b) for their excellent technical support. We used the programme *Ocean Data View* to make Figures 2, 4, 5 and the Figures in Supplement fs01 and thank Rainer Schlitzer for supplying this open access programme. We are grateful to Marcel M.M. Kuypers, Phillis Lam, and Marlene M. Jensen for discussions and kindly providing their ammonium data. Katharina Six and Francesca Guglielmo have helped us with many fruitful discussions and suggestions. Two anonymous reviewers have helped to improve the manuscript with their very constructive comments. Financial support for the Meteor cruise came from the Deutsche Forschungsgemeinschaft (DFG Grant No. GA 755/4-1).

SUPPLEMENT

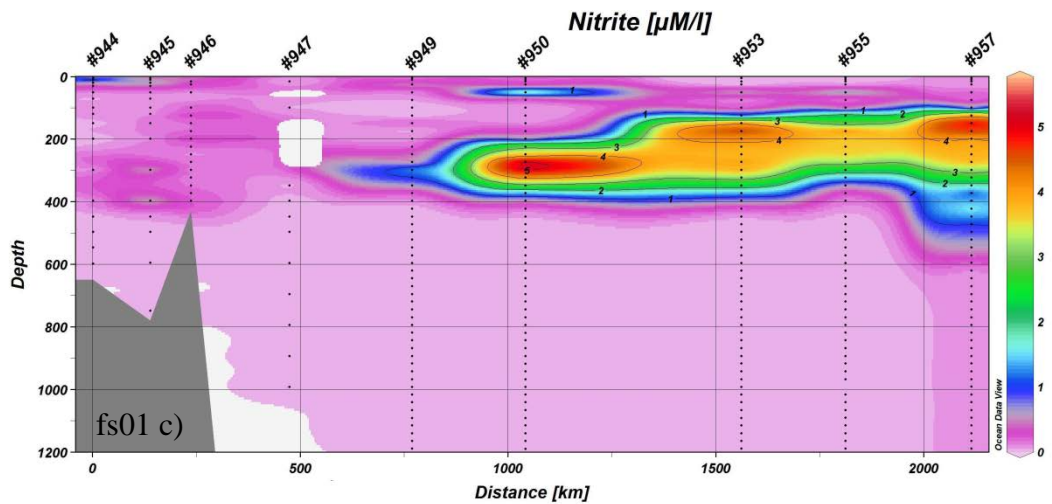
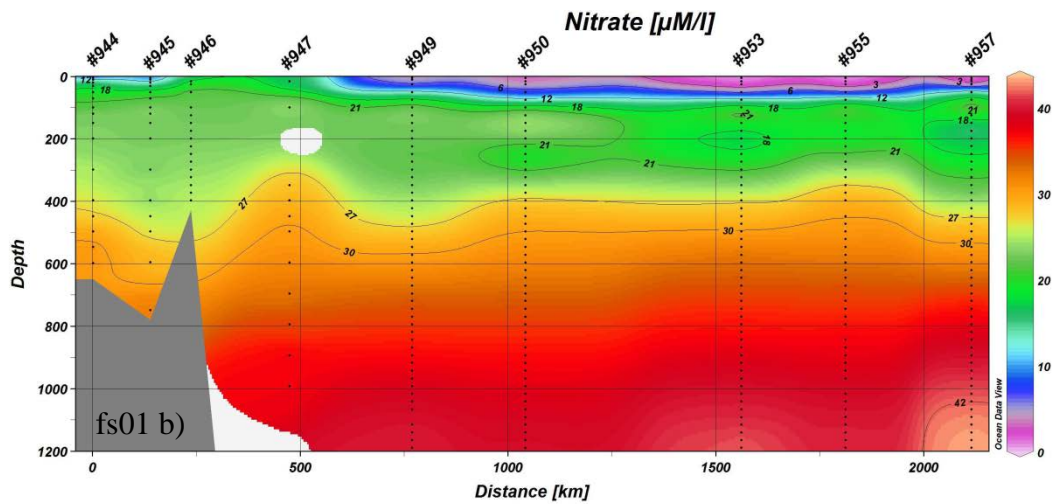
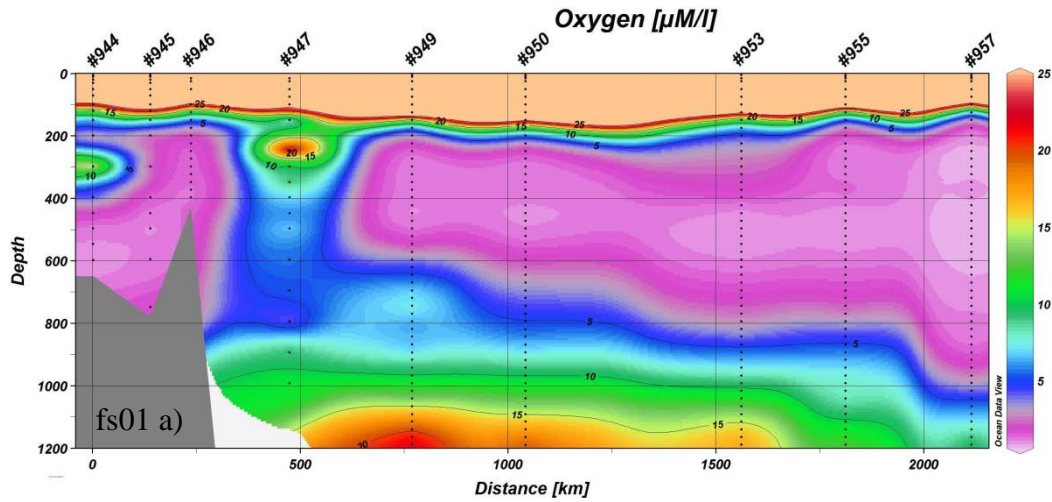
Supp ts01:

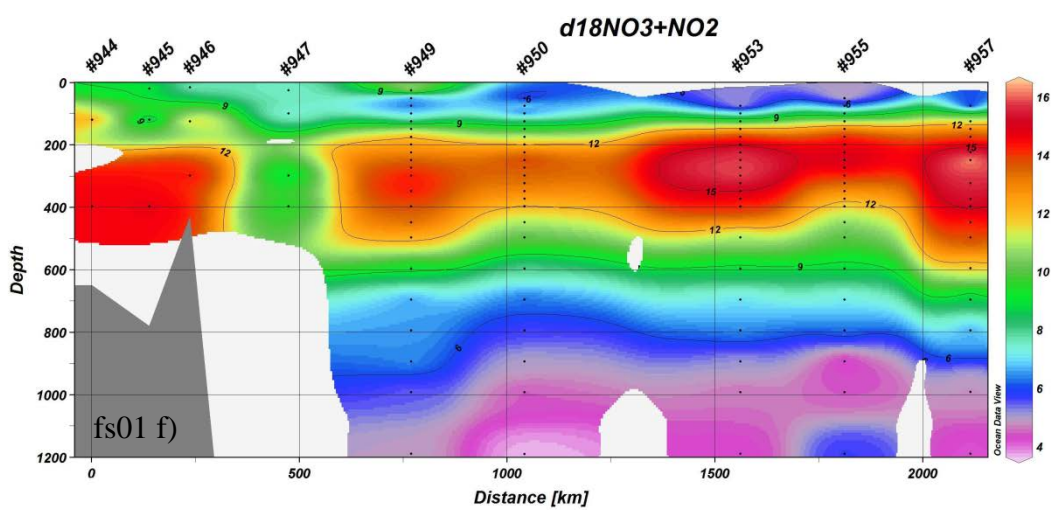
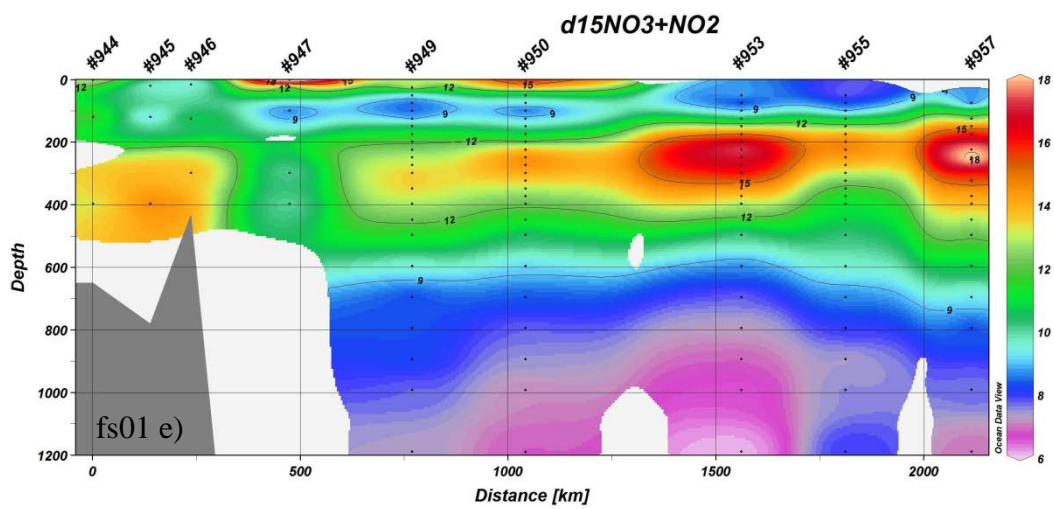
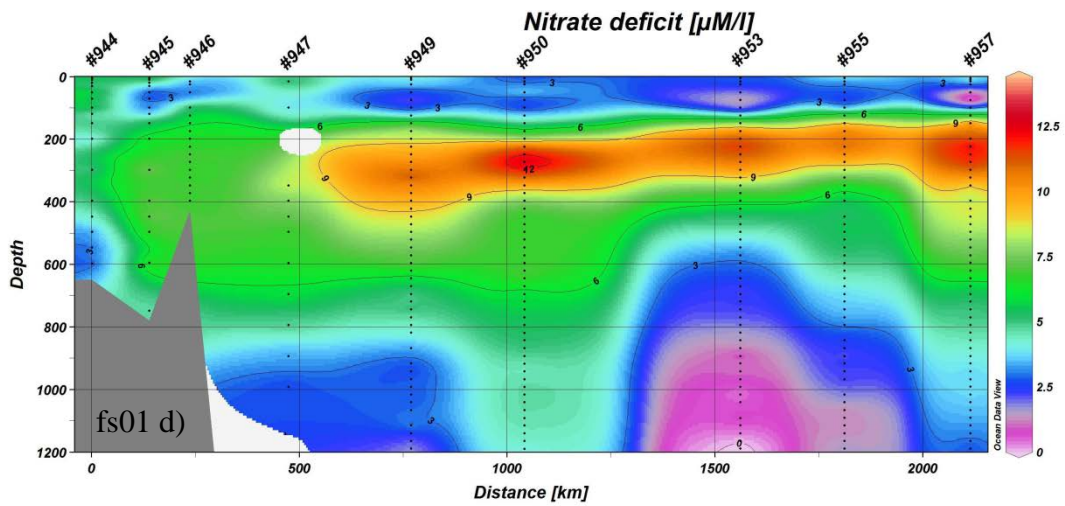
Sampling locations:

Station No.	Latitude	Longitude
944	21°55.96'N	59°48.15'E
945	20°43.73'N	59°23.89'E
946	20°06.11'N	58°44.37'E
947	18°00.00'N	59°00.00'E
949	16°26.00'N	61°15.00'E
950	15°15.00'N	63°30.00'E
953	17°00.00'N	68°00.00'E
955	19°06.00'N	67°06.00'E
957	20°34.00'N	64°40.00'E

Supp fs01:

Cross-sections of oxygen (a) nitrate (b), nitrite (c), nitrate deficit (d), $\delta^{15}\text{N}_{\text{NO}_3+\text{NO}_2}$ (e) and $\delta^{18}\text{O}_{\text{NO}_3+\text{NO}_2}$ (f) along the cruise track of Meteor 74/1. The horizontal distance is given in km from station 944. Units in Figs. a-e are μM and units in Figs. e and f are ‰.





Supp text01:

Fractionation factors ϵ obtained by the steady state (open system) model plotting 1-f against $\delta^{15}\text{N}_{\text{NO}_3+\text{NO}_2}$, $\delta^{18}\text{O}_{\text{NO}_3+\text{NO}_2}$ or $\delta^{15}\text{N}_{\text{NO}_3}$, respectively, are given in table supplement ts02 for comparison with the results of the Rayleigh model in Table 3 of the manuscript. The open system assumes that the substrate is replenished constantly (Sigman, et al., 2009a) so that:

$$\delta^{15}\text{N}_{\text{substrate}} = \delta^{15}\text{N}_{\text{initial.substrate}} - \epsilon(1-f) \quad (15)$$

with f being the proportion of the original fraction of the substrate remaining. The stable isotopic ratio is calculated according to:

$$\delta^{15}\text{N}_{\text{product}} = \delta^{15}\text{N}_{\text{initial.substrate}} - \epsilon(f) \quad (16).$$

Using the regressions obtained from the Rayleigh and, respectively, the steady state (open system) model, the stable isotopic values increase with ongoing denitrification along the curves shown in figure supplement Figure fs02. Clearly, the values from the ODZ of the Arabian Sea are in an f range in which both models produce very similar results.

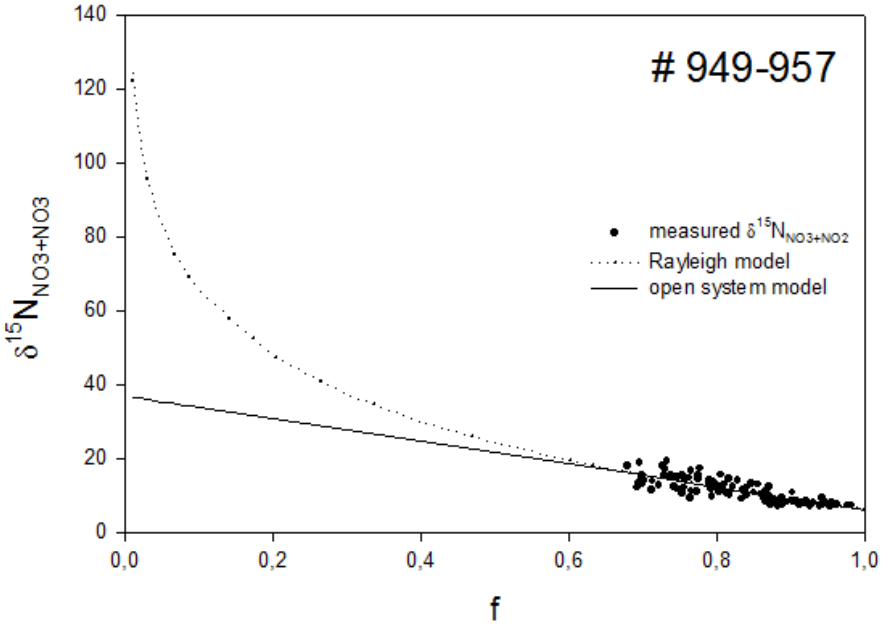
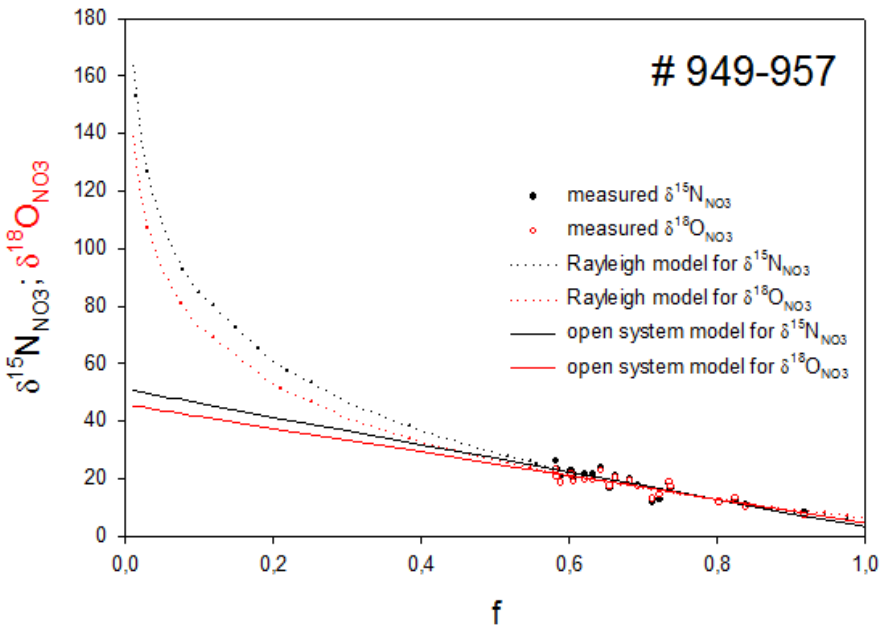
References

Sigman, D., K. L. Karsh, and K. L. Casciotti (2009), Ocean process tracers: Nitrogen isotopes in the ocean, in Encyclopedia of Ocean Sciences (update from 2001), edited by J. H. Steele, et al., pp. 4138-4153, Academic Press, London.

Supp ts02:

100-1200m Station No.	Nitrate+Nitrite		
	15e	18e	15e/18e
949 21.7	-	-	
950 40.8	-	-	
953 40.0	-	-	
955 32.9	-	-	
957 43.1	-	-	
949-957	30.7	-	-
		Nitrate	
949-957	47.8	40.6	1.2

Supp fs02:



Supp text02:

Model description:

$$d(\text{NO}_3)/dt = [(\text{NO}_3)_{\text{in}} - (\text{NO}_3)_{\text{out}} + (\text{NO}_3)_{\text{nit}} - (\text{NO}_3)_{\text{red}} + (\text{NO}_2)_{\text{ox}}]/\text{Volume} \quad (17)$$

$$d(\text{NO}_2)/dt = [(\text{NO}_3)_{\text{red}} - (\text{NO}_2)_{\text{ox}} - (\text{NO}_2)_{\text{red}} - (\text{NO}_2)_{\text{out}}]/\text{Volume} \quad (18)$$

both equations were solved for ^{15}N and ^{14}N .

Isotopic fraction was considered during nitrification ((NO_3)nit), nitrate reduction ((NO_3)red) and nitrite oxidations ((NO_2)ox) and is described below.

$(\text{NO}_3)_{\text{in}}/(\text{NO}_3)_{\text{out}}/(\text{NO}_2)_{\text{out}}$:

In order to test our assumption we produced a small model for the upper part of the OMZ (Fig. 7 in manuscript). The box encompasses the secondary nitrite maximum and ranges from a water-depth of 125 m to 350 m as seen in profile 953 (Fig. 2.3 in the manuscript). The spatial expansion of the secondary nitrate maximum accounts to $1.95 \cdot 10^{12} \text{ m}^2$ (Naqvi et al., 1987) suggesting a volume of $438.75 \cdot 10^{12} \text{ m}^3$. The in- and outflow of water was calculated by dividing the volume of water by the mean residence time of water within the OMZ. Although estimates of the residence times vary between 1 and 50 years, we used 10 years because it is widely believed to be the most appropriate estimate. Nitrate inputs were calculated by multiplying the inflow with a nitrate concentration of 34 mmol/m^3 .

The $\delta^{15}\text{N}$ of incoming nitrate ($\delta^{15}\text{NNO}_3$) was assumed to be 7 permill.

$$(\text{NO}_3)_{\text{in}} = (438.75 \cdot 10^{12} / 10) \cdot 0.034 = 1.49 [10^{12} \text{ mol/yr}] \quad (19)$$

$$(\text{NO}_3)_{\text{out}} = (438.75 \cdot 10^{12} / 10) \cdot (\text{NO}_3 \text{ concentration in the box}) [10^{12} \text{ mol/yr}] \quad (20)$$

$$(\text{NO}_2)_{\text{out}} = (438.75 \cdot 10^{12} / 10) \cdot (\text{NO}_2 \text{ concentration in the box}) [10^{12} \text{ mol/yr}] \quad (21)$$

$(\text{N}_{\text{org}})_{\text{in}}/(\text{N}_{\text{org}})_{\text{out}}/(\text{N}_{\text{org}})_{\text{rem}}$:

The second source of nitrogen is the import of organically bound nitrogen that was exported from the euphotic zone into the OMZ. There are a variety of equations that allow to calculate the organic carbon (OC) flux at all water depths if the primary production (Pp) is known. Based on satellite-derived data on primary production and results derived from sediment trap experiments such an equation was adapted to the condition found in the Arabian Sea (Rixen et al., 2002):

$$\text{OC} = 0.01 \text{Pp}^2 / \text{water-depth}^{0.628} \quad (22)$$

The mean primary production in the Arabian Sea of $180 \text{ gC m}^2 \text{ yr}^{-1}$ was used to calculate the organic carbon flux at the top (125 m) and the bottom (350 m) of the considered box. The

difference between these fluxes indicates the amount of organic matter that was remineralised within the box, which was converted into organic nitrogen by using the Redfield ratio.

$$(N_{\text{org}})_{\text{in}} = (0.01 \text{ Pp2/water-depth}^{10.628}) / (\text{atomic weight of carbon}) / (\text{Redfield C/N ratio})$$

$$[\text{mol N/yr}] \quad (23)$$

$$(N_{\text{org}})_{\text{out}} = (0.01 \text{ Pp2/water-depth}^{20.628}) / (\text{atomic weight of carbon}) / (\text{Redfield C/N ratio})$$

$$[\text{mol N/yr}] \quad (24)$$

$$(N_{\text{org}})_{\text{rem}} = (N_{\text{org}})_{\text{in}} - (N_{\text{org}})_{\text{out}} \quad (25)$$

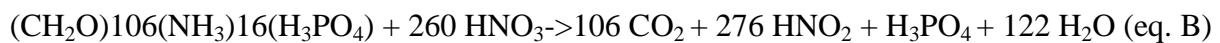
Three different remineralisation processes were considered: (a) nitrification in the course of which N_{org} is converted to nitrate (eq. A) and the heterotrophic denitrification which is a chain of reactions starting with nitrate reduction (eq. B) followed by the nitrite reduction to N_2 (eq. C).

Nitrification ($N_{\text{org}} \rightarrow \text{NO}_3$):

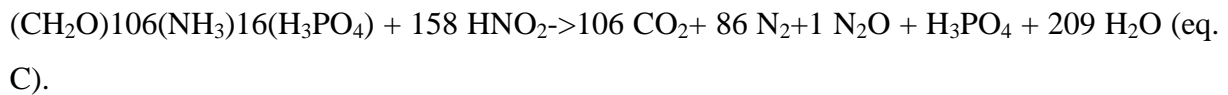


Denitrification:

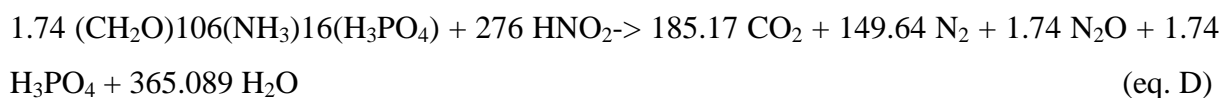
1.: ($N_{\text{org}} + \text{NO}_3 \rightarrow \text{NO}_2$):



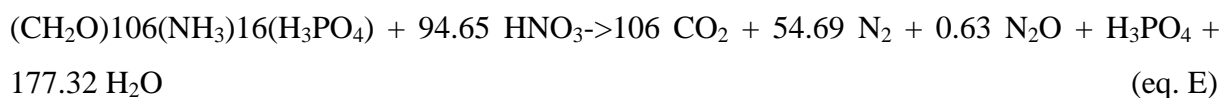
2.: ($N_{\text{org}} + \text{NO}_2 \rightarrow \text{N}_2$):



In order to balance denitrification (the amount of HNO_2 that is produced during the first and consumed during the second step) the eq. C has to be multiplied by 1.74. This results in the following net equation:



adding eqs. B and D and dividing it by 2.74 results in (eq. E):



The amount of N_{org} that was decomposed by the three mechanisms was determined as follows:

Nitrification ($N_{\text{org}} \rightarrow \text{NO}_3$)

$$(N_{\text{org}})_{\text{rem1}} = (N_{\text{org}})_{\text{rem}} * (\text{Fac10}) \quad (26)$$

Denitrification (1): ($N_{\text{org}} + \text{NO}_3 \rightarrow \text{NO}_2$)

$$(N_{org})rem2 = ((N_{org})rem * (1-Fac10)) * (2.74-Fac11) / 2.74 \quad (27)$$

Denitrification (2): $(N_{org} + NO_2 \rightarrow N_2)$

$$(N_{org})rem3 = ((N_{org})rem * (1-Fac10)) * (Fac11 / 2.74) \quad (28)$$

$(NO_3)nit$ is the amount of nitrate produced during the nitrification. An isotopic fractionation factor ($^{15}\epsilon$) of 2 permill was considered for this reaction.

$$\delta^{15}N(NO_3)nit = \delta^{15}N(N_{org})rem1 - 2 \text{ [‰]} \quad (29)$$

The produced $^{15}NO_3$ and $^{14}NO_3$ were added to the $^{15}NO_3$ and $^{14}NO_3$ pool in the box and subtracted from ^{14}N and ^{15}N of organic nitrogen (N_{org}) that continues to sink through the OMZ.

$$(NO_3)nit = (N_{org})rem1 \text{ [mol/yr]} \quad (30)$$

$(NO_3)red$ is the nitrite produced during the first step of denitrification (see eq. 2). An isotopic fractionation factor ($^{15}\epsilon$) of 25 permill was considered.

$$(NO_3)red = [(N_{org})rem2] + [(260/16) * (N_{org})rem2] \text{ [mol/yr]} \quad (31)$$

where $(N_{org})rem2$ is the amount of organic N that is first converted to NO_2 considering a $^{15}\epsilon$ of 2 ‰:

$$\delta^{15}N(NO_2)rem2 = \delta^{15}N(N_{org})rem2 - 2 \text{ [‰]} \quad (32)$$

and $[(260/16) * (N_{org})rem2]$ is the respective amount of nitrate taken from the pool (NO_3 pool) (see eq. B) considering a $^{15}\epsilon$ of 25 ‰.

$$\delta^{15}N(NO_2)red = \delta^{15}N(NO_3 \text{ pool}) - 25 \text{ [‰]} \quad (33)$$

The produced $^{15}NO_2$ and $^{14}NO_2$ were added to the $^{15}NO_2$ and $^{14}NO_2$ pool in the box and subtracted from the pool of NO_3 and the sinking organic N.

$(NO_2)red$ is the N_2 formation during the second part of denitrification (see eq. C).

$$(NO_2)red = [(N_{org})rem3] + [(100/16) * (N_{org})rem3] \text{ [mol/yr]} \quad (34)$$

$(NO_2)ox$: We assume certain fraction (Fac12) of the nitrite which accumulates within the box during the oxidation of nitrite to nitrate.

$$(NO_2)ox = (\text{amount of } NO_2 \text{ in the box}) * fac \ 12 \text{ [mol/yr]} \quad (35)$$

An isotopic fractionation factor ($^{15}\epsilon$) of -13 permill was considered.

$$\delta^{15}N(NO_3) = \delta^{15}N(NO_2 \text{ ox}) + 13 \text{ [‰]} \quad (36)$$

The produced $^{15}NO_3$ and $^{14}NO_3$ were added to $^{14}NO_3$ and $^{15}NO_3$ in the pool and subtracted from the $^{14}NO_2$ and $^{15}NO_2$ pool in the box.

Model run:

Each step was run for 200 years to make sure that steady state was reached. Accordingly, the model was running for 1000 years whereby the conditions were changed five times (Fig. 2.8 in manuscript).

(I) No import of N_{org} /no biology:

For the first 200 model years there was no remineralisation of organic nitrogen and the mean nitrate concentration reached a value of 31 mmol/m^3 ; nitrite concentration were 0 mmol/m^3 and $\delta^{15}\text{NNO}_3$ was 7 permill as prescribed.

(II) No denitrification:

In the second step after the model year 200 the entire organic nitrogen was decomposed and converted into nitrate via nitrification. Accordingly, the nitrate concentration increased by approximately 4 mmol/m^3 and the $\delta^{15}\text{NNO}_3$ was reduced slightly as the lighter ^{14}N is preferentially decomposed.

(III) Denitrification:

In the third step the nitrification was reduced and the remaining organic nitrogen was remineralised during denitrification. Consequently the nitrate concentration decreased and the nitrite concentration increased. Due to the strong discrimination against the heavier ^{15}N during nitrate reduction ($^{15}\epsilon = 25 \text{ permill}$) the remaining nitrate within the box became heavier and reached values around 20 permill as measured at the profile 953 (Fig. 2.3). Assuming furthermore that approximately 24% of the produced nitrite is not reduced to N_2 leads to nitrite concentrations of around 5 mmol/m^3 which also agrees quite well with measurements at profile 953 (Fig. 2.3). However, the resulting $\delta^{15}\text{NNO}_2$ ratios with values of -6 permill are much higher than the calculated ratios of -16 permill.

(IV) No nitrification/100% denitrification:

Assuming in a fourth step that the entire organic nitrogen was decomposed during the denitrification further increases the $\delta^{15}\text{NNO}_2$.

(V) 100% denitrification and nitrite oxidation:

Considering in the fifth step that 60% of the produced nitrite is not reduced to N_2 and that 40% of the accumulated nitrite is oxidized to nitrate leads to $\delta^{15}\text{NNO}_2$ values

similar to the ones measured at profile 953. The decrease in $\delta^{15}\text{NNO}_2$ is caused by the negative isotopic fraction during nitrite oxidation ($^{15}\epsilon = -13$ permil), which appears to be a process explaining the low $\delta^{15}\text{NNO}_2$ values in the upper part of the OMZ in the Arabian Sea. The respective mass balance is given in Fig. 2.7 of the manuscript.

Model run/factors:

(I) No biology no factors

(II) No Denitrification Fac 10 = 1.00

(III) Denitrification Fac10 = 0.08; Fac11 = 2.55; Fac12 = 0.00

(IV) 100% Denitrification Fac10 = 0.00; Fac11 = 2.55; Fac12 = 0.00

(V) Nitrite oxidation Fac10 = 0.00; Fac11 = 2.00; Fac12 = 0.40

References:

- Naqvi, S. W. A. (1987), Some aspects of the oxygen-deficient conditions and denitrification in the Arabian Sea, *Journal of Marine Research*, 45, 1049-1072.
- Rixen, T., Guptha, M.V.S., Ittekkot, V., 2002. Sedimentation. In: Watts, L., Burkill, P.H., Smith, S. (Eds.), Report of the Indian Ocean Synthesis Group on the Arabian Sea Process Study. JGOFS International Project Office, Bergen, pp. 65-73.

3 N-cycling and balancing of the N-deficit generated in the oxygen-minimum zone over the Namibian shelf – an isotope based approach

Birgit Nagel, Kay-Christian Emeis, Anita Flohr, Tim Rixen, Tim Schlarbaum, Volker Mohrholz, Anja van der Plas

Published in March 2013 in: JOURNAL OF GEOPHYSICAL RESEARCH

(BIOGEOCHEMISTRY)

ABSTRACT

The northern Benguela upwelling system is a nutrient-replete region with high plankton biomass production and a seasonally changing oxygen minimum zone. Nitrate:phosphate ratios in fresh upwelling water are low due to denitrification in the near-seafloor oxygen minimum zone and phosphate efflux from sediments. This makes the region a candidate for substantial dinitrogen fixation, for which evidence is scarce. Nutrient and oxygen data, N isotope data of nitrate, nitrogen isotope ratios of particulate matter, particulate organic carbon content and suspended matter concentrations on a transect across the shelf and upper slope at 23°S illustrate N-cycling processes and are the basis for estimating the contribution of N-sources and N-sinks to the reactive nitrogen pool. It appears that N-removal due to denitrification exceeds N gain by N₂ fixation and physical mixing processes by a factor of >6, although inorganic N:P ratios again increase as surface water is advected offshore. Nitrate and ammonium regeneration, nutrient assimilation with N:P < 16, shelf break mixing, atmospheric input and N₂ fixation all contribute to the restoration of inorganic N:P ratios back to Redfield conditions, but in seasonally changing proportions. The Benguela upwelling system thus is a nutrient source for the oceanic mixed layer where N-sources and N-sinks are not in balance and Redfield conditions can only re-adjust by advection and mixing processes integrated over time.

3.1. INTRODUCTION

Upwelling systems are the largest marine source of CO₂ to the atmosphere and their immense primary production fueled by upwelled nutrients far outweighs their modest regional extent (Watson, 1995; Wetzel *et al.*, 2005). Productivity eventually re-captures the outgassed CO₂ by phytoplankton assimilation. But it is questionable if CO₂ outgassing and uptake are in direct balance in individual upwelling systems. Because they often tap oxygen-deficient intermediate water masses, upwelling shelves are prone to oxygen deficiency aggravated by very high oxygen demand generated by remineralisation of sinking organic matter (Monteiro *et al.*, 2006). Oxygen-deficient coastal upwelling often does not supply nutrients into the euphotic zone in Redfield ratios, but with surplus of phosphate over nitrate (termed P* by (Deutsch *et al.*, 2007)), because either is nitrate used to oxidize organic matter in the absence of dissolved O₂ (Lipschultz *et al.*, 1990), or phosphate is added from anoxic sediments high in organic carbon and phosphorus overlying the shelf (Bailey, 1991). In the case that inorganic N:P ratios of upwelled waters are smaller than 16, current understanding is that there will be a zone at the fringes of the high productivity belt where nitrate is depleted by assimilation, and phosphate remains in aged upwelling waters, triggering the “Redfield homeostat” of diazotrophic N₂ fixation until the nitrate deficit is filled (Rixen *et al.*, 2005; Rixen *et al.*, 2009; Tyrrell, 1999). If this basic concept is true, the CO₂ budget of an upwelling system remains constant on time scales of years to decades and on spatial scales far beyond the immediate coastal upwelling area, since the N deficits produced in hypoxic water masses are balanced by N₂ fixation at the fringes of the upwelling region and the hemipelagic ocean.

One example of such a system is the Benguela upwelling system (BUS) where several upwelling cells exist along the Namibian and South African coast due to the interaction of trade winds with coastal topography (Shannon and Nelson, 1996). The northward component of the Southeast Trades drives upwelling and causes offshore Ekman transport in the surface mixed layer. Near-seafloor onshore transport and upwelling from 50 to 200 m water depth compensate for the wind-driven water deficit. The BUS is part of the eastern boundary current system of the south Atlantic. Off central and northern Namibia, the confluence of the northward flowing Benguela Current and the poleward Angola current form a transition zone between central water of tropical and subtropical origin. Eastern South Atlantic Central Water (ESACW; Fig. 3.1a) is advected within the Benguela current from the Agulhas region equatorwards as far as the Angola Benguela Frontal Zone at 17°S (Mohrholz *et al.*, 2001). The Angola current and its subsurface extension, the poleward undercurrent (PU), transport nutrient-rich and oxygen-depleted South Atlantic Central Water (SACW) from the Angola

Gyre along the shelf break (Fig. 3.1a). Its proportion in the upwelling water controls the intensity of the oxygen minimum zone (OMZ), which is most pronounced on the northern Benguela shelf (Inthorn *et al.*, 2006a; Mohrholz *et al.*, 2008; Monteiro *et al.*, 2006). Upwelling mainly occurs at the coast (Mohrholz *et al.*, 2008), but also over the shelf due to a belt of negative wind stress curl (Fennel *et al.*, 2012). Also shelf break upwelling was observed (Barange and Pillar, 1992).

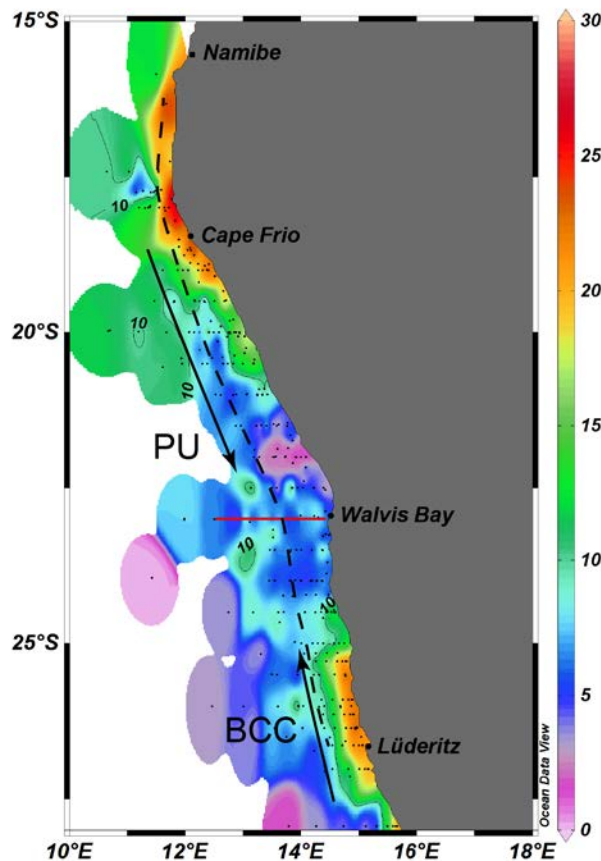


Fig. 3.1a: Map of the study area showing nitrate concentrations in surface water (0-5 m, data taken from the Namibia National Collection of Bottle Data, 1906-1990). Red line labels 23°S-transect where detailed sampling was carried out during the three cruises in 2008, 2010 and 2011. Dashed line indicates location of the shelf break and arrows mark the Benguela Coastal Current (BCC) and the Poleward Undercurrent (PU) supplying ESACW (Eastern South Atlantic Central Water) and SACW (South Atlantic Central Water), respectively.

Water mass composition and thus oxygenation on the shelf vary throughout the year owing to seasonal changes in the wind-driven Ekman regime (Fig. 3.1b). High SACW contributions (80 to 100%) are found along the 23°S transect off Walvis Bay in austral summer (February/March) when the PU is most active and the cross-shelf circulation is weak,

so that ventilation of the bottom water is impeded (Mohrholz *et al.*, 2008). The cross-shelf circulation is strongest in the peak upwelling season in August/September and brings oxygen-rich ESACW from the shelf break onto the shelf (Mohrholz *et al.*, 2008). Hypoxia and anoxia on the shelf are thus mainly controlled by the water mass composition, but oxygen demand from high organic matter fluxes and degradation reduce original O₂ concentrations (Monteiro and Van der Plas, 2006) and create conditions conducive for anaerobic pathways of organic matter degradation. Oxygen concentrations below 10 μM and $\sim 5 \mu\text{M}$ stimulate anammox and heterotrophic denitrification, respectively (Cline and Kaplan, 1975; Jensen *et al.*, 2008), and cause nitrate deficits over phosphate in OMZs that are transferred into surface waters by upwelling (Tyrrell and Lucas, 2002).

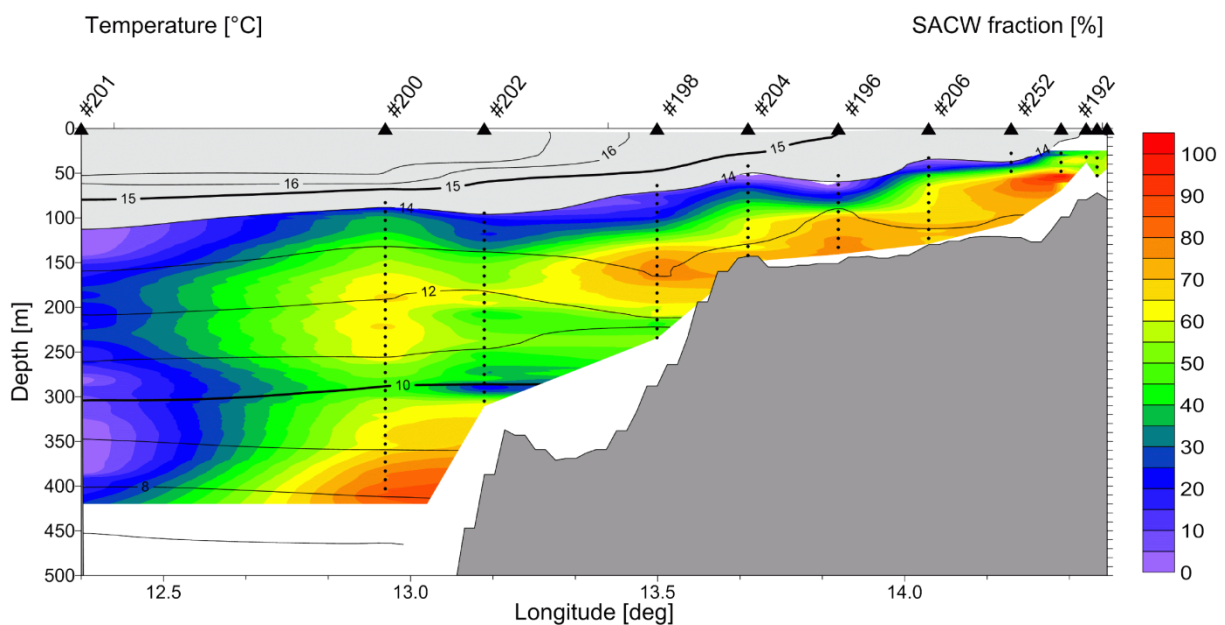


Fig. 3.1b: Water mass distribution (% SACW, colours) and temperature (contours) on the transect at 23°S during expedition M76-2 (May-June 2008).

Nitrate reduction in the water column – the first step of heterotrophic denitrification - and presumably also anammox are associated with kinetic fractionation of stable N isotopes causing an enrichment of the heavier ¹⁵N isotope in the residual nitrate pool (Konovalov *et al.*, 2008; Sigman *et al.*, 2005). The fractionation factor (ϵ) is the difference between the isotopic composition of the source and the product (Mariotti *et al.*, 1981). Heterotrophic denitrifying bacteria and nitrate assimilating phytoplankton discriminate against the heavier ¹⁵N isotope with a fractionation factor of 25‰ and 5‰, respectively (Granger *et al.*, 2008; Granger *et al.*,

2004). Although large reactive nitrogen deficits over phosphate occur in upwelling water, there is no experimental evidence for significant N_2 fixation in the BUS (Sohm *et al.*, 2011); Wasmund, pers. comm., 2011). This is puzzling, because inorganic N:P ratios are evidently restored to Redfield ratios in modified upwelling water advected offshore (Wasmund *et al.*, 2005) and seem to exemplify the P*-concept (Deutsch *et al.*, 2007) that links N_2 fixation in time and space to the denitrification zones of the ocean. In the absence of evidence for N_2 fixation several alternative processes have been invoked, such as shelf break upwelling in a second upwelling cell (Barange and Pillar, 1992; Emeis *et al.*, 2009), or non-Redfield assimilation stoichiometry (Weber and Deutsch, 2010).

Here, we use data of oxygen and nutrient concentrations as well as stable isotope compositions of nitrogen in nitrate ($\delta^{15}N_{NO_3}$) and $\delta^{15}N$ ratios of particulate nitrogen ($\delta^{15}N_{PN}$) as well as particulate organic carbon content (POC) to investigate N-cycling processes in the BUS and the isotopic composition of nitrate as a fingerprint of its origin. With the data, we quantify the nitrate deficit generated by denitrification and phosphate release, estimate how much denitrification contributes to the regional nitrate deficit, and identify mechanisms that restore the inorganic N:P ratios in the mixed layer of the adjacent South Atlantic.

3.2. MATERIALS AND METHODS

3.2.1. Sampling

Water samples were taken with a CTD/rosette sampler during cruises M76-2 (May/June 2008), D-356 (August/September 2010) and MSM17-3 (February/March 2011) and were filtered over pre-combusted GF/F Filters onboard. Filtrates were stored frozen in acid-washed polypropylene bottles for nutrient analysis and isotope analysis. Since the main focus of all cruises was on the 23°S transect and sampling was most detailed there, we concentrate on this transect.

Particulate matter sampling was carried out by filtration onboard. Water was filtered over pre-weight and pre-combusted (450°C) GF/F Filters (Whatman). Filters were dried immediately after filtration at 40°C for 48h.

3.2.2. Analytical Methods

Nutrients of M76-2 samples were measured with a BRAN & LUEBBE autoanalyser in the home laboratory in Hamburg by applying standard methods. Nutrient analyses of D-356 were carried out onboard and samples of MSM17-3 were measured in the home laboratory in Bremen. Standard methods and a SKALAR autoanalyser were used for the samples of D-356 and MSM17-3. Oxygen concentrations in discrete samples were measured by using Winkler methods and were further used to calibrate oxygen data obtained from the CTD.

POC was measured using a Thermo Flash EA 1112. Briefly, homogenized samples were weighed into silver capsules and inorganic carbon was removed by adding 1M HCl suprapur prior to analyses. All POC data are given in weight-%.

$\delta^{15}\text{N}$ of nitrate was determined using the “denitrifier method” (Casciotti *et al.*, 2002; Sigman *et al.*, 2001a) and are reported in ‰ using the delta-notation

$$\delta^{15}\text{N}_{\text{sample}} = ((^{15}\text{N}/^{14}\text{N})_{\text{sample}} / (^{15}\text{N}/^{14}\text{N})_{\text{reference}} - 1) * 1000 \quad (37)$$

with air N_2 as reference for $^{15}\text{N}/^{14}\text{N}$. The values were calibrated using IAEA-N3 ($\delta^{15}\text{N}_{\text{NO}_3} = +4.7\text{‰}$) and USGS-34 ($\delta^{15}\text{N}_{\text{NO}_3} = -1.8\text{‰}$; Böhlke *et al.*, 2003). A potassium nitrate standard was measured twice within each run for quality assurance. Isotope values were corrected using the single point correction referring to IAEA-N3 for $\delta^{15}\text{N}_{\text{NO}_3}$. The standard deviation for IAEA-N3 was 0.3‰, which is within the same specification for $\delta^{15}\text{N}_{\text{NO}_3}$ for at least duplicate measurements of the samples. Since nitrite was not removed prior to isotope analyses and since *Pseudomonas aureofaciens* used for the “denitrifier method” consume both nitrate and nitrite, we have to perform a nitrite correction of $\delta^{15}\text{N}$ values in samples with significant nitrite concentrations (more than 1 μM). The correction was done using the equation:

$$\delta^{15}\text{N}_{\text{NO}_2} = ((\text{NO}_3 + \text{NO}_2) * \delta^{15}\text{N}_{\text{NO}_3+\text{NO}_2}) - (\text{NO}_3 * \delta^{15}\text{N}_{\text{NO}_3}) / \text{NO}_2 \quad (38)$$

for samples from the bottom water of station #206 and #252. Because we lack genuine nitrite $\delta^{15}\text{N}$ values for the BUS, we have to resort to literature data. In the Arabian Sea OMZ $\delta^{15}\text{N}_{\text{NO}_2}$ values are calculated from equation (2) to average -18.1‰ (Gaye, B., B. Nagel, K. Dähnke, T. Rixen, and K.-C. Emeis, Evidence of coupled denitrification and nitrification in the ODZ of the Arabian Sea from paired stable isotopes of nitrate and nitrite, resubmitted to *Global Biogeochemical Cycles*.) which is in accordance with nitrite isotope data from the Eastern Tropical North Pacific OMZ (Casciotti and McIlvin, 2007).

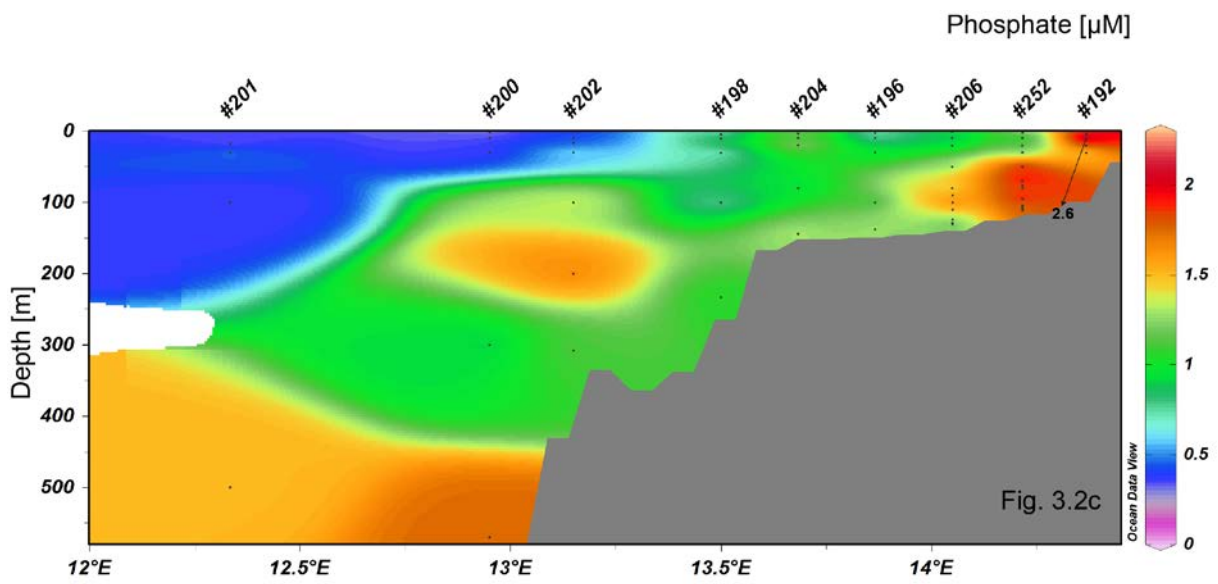
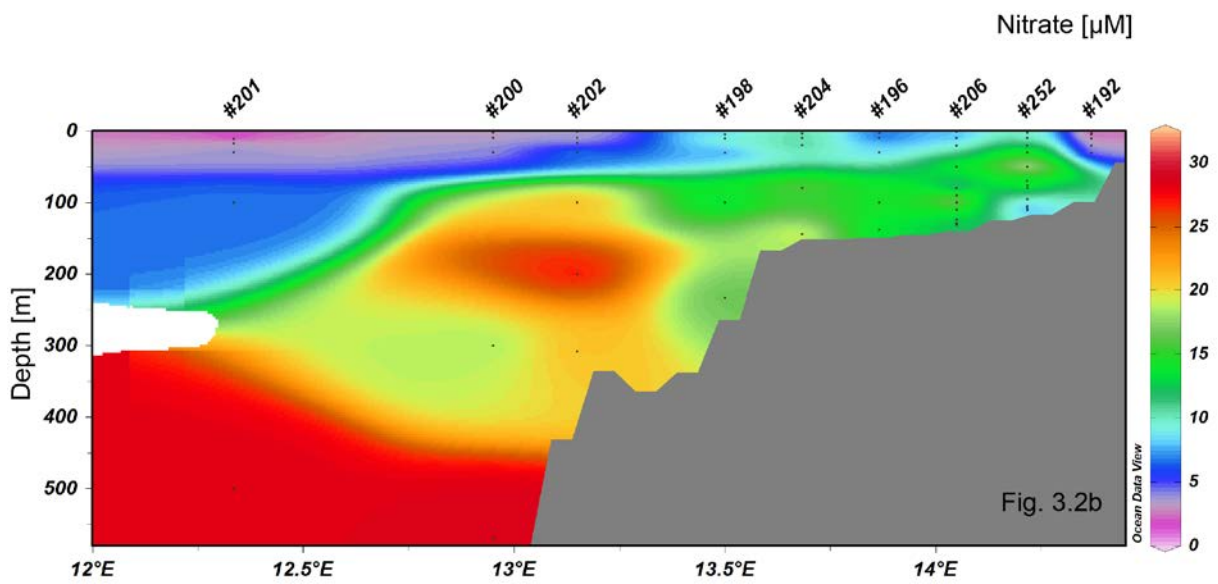
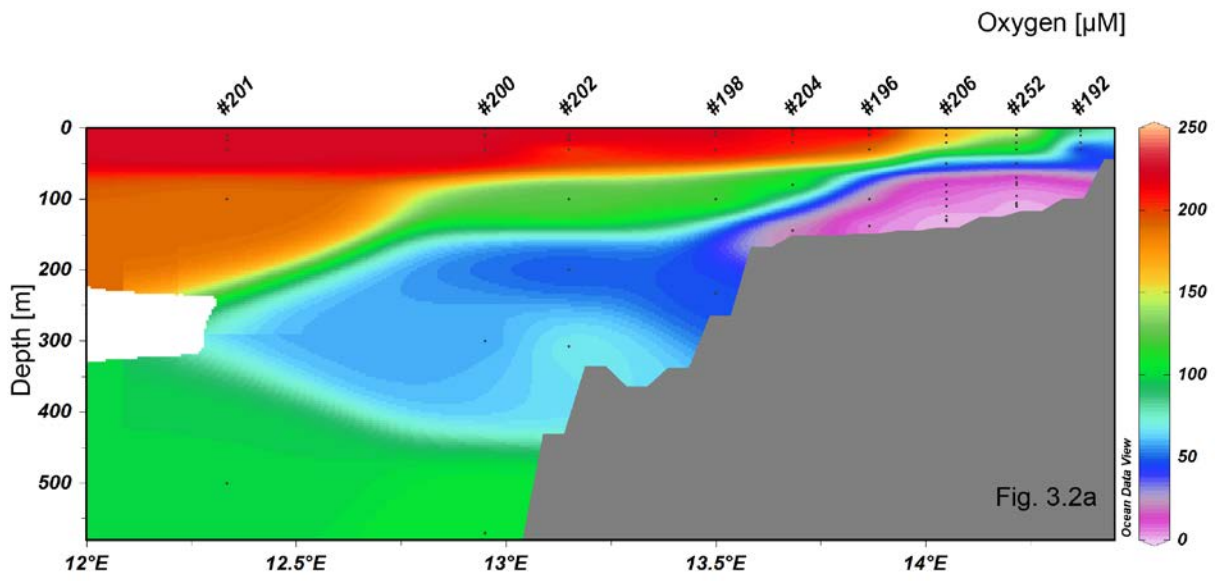
$\delta^{15}\text{N}_{\text{PN}}$ ratios were measured using a Thermo Delta Plus XP mass spectrometer after combustion in a Thermo Flash EA 1112. A single-point calibration was performed with IAEA-N1 standard (Bahlmann *et al.*, 2010). Within each run IAEA-N2 and IVA Sediment standards have been measured to assure measurement quality and to assess the laboratories

long-term measurement performance. The standard deviation for IAEA-N1 was less than 0.2 ‰ and duplicate measurements of suspended matter samples differ less than 0.3‰ due to inhomogeneous particle coverage of filters.

3.3. RESULTS

We concentrate on the data obtained for the sampling period in May/June 2008, when the shelf was partially anoxic, and use nutrient data from D-356 and MSM17-3 to demonstrate the high seasonal variability on the Namibian shelf. In May/June 2008 moderate coastal upwelling of water from 100 to 150 m water depth occurred at 23°S. On the shelf, the subsurface SACW contribution (Fig. 3.1b) was highest (< 85%, 50 m) on the inner shelf in the coastal upwelling region and decreased towards the outer shelf (< 65%, 200 m). A patch of low SACW fraction (<40%) was found above the bottom at the shelf break (station #202). A distinct thermocline was present within the upper 50 m above the shelf break and further offshore. We found suboxic conditions (< 20 μM) in the bottom water of the inner shelf at 23°S and even surface waters near the coast were oxygen depleted (O_2 < 80 μM ; Fig. 3.2a). The subsurface OMZ spread into the hemipelagic ocean where minimum O_2 concentrations ranged between 40 and 60 μM .

Nitrate concentrations (Fig. 3.2b) in the mixed layer were lowest near the coast and at the offshore station #201 (< 2 μM). A “nitrate plume” above the shelf break with significantly elevated concentrations by > 5 μM compared to the adjacent stations lifted the nitracline up into the thermocline. A similar pattern was observed for phosphate (Fig. 3.2c): elevated concentrations occurred above the shelf break, but differing from nitrate, highest concentrations (> 1.5 μM) were found near the coast. Nitrite concentrations (Fig. 3.2d) above 1 μM were restricted to suboxic bottom water on the inner shelf with a maximum of 4.4 μM at 60 cm above the seafloor at station #252. Ammonium concentrations (Fig. 3.2e) were above 1 μM throughout the inner shelf, with maximum values in coastal surface water between 6 and 7 μM , and above 8 μM at the seafloor (#206).



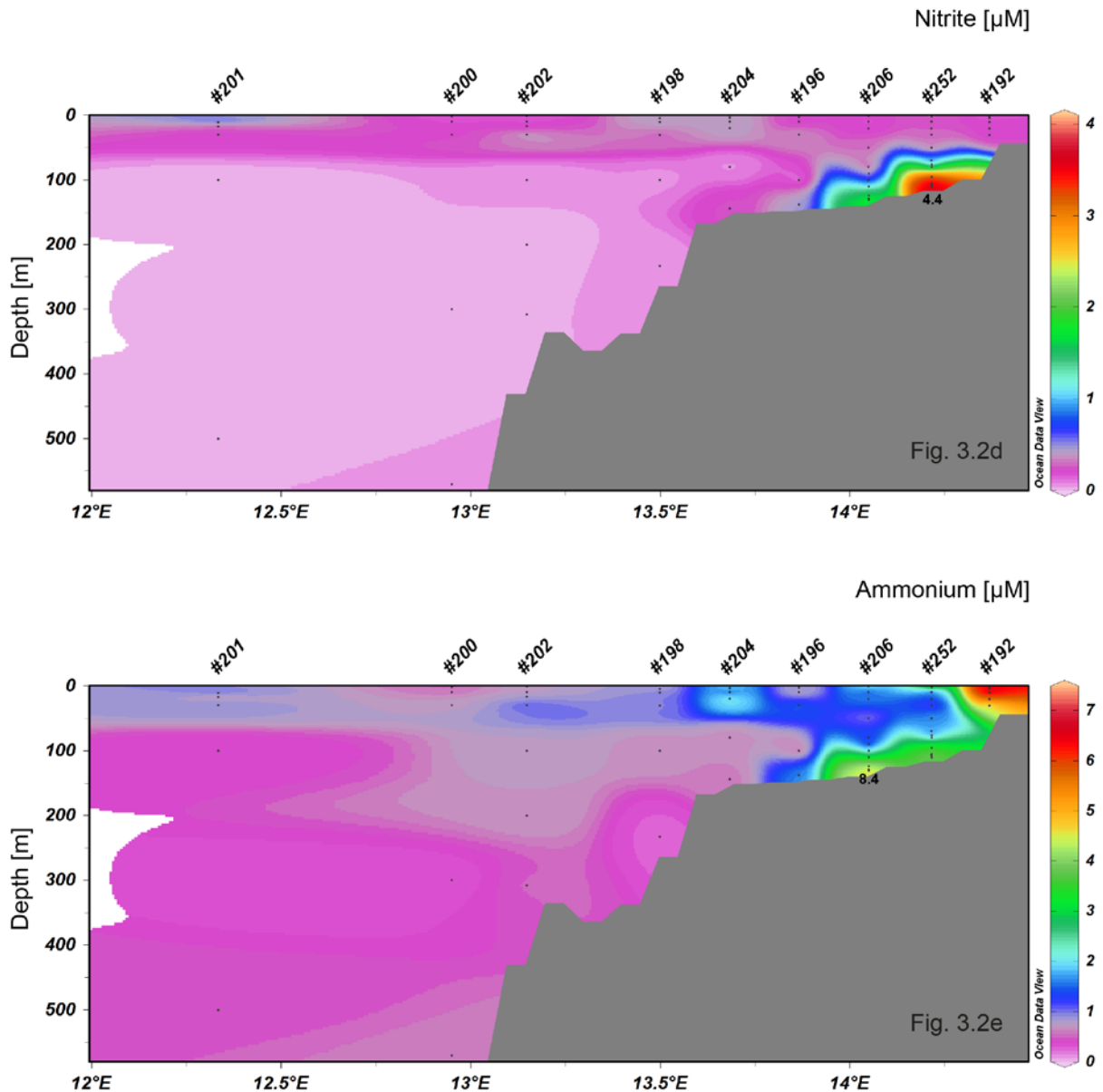


Fig. 3.2: Interpolated concentrations during M76-2 (May-June 2008) on the 23°S transect normal to the coast. a) oxygen; b) nitrate; c) phosphate; d) nitrite and e) ammonium. Numbers mark individual concentrations that deviate from the colour code due to steep concentration gradients.

Suspended matter concentrations (SPM, see supplement S1) and particulate organic carbon content (POC, see supplement S2) correlated near the seafloor. Both increased in bottom water towards the inner shelf from 4.9 mg/l to ~30 mg/l in the bottom nepheloid layer and from 2.8% to 6.0%, respectively. SPM concentrations were high in surface water near the coast (~19 mg/l) at co-occurring low POC concentrations of 2.7% to 2.9%. SPM concentrations decreased in surface water in offshore direction to 4.2 mg/l at the most offshore station. POC content in surface water was high at stations #206 and #198. Further

offshore, high POC contents in surface waters were observed at co-occurring low SPM concentrations and vice versa. At offshore station #201 a pronounced deep surface SPM maximum (18 mg/l) occurred at 17 m water depth at a remarkably low POC content of 1.2%. Bottom waters at the shelf break were rich in SPM (12.5 mg/l at 5 m above seafloor) and POC (4%) compared to the surrounding waters.

Bottom waters at the shelf break had excess reactive nitrogen with respect to phosphate. DIN/P ratios (see supplement S3) were calculated as $(\text{NO}_3^- + \text{NO}_2^- + \text{NH}_4^+)/\text{PO}_4^{3-}$ and ranged between 21 and 16 at the outer shelf stations. DIN/P ratios decrease on the inner shelf down to 3.4 in coastal surface water.

The $\delta^{15}\text{N}_{\text{NO}_3}$ of water at the shelf edge – the source for upwelling waters over the shelf - ratios ranged from 5.7‰ to 6.7‰ (Fig. 3a). These values are slightly higher than deep ocean nitrate originating from subduction around the polar front (5.5‰; Sigman *et al.*, 2001b). By contrast, bottom water nitrate on the inner shelf OMZ was most enriched in ^{15}N ($\delta^{15}\text{N}_{\text{NO}_3}$ values between 28 and 29.6‰) at station #252. The nitrite correction (eq. 2) was performed for these samples because nitrite content was 32% of the combined $\text{NO}_2^- + \text{NO}_3^-$ pool. High $\delta^{15}\text{N}_{\text{NO}_3}$ values (< 13.9‰) were also found within the mixed layer at the most distal station #201 on the 23°S transect, where nitrate concentrations dropped below 2 μM . Stable nitrogen isotope ratios of particulate nitrogen ($\delta^{15}\text{N}_{\text{PN}}$) ratios ranged between 3.0‰ in the surface water at the most distal station (#201) and 11.0‰ in intermediate water (50 m) at nearshore station #252 (Fig. 3b). $\delta^{15}\text{N}_{\text{PN}}$ were low (< 5.5‰) in surface waters at the outer shelf and upper slope. High $\delta^{15}\text{N}_{\text{PN}}$ (> 7‰) characterised all suspensions in intermediate and bottom water with the exceptions of shelf break bottom water (6.2‰) and bottom water at station #206 (6.7‰).

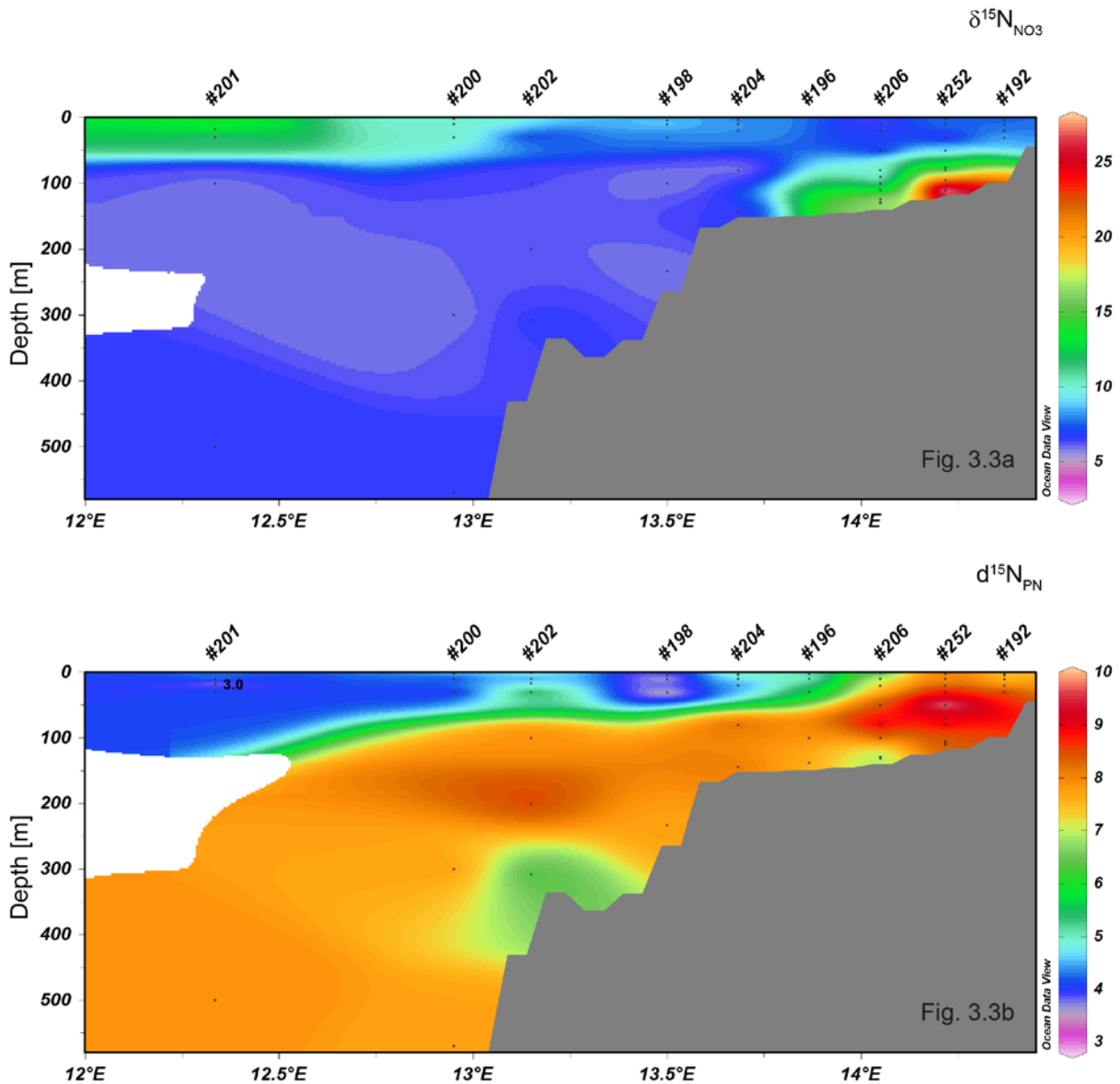


Fig. 3.3: Interpolated isotopic compositions in ‰ during M 76-2. a) $\delta^{15}\text{N}_{\text{NO}_3}$; b) $\delta^{15}\text{N}_{\text{PN}}$

3.4. DISCUSSION

N-loss processes such as heterotrophic denitrification and anammox are known to occur in the Benguela OMZ (Kuypers *et al.*, 2005; Tyrrell and Lucas, 2002), but there is only little experimental evidence for N_2 fixation balancing the N-loss, and the rates observed were too low to compensate the N-loss (Sohm *et al.*, 2011). Despite a pronounced N-deficit on the inner Namibian shelf, however, we find a balanced inorganic N:P ratio ($(\text{NO}_3^- + \text{NO}_2^- + \text{NH}_4^+)/\text{PO}_4^{3-}$) of ~ 16 in surface water offshore the shelf break in May/June 2008. This suggests a source of inorganic N in surface water advected from the shelf to the open ocean.

Below we address the question if the BUS is a closed system in which N-losses are compensated by N-supply restoring Redfield conditions. If this is not the case and N-losses exceed N-supply, the BUS would be a sink of fixed N, thus weakening the CO₂ uptake capacity of the regional biological pump. We then investigate seasonal variability linked to water mass and oxygen dynamics, and attempt to quantify the deficit of inorganic N transferred into the adjacent hemipelagic ocean.

3.4.1. Processes of N-Cycling on the Namibian Shelf

Our discussion of data and transformations of reactive N follows mainly a 2D cross shelf circulation model view. This is applicable to the circulation on the shelf, but has some weaknesses for the shelf break and adjacent oceanic stations. Mohrholz *et al.* (2008) have shown that the cross shelf circulation on the shelf is controlled by upwelling dynamics with offshore Ekman transport in the mixed layer and an onshore compensation flow below the thermocline. Offshore of the shelf edge and below the surface layer the circulation is dominated by meridional currents, namely the Benguela current and the poleward undercurrent. Although the meridional flow on the shelf is prominent (Monteiro and Van der Plas, 2006; Monteiro *et al.*, 2008), one can interpret the conditions observed on the transect off Walvis Bay as a projection of the 3D picture onto a 2D transect. This is because the meridional extent of the upwelling area is large compared to the shelf width. Further assuming that processes are uniform along the coast, a 2D transect depiction is mainly controlled by cross shelf dynamics. This assumption is also applicable for the surface mixed layer beyond the shelf edge, because the Ekman offshore transport dominates the flow on longer time scales.

Phosphate and ammonium concentrations (Fig. 3.2c and 3.2e) increase in bottom water from the outer shelf towards the coast. The increase is caused by intense remineralisation of organic matter in sediments of the inner shelf. Ammonium and phosphate diffuse out of the sediments under low oxygen conditions (Neumann, 2012). The benthic ammonium supply is entrained into the cross shelf flow and wells up near the coast.

Significant amounts of nitrate in sub-thermocline water on the shelf are consumed within the OMZ on the inner shelf (Fig. 3.2b) as soon as decreasing oxygen concentrations reach the threshold of ~ 5-10 μM for heterotrophic denitrification and anammox (Cline and Kaplan, 1975; Jensen *et al.*, 2008). In sub-thermocline water on the outer shelf and at station #206 $\delta^{15}\text{N}_{\text{NO}_3}$ and $\delta^{18}\text{O}_{\text{NO}_3}$ (data not shown) change in parallel. This pattern is consistent with

nitrate reduction (the first step of heterotrophic denitrification; Granger *et al.*, 2008), which was detected in the bottom nepheloid layer throughout the OMZ in low rates (Füssel *et al.*, 2011). The $\delta^{15}\text{N}_{\text{NO}_3}$ and $\delta^{18}\text{O}_{\text{NO}_3}$ values continue to rise towards the inner shelf while the nitrate deficit (N_{def} ; see supplement S4) increases. This indicates progressive nitrate consumption by nitrate reduction. Other nitrate and nitrite consuming processes which could account for the evolving nitrate deficit in the deep water over the shelf at 23°S are anammox and dissimilative nitrate reduction to ammonium (DNRA). Anammox is possibly the dominant reason for the N-deficit on the Namibian shelf (Kuypers *et al.*, 2005) and anammox rates exceed nitrate reduction rates at station #252 (Füssel *et al.*, 2011). Nitrate ammonifiers were not evident at station #252 (Füssel *et al.*, 2011) and not responsible for decreasing nitrate concentrations in waters of the OMZ. From our data we cannot definitely state which process is the most effective in eliminating reactive N before the water upwells into the euphotic mixed layer.

As the upwelled water moves across the shelf, the $\delta^{15}\text{N}_{\text{NO}_3}$ values in surface waters decrease from the stations closest the coast to roughly the shelf break. Near the coast, particulate matter that is apparently produced in the surface layer by phytoplankton has higher $\delta^{15}\text{N}_{\text{PN}}$ values than $\delta^{15}\text{N}$ of the ambient nitrate. This suggests that a relatively ^{15}N -enriched N-source is assimilated by phytoplankton, whereas a relatively ^{15}N -depleted source adds to the dissolved nitrate pool. For both, the branching of high ambient ammonium concentrations into either biomass (ammonium assimilation) or nitrate (nitrification) is a good candidate (Wankel *et al.*, 2007).

High ammonium concentrations (Fig. 3.2e) in coastal surface water most likely originate from two sources. The first is benthic remineralisation of organic matter, because both ammonium and phosphate concentrations are elevated in freshly upwelled waters near the coast. In addition to the benthic source, an ammonium source from ammonification of particulate nitrogen in the water column is indicated by a vertical decrease of SPM concentrations from the mixed layer (~ 10 mg/l) to 50 m water depth (~ 5 mg/l; see supplement S1). Additionally, POC content decreases in the upper 50 m of station #252 (see supplement S2). At the same time, the average $\delta^{15}\text{N}_{\text{PN}}$ ratio of the sinking material increases from 7.8‰ in the mixed layer to 9.5‰ at 50 m water depth (Fig. 3.3b), indicating a preferential release of ^{15}N depleted ammonium during ammonification. The ammonium mixture produced is partly assimilated and causes the mismatch between $\delta^{15}\text{N}_{\text{NO}_3}$ and $\delta^{15}\text{N}_{\text{PN}}$ seen at station #252. Here, particles in the surface water have higher $\delta^{15}\text{N}$ ratios than ambient nitrate ($\delta^{15}\text{N}_{\text{PN}} = 8.3\text{‰}$ versus $\delta^{15}\text{N}_{\text{NO}_3} = 7.5\text{‰}$ and 7.8‰), whereas biomass from assimilation

of that nitrate should have a $\delta^{15}\text{N}_{\text{PN}}$ that is 5‰ more negative than ambient $\delta^{15}\text{N}_{\text{NO}_3}$ (Granger *et al.*, 2004). This implies that assimilation of isotopically enriched ammonium – associated with a fractionation factor of 6 to 27‰ (Hoch *et al.*, 1992; Wankel *et al.*, 2007; Waser *et al.*, 1998) - raises the $\delta^{15}\text{N}_{\text{PN}}$.

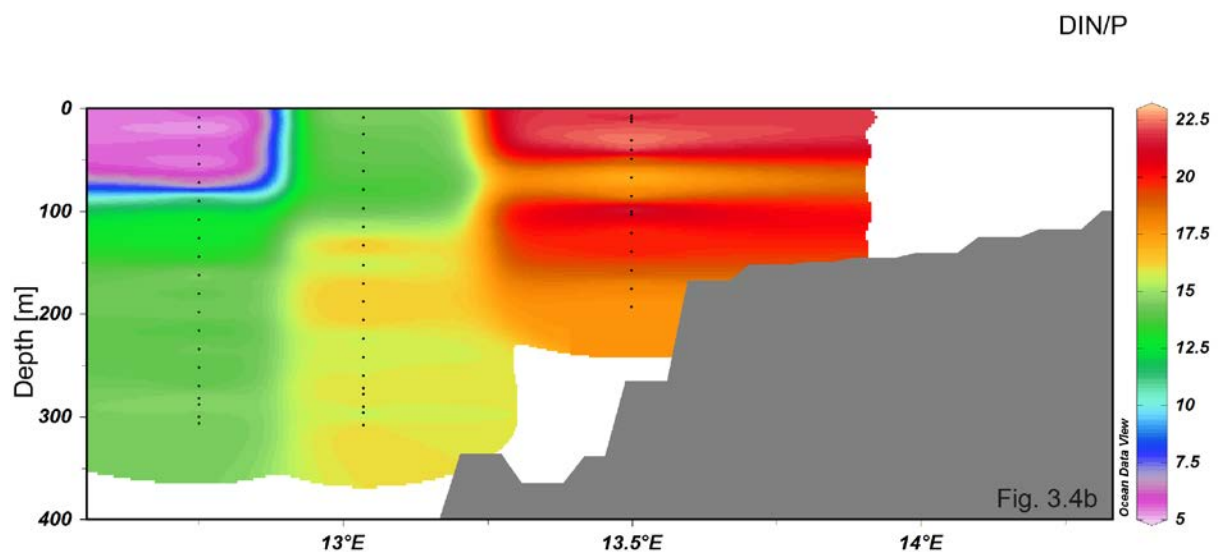
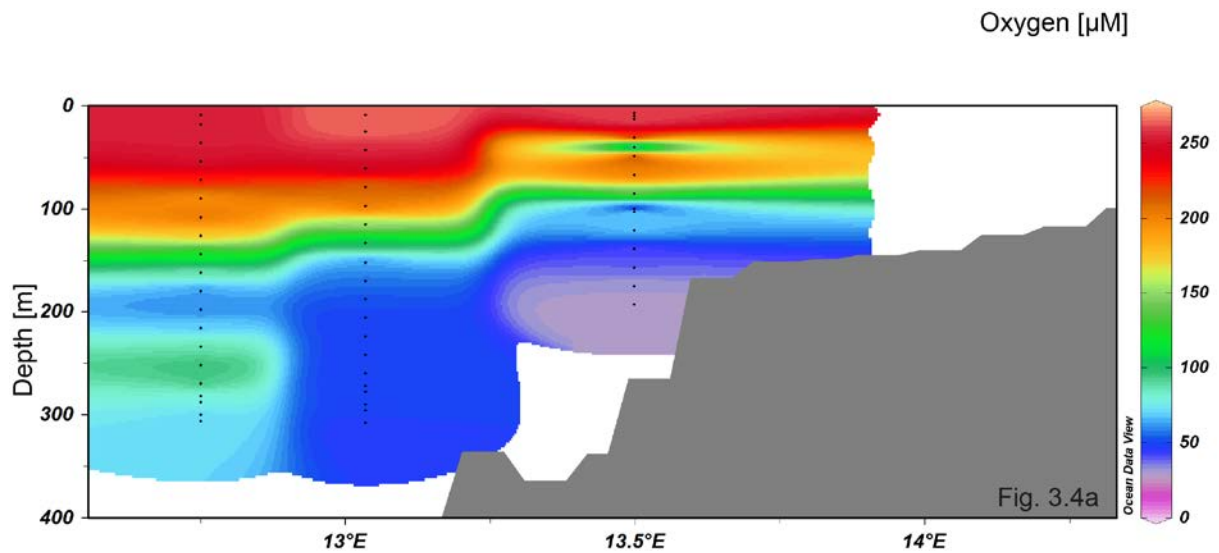
Additions from nitrification of ammonium on the other hand decrease the $\delta^{15}\text{N}$ of the nitrate pool, because marine nitrification discriminates strongly against ^{15}N ($^{15}\epsilon$ between 14 and 19‰; Casciotti *et al.*, 2003). The branching of ammonium fluxes to either nitrification or ammonium assimilation, associated with different fractionation factors, thus leads to nitrate that is more ^{15}N -depleted than the suspended matter produced by ammonium assimilation of the residual (Wankel *et al.*, 2007).

$\delta^{15}\text{N}_{\text{PN}}$ ratios (Fig. 3.3b) decrease in offshore direction from 7.2‰ at station #206 to values between 5.5‰ and 3.8‰ at the shelf break (station #198) coincident with decreasing ammonium concentrations (Fig. 3.2e). Nitrate rather than ammonium is the predominant N-source for primary production offshore of station #206 and low $\delta^{15}\text{N}_{\text{PN}}$ ratios mimic low $\delta^{15}\text{N}_{\text{NO}_3}$ ratios of newly produced nitrate (see also Granger *et al.*, 2011). The production of nitrate in the oxygen gradient of OMZs is a typical feature also known from the Eastern Tropical North Pacific (Ward and Zafiriou, 1988), the Eastern Tropical South Pacific (Lipschultz *et al.*, 1990; Ward *et al.*, 1989) and from the Arabian Sea (Gaye, B., B. Nagel, K. Dähnke, T. Rixen, and K.-C. Emeis, Evidence of coupled denitrification and nitrification in the ODZ of the Arabian Sea from paired stable isotopes of nitrate and nitrite, resubmitted to *Global Biogeochemical Cycles*). As surface water moves offshore with the Ekman transport, decreasing primary production at decreasing nitrate concentrations causes decreasing SPM concentrations (see supplement S1). A contribution of N_2 fixation is seen in the oceanic end member (station #201), where nitrate is almost completely consumed (Fig. 3.2b), but SPM concentration is high and has a low $\delta^{15}\text{N}_{\text{PN}}$ value of 3.0‰ (Fig. 3.3b). Nitrate in surface water of station #201 is almost consumed (0.14 μM at 11 m water depth) and $\delta^{15}\text{N}_{\text{NO}_3}$ and $\delta^{15}\text{N}_{\text{PN}}$ at 17 m water depth are 13.9‰ and 3.0‰, respectively. Beyond the shelf break, *Trichodesmium* occasionally occurs and one to ten *Trichodesmium* colonies per m^3 were encountered in plankton nets in February 2011 in the northern BUS (H. Auel, pers. comm., 2011).

3.4.2. Seasonal Variability of Water Masses and Nutrient Composition on the Namibian Shelf

Nutrient concentrations and nutrient ratios in the northern BUS are highly variable due to the seesaw of two distinct water masses caused by physical processes. Nutrient-depleted and oxygenated ESACW mixes on the shelf with nutrient-rich and oxygen-depleted SACW between the Lüderitz upwelling cell (26°S) and the Angola-Benguela-Frontal-Zone at 17°S (Mohrholz *et al.*, 2008). Since ESACW and SACW have completely different oxygen and nutrient concentrations (as well as differing nitrate/phosphate ratios), prevailing upwelling conditions control oxygenation and nutrient conditions over the shelf. This is illustrated in Fig. 3.4 that depicts two different situations on the 23° transect. In August/September 2010 (cruise D356), DIN/P ratios on the shelf ranged between 13.6 and 22.8 (Fig. 3.4b) when intense upwelling occurred in the northern BUS. In this season, a weak poleward undercurrent and strong cross-shelf compensation currents transported waters with high ESACW proportions onto the shelf (Mohrholz *et al.*, 2008). This mixture had high inorganic N/P ratios. Poole and Tomczak (1999) propose low N:P ratios of ~ 9 for the ESACW in their water mass definitions of the Atlantic Ocean. But they define the core depth of ESACW between 350 and 600 m, which is below our sampling depths. Because oxygen concentrations on the shelf are > 30 µM (Fig. 3.4a) denitrification and release of ammonium and phosphate from sediments were inhibited so that the high inorganic N:P ratios of upwelling source waters reached the surface. Bottom water DIN/P ratios increased from the outer to the inner shelf, where sulphur bacteria abundantly inhabiting the benthic boundary layer take up phosphate during oxic periods to store it within the cells as polyphosphate (Brock and Schulz-Vogt, 2011). Consequently, arriving high DIN:P ratios further increase and are transported into surface water by upwelling and Ekman transport. By contrast a weak cross-shelf compensation current and strong poleward undercurrent activity controlled the water mass composition in the northern BUS during cruise MSM17-3 in February/March 2011. ESACW had retracted to the South and the dominance of oxygen-poor SACW (with DIN/P ratios around 16:1) promoted the development of suboxic conditions on the shelf (Fig. 3.4c). This stimulated heterotrophic denitrification and anammox and created an N-deficit by either denitrification or phosphate release from sediments leading to lowered DIN/P ratios (Fig. 3.4d). Phosphate can be released from the seafloor under anoxic conditions from internal sources from the inner-shelf organic-rich diatomaceous mud (Bailey, 1991). Under changing oxic/anoxic conditions, phosphate-sequestering bacteria play a role in generating recent concretionary phosphorites on the landward flank of the diatomaceous mudbelt and in

releasing mediate phosphorous from sediments (Nathan *et al.*, 1993). This source likely contains a contribution from large sulphur bacteria inhabiting the diatomaceous mud on the inner shelf: Under anoxic conditions and sulphide exposure, intracellular polyphosphate stored under oxic conditions is decomposed and released to pore water (Brock and Schulz-Vogt, 2011). Because sediment pore water and ambient bottom water are in isotopic disequilibrium regarding oxygen isotopes of phosphate ($\delta^{18}\text{O}_\text{P}$), the imprint of regenerated phosphate is evident under anoxic conditions (Goldhammer *et al.*, 2011) and further decreases the DIN/P ratio in the water column on the inner shelf. Phosphate concentrations in pore water of the diatomaceous mud reach up to $< 500 \mu\text{M}$ in 10 to 20 cm below seafloor (Goldhammer *et al.*, 2011) and increase to $> 1000 \mu\text{M}$ during prolonged suboxic periods over the central Namibian shelf (Bartholomae and van der Plas, 2007; van der Plas *et al.*, 2007).



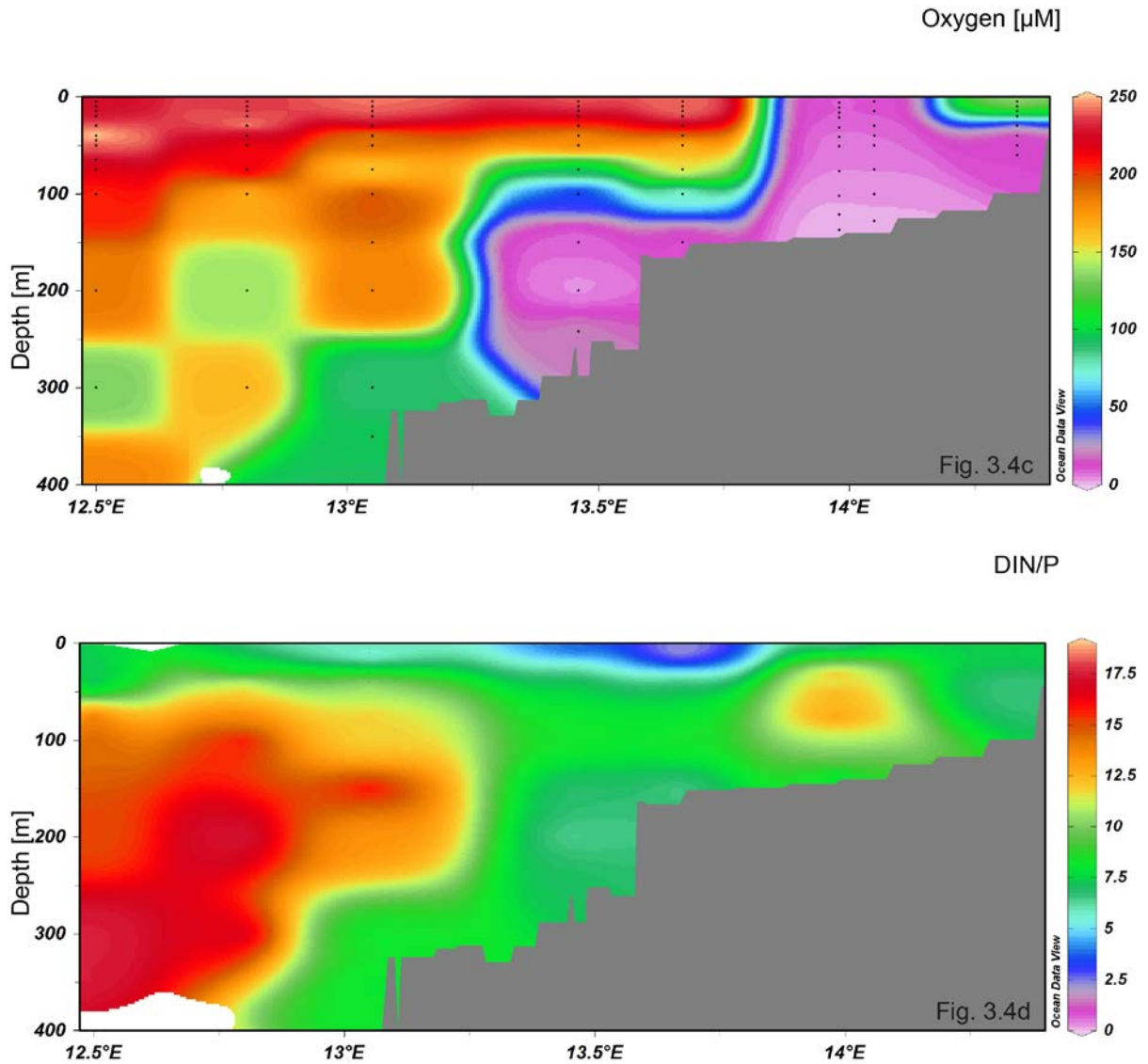


Fig. 3.4: O_2 concentrations on the 23°S transect (3.4a) show enhanced oxygenation during Aug/Sep 2010 that was caused by strong upwelling and cross-shelf currents transporting ESACW with elevated DIN/P ratios (3.4b) onto the shelf. In February/March 2011 the OMZ (3.4c) covered almost the entire shelf and molar DIN/P ratios (3.4d) decreased from 17.5 above the upper slope to 5 in coastal surface water.

3.4.3. Quantification of the Nitrate Deficit and Denitrification

N loss or P gain both affect the local deficit of inorganic N (N_{def}) in the system. Devol *et al.* (2006) defined N_{def} as the difference between the preformed N:P conditions (N^{pref}) and the measured inorganic N-pool (NO_3^- , NO_2^- and NH_4^+):

$$N_{\text{def}} = N^{\text{pref}} - N^{\text{meas}} \quad (39),$$

To estimate the local N^{pref} we plotted DIN ($[\text{NO}_3^-] + [\text{NO}_2^-] + [\text{NH}_4^+]$) versus $[\text{PO}_4^{3-}]$ from water samples that were not affected by denitrification and phosphate release ($O_2 > 65 \mu\text{M}$)

nor by assimilation processes (50 – 500 m water depth). The slope of the regression in Fig. 3.5 is 18.22 and the intercept on the PO_4^{3-} -axis is 0.01, so that:

$$N^{\text{pref}} = 18.22 * (\text{PO}_4^{3-} - 0.01) \quad (40).$$

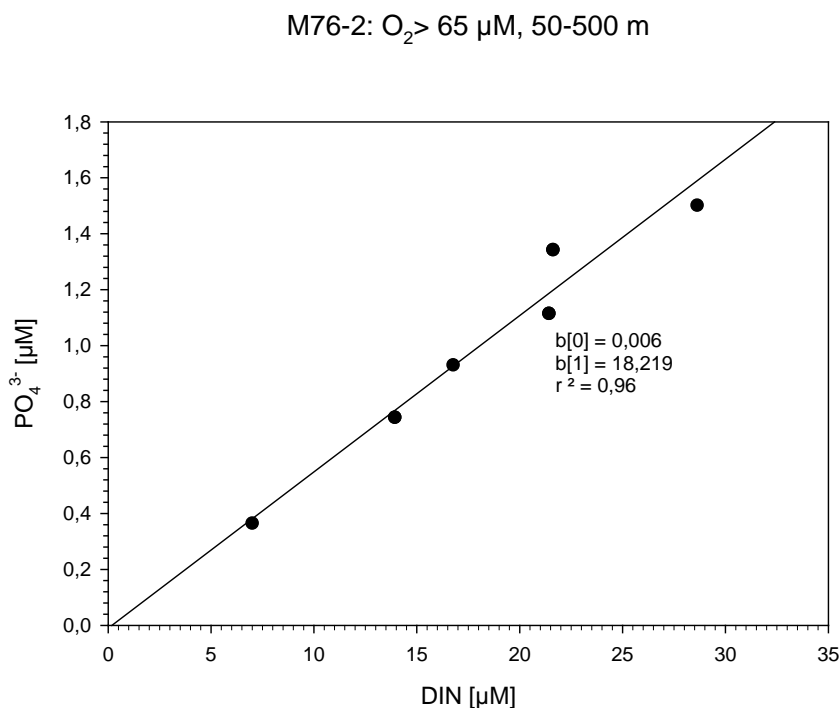


Fig. 3.5: Linear correlation between dissolved inorganic nitrogen ($\text{NO}_3^- + \text{NO}_2^- + \text{NH}_4^+$) and phosphate of sampling sites from M76-2 on the 23 °S-transect between 50 and 500 m water depth and $\text{O}_2 > 65 \mu\text{M}$.

Offshore of the shelf break N_{def} (see supplement S4) is negative between 100 and 650 m water depth and mirrors a slight N excess over phosphate. N_{def} increases towards the mixed layer and laterally towards the shelf, to maximum values in coastal surface water at station #192 (27.2 μM) and within the bottom nepheloid layer at #252 (28.6 μM).

During the expedition M76-2 in May/June 2008, upwelling source water at the shelf break had DIN:P ratios ~20:1 (see supplement S3) that correspond to a N_{def} of ~ -2 μM . This is in accordance with nutrient data for SACW of van der Plas *et al.* (2007). During onshore advection with the cross-shelf compensation current, O_2 concentrations decrease from 70 μM to 0 μM in inner shelf bottom water. Assuming a threshold for heterotrophic denitrification of ~5 μM and of ~10 μM for anammox (Cline and Kaplan, 1975; Jensen *et al.*, 2008) both processes are feasible on the inner shelf below 70 m water depth. There, heterotrophic denitrification, anammox, and phosphate release decrease the inorganic N:P ratio to 7.1 (see

supplement S3) and cause a N_{def} of 28.6 μM in the bottom water of station #252 (see supplement S4). Integrated over the water column at 23°S and at O_2 concentrations below 10 μM a cumulative N_{def} of 3 M N per m^2 is generated by all three processes. Taking into account that the OMZ is roughly situated above the diatomaceous mud belt, which has an extension of 18 000 km^2 (Emeis *et al.*, 2004), we calculate an N_{def} amounting 0.75 Tg N for that area in May/June 2008. Water on the shelf moves eastward at a rate of 550 km per annum (Mohrholz *et al.*, 2008), so that water in the OMZ is completely exchanged 4.5 times a year. Assuming that the lower 30 m of the water column are suboxic for 9 months per year (Bartholomae and van der Plas, 2007; Joubert, 2006) our estimate for the inorganic N deficit relative to phosphate amounts 2.5 Tg N per annum for the water column above the diatomaceous mud belt. This is in the same range of calculations by Kuypers *et al.* (2005) who attributed a loss of fixed N of 1.4 ± 1 Tg on an area of 100,000 km^2 to anammox.

To calculate the contribution of heterotrophic denitrification to N_{def} , we use the stable nitrate isotope data set. Heterotrophic denitrification is associated with a fractionation factor of 25‰ for stable N and O isotopes of nitrate (Granger *et al.*, 2004; Sigman *et al.*, 2009b; Voss *et al.*, 2001), leaving the residual nitrate isotopically enriched. In an upwelling system nitrate is supplied constantly to the OMZ so that heterotrophic denitrification follows the “open system model” rather than the “Rayleigh closed system” model (Sigman *et al.*, 2009a).

Using the equation:

$$\delta^{15}\text{N}_{\text{reactant}} = \delta^{15}\text{N}_{\text{initial}} + \varepsilon (1-f) \quad (41)$$

for nitrate N isotopes, we calculated the contribution of denitrification to the N_{def} . Source nitrate at the shelf break had a $\delta^{15}\text{N}_{\text{NO}_3}$ of 6.1‰, and f was calculated according to Mariotti *et al.* (1981):

$$f = (\text{NO}_3^-) / (\text{NO}_3^- + N_{\text{def}}) \quad (42).$$

The observed depth-integrated and nitrite-corrected average $\delta^{15}\text{N}_{\text{NO}_3}$ of 18.1‰ within the OMZ requires that ~ 48% of the nitrate arriving at the core of the OMZ have to be eliminated by heterotrophic denitrification. Looking at the nitrate concentrations (Fig. 3.2b), we find that this isotope-based calculation underestimates the nitrate elimination due to heterotrophic denitrification: water enters the OMZ containing ~18 μM nitrate and lowest nitrate concentrations in the core of the OMZ are 7.0 μM . Annual heterotrophic water column denitrification above the diatomaceous mud belt amounts 0.25 Tg N assuming an average suboxic depth interval of 30 m ($\text{O}_2 < 10 \mu\text{M}$) for nine months per year and a mean residence time of water of 80 days. According to this calculation only 10% of the total N_{def} were due to heterotrophic denitrification during M76-2 in May/June 2008. Other candidates causing the

N_{def} are phosphate release from sediments and anammox that is thought to eliminate the majority of reactive N within the northern BUS (Füssel *et al.*, 2011; Kuypers *et al.*, 2005).

3.4.4. Restoration of Surface Water N:P Ratio

The N-deficit in surface water is advected offshore from the coast by the Ekman transport and decreases successively from 27.2 μM to 0.2 μM at station #201 (see supplement S4). Possible N-sources for filling the N-deficit in the Benguela region are: (1) atmospheric or land input, (2) N_2 fixation, (3) assimilation of nutrients with N:P ratio < 16 , (4) nitrification or (5) shelf break upwelling or mixing.

Atmospheric dry deposition in the Atlantic Ocean between 30°S and 10°S has N:P ratios much above 16 and therefore is a potential N-source. The atmospheric nitrate input in the open Atlantic Ocean between 25 and 17°S is relatively low ($< 20 \mu\text{M m}^{-2} \text{ d}^{-1}$; Baker *et al.*, 2003). Many arid environments have highly alkaline soils where ammonia is emitted to the atmosphere (McCalley and Sparks, 2008). Dry deposition of ammonium is unlikely since NH_4^+ and organic N are associated with fine mode aerosols ($< 1 \mu\text{m}$; Baker *et al.*, 2003) but fine sands dominate the sediments immediately along the Namibian coast where elevated ammonium concentrations occur. Ammonium concentrations in coastal surface water range between $< 7 \mu\text{M}$ in May/June 2008 (Fig. 3.2e) and 0.7 μM in February/March 2011 (data not shown) during times of weak trade wind and upwelling activity. We attribute changing ammonium concentrations in surface water to remineralisation processes at the sediment-water interface and the upwelling intensity rather than to atmospheric inputs.

N_2 fixation rates in the BUS or the adjacent South Atlantic Gyre are generally low. Highest N_2 fixation rates ($< 8 \text{ nmol N l}^{-1} \text{ d}^{-1}$) were found within or near the BUS where high nitrate concentrations did not exclude N_2 fixation (Sohm *et al.*, 2011). This agrees with our data from May/June 2008 where patches of negative $\delta^{15}\text{N}_{\text{PN}}$ (-1.8‰) occurred on the Namibian shelf at 20°S (data not shown). We find no isotopic indication of N_2 fixation in surface water above the shelf at 23°S in either $\delta^{15}\text{N}$ of nitrate or in $\delta^{15}\text{N}_{\text{PN}}$. Over the continental slope at the most offshore station #201, however, we find balanced N:P ratios where nitrate is almost completely consumed in the mixed layer (Fig. 3.2b) and particulate matter has a $\delta^{15}\text{N}$ of 4.9‰ (Fig. 3.3a). Suspended matter concentrations in the deep mixed layer (17 m water depth) are high and comparable to those in surface water near the coast (18 mg/l; see supplement S1). This indicates stimulated phytoplankton activity in surface water. Intense remineralisation reduces POC content (see supplement S2) from surface water (4.3%)

to the deep mixed layer (1.2%). Summarizing, we find nutrient-depleted surface water at station #201 (Fig. 3.2), a deep-surface SPM maximum, and low $\delta^{15}\text{N}_{\text{PN}}$ values of 3.0‰ at co-occurring high $\delta^{15}\text{N}_{\text{NO}_3}$ values of 13.9‰. This pattern is consistent with N_2 fixation. If it is indeed present, this is likely a small contribution, because the N_{def} in surface water (0-20 m) drops by only 0.05 M/m^2 between stations #202 and #201. The corresponding N-supply by fixation to the BUS at 23°S is 6 times less than the N-loss estimated from nitrate isotopes.

Another mechanism for N:P ratio restoration is the consumption of nutrients with N:P <16 under nutrient-replete conditions (Geider and La Roche, 2002; Weber and Deutsch, 2010). In our study area, diatoms dominate phytoplankton on the inner shelf and nutrient-replete conditions favour nutrient assimilation with N:P <16.

Even if organic matter N:P ratios are below Redfield, remineralisation releases nutrients with proportional N:P of ~16 and thus helps to increase the initially low inorganic N:P ratio at the coast. Nitrification of ammonium from benthic and water-column sources plays an important role in the surface water of the inner shelf (see discussion above). Although the supply of preformed nitrate in upwelling systems is large, evidence for quantitatively significant nitrification within OMZs is accumulating (Füssel *et al.*, 2011; Lam *et al.*, 2011; Gaye, B., B. Nagel, K. Dähnke, T. Rixen, and K.-C. Emeis, Evidence of coupled denitrification and nitrification in the ODZ of the Arabian Sea from paired stable isotopes of nitrate and nitrite, resubmitted to *Global Biogeochemical Cycles.*), and recycling of ammonium from particles and sediments contributes to the increase of N:P ratios offshore.

Finally, shelf break upwelling and turbulent mixing across the thermocline are episodic processes that dilute and mask the N-deficit in modified upwelling water because inorganic N:P ratios in subsurface waters at the shelf break are above 16. Shelf break upwelling is reported to be active during high wind speed periods (Barange and Pillar, 1992; Pichevin *et al.*, 2005) and is caused by negative wind stress curl that roughly coincides with the shelf break. Using an analytical model Fennel and Lass (2007) and Fennel *et al.* (2012) have shown that the structure of the wind field off Namibia forces curl-driven upwelling on the entire shelf. This process supplies nutrients from the subsurface layers into the euphotic zone. Additionally, the breaking of internal waves and tides at the shelf edge increases the turbulent diapycnal mixing and also contributes to the entrainment of nutrients into the upper layer (Mohrholz and Heene, 2011). Elevated SPM concentrations (supplement S1) and high $\delta^{15}\text{N}_{\text{PN}}$ ratios (Fig. 3.3c) in warm stratified surface water at the 23°S transect image a recent shelf break upwelling phase and a late stage plankton bloom due to an uplift of the nitracline (Fig. 3.2b) and $\delta^{15}\text{N}_{\text{NO}_3}$ isolines (Fig. 3.3a). Shelf break mixing thus is an episodic phenomenon,

but elevated biomass concentrations in surface water above the shelf break have been encountered on other cruises (N. Wasmund, pers. comm., 2011). The water mass analysis (Fig. 3.1b) illustrates a dominating ESACW-portion at station #201. As shown above, ESACW imports nutrients with elevated inorganic N/P ratios and thus contributes to balance the N_{def} .

The N-deficit generated in the OMZ cannot always be balanced as suggested by inorganic N/P ratios in surface water encountered during expeditions D356 and MSM17-3 (Fig. 3.4). During late austral summer (MSM17-3; February/March 2011), when the OMZ spreads over the entire shelf (Fig. 3.4c), DIN/P ratios in surface water were constantly < 7.5 at nitrate concentrations offshore the inner shelf break $< 1.5 \mu\text{M}$. Even surface water temperatures around 20.5°C apparently did not stimulate N_2 fixation anywhere on the transect. DIN/P ratios in surface water from September 2010 (expedition D356; Fig. 3.4b) drop from ~ 22 to ~ 6 in offshore direction at surface water temperatures of 16.6°C at the most offshore station. This implies that the modified upwelling water still hosted the N-deficit generated during times when the water parcel was situated in the OMZ weeks to months before.

3.5. SUMMARY AND CONCLUSIONS

The northern BUS is a highly variable system, because it depends on the seasonally changing water-mass mixture over the shelf. This creates conditions leading to rapidly changing nutrient supply to surface waters over the shelf and in the adjacent hemipelagic ocean, to highly variable nutrient ratios in the modified upwelling waters, and to seasonally changing oxygenation on the shelf. Owing to the seesaw of two distinct water masses, N-cycling processes change or shift spatially. In May/June 2008 denitrification occurred in the moderately extended OMZ. Ammonium produced during benthic remineralisation and during ammonification of organic matter in the water column accumulates in the OMZ and welled up near the coast. The branching of ammonium to either ammonium assimilation or nitrification leads to ^{15}N -enriched particulate matter and replenishes the nitrate pool. Nitrate assimilation dominated primary production above the outer shelf.

In the BUS we calculate that the total N-deficit of 2.5 Tg N per year is created in the oxygen deficient water column overlying the shelf. Using the isotope-based “open system model” from Sigman *et al.* (2009a), we calculate that only 0.05 Tg N of this deficit is generated by denitrification of preformed nitrate. The global annual N-loss due to water-column denitrification matches 150 Tg (Codispoti *et al.*, 2001). About one half of reactive N

is removed in the three major OMZs located in the Arabian Sea (about 50 Tg N a⁻¹; Devol *et al.*, 2006), in the Eastern Tropical North Pacific and in the Eastern Tropical South Pacific (25 to 50 Tg a⁻¹ in each region; Codispoti *et al.*, 2001; Devol, 2008). Compared to these large-volume OMZs the Benguela OMZ is only a minor sink of oceanic reactive N.

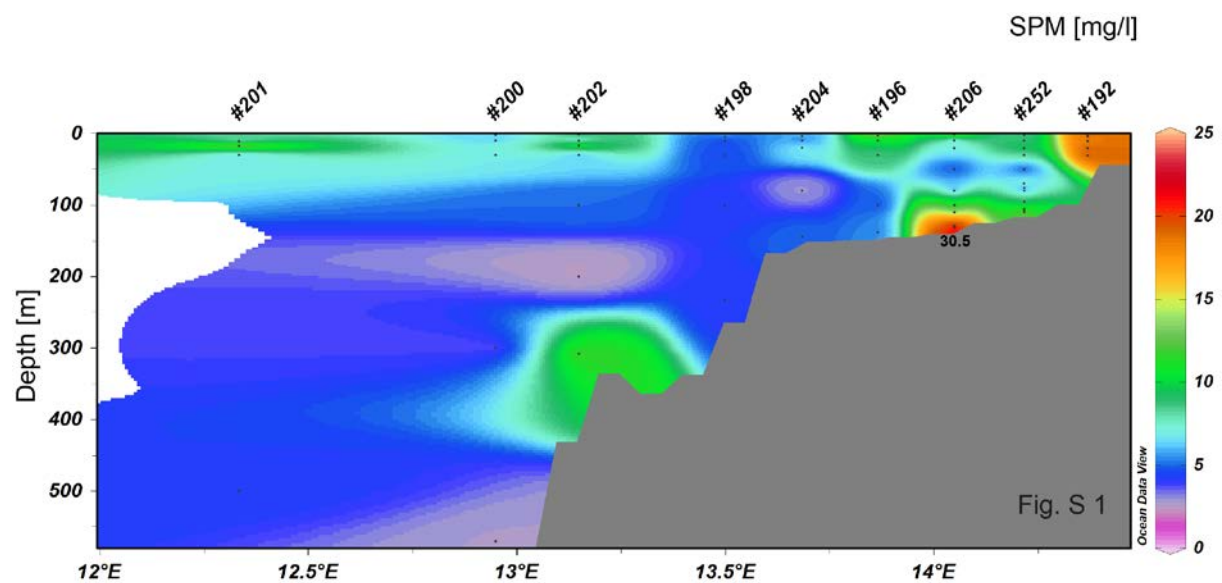
The P*-concept of Deutsch *et al.* (2007) links oceanic N₂ fixation with zones of reactive N removal in time and space. Possibly due to the intense seasonal variability, the BUS N₂ fixation rate is low and differs from other upwelling areas (e.g. Deutsch *et al.*, 2007; Fernandez *et al.*, 2011), although conditions of modified upwelling water advected into the adjacent hemipelagic ocean are conducive for N₂ fixation. Our isotope-based estimate and mass-balanced calculation illustrate that denitrification in the OMZ exceeds N₂ fixation offshore by a factor of 6. In spite of this, the N-deficit generated in the OMZ was filled in offshore surface waters in May/June 2008 most probably due to physical mixing of sub-thermocline water with surface water at the shelf-break that diluted the N deficit. The BUS is a dynamic system where N-loss and N-supply are temporally and spatially decoupled. The associated variability in nutrient ratios exported to the hemipelagic ocean may be the reason why diazotrophic N₂ fixation is a sporadic and subordinate N-source in the system.

ACKNOWLEDGEMENTS

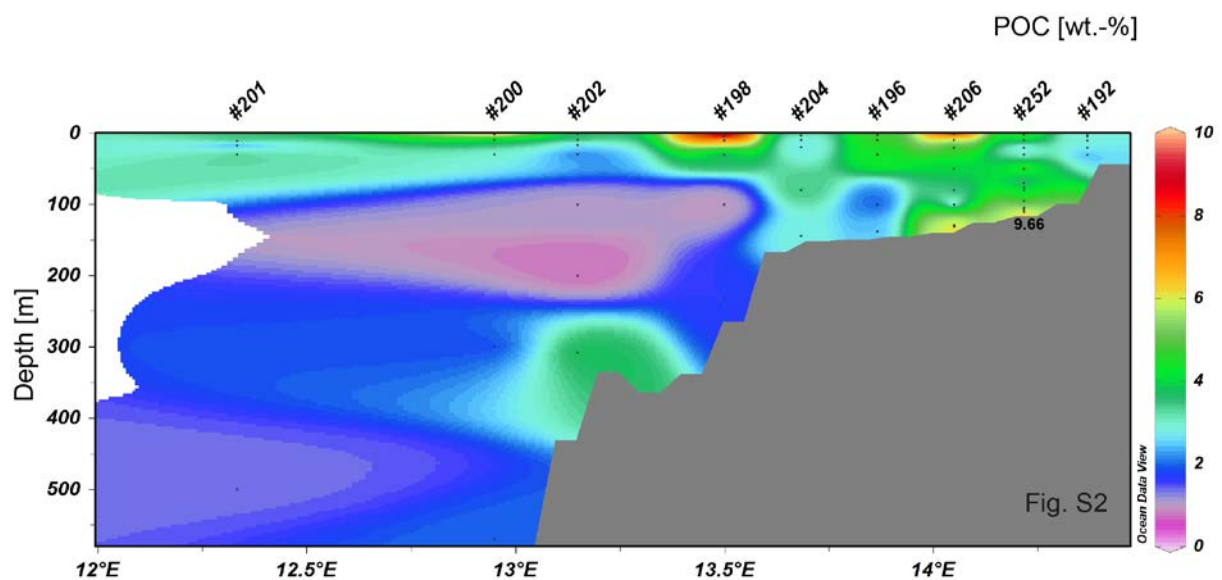
We thank the captains and crews of R/V Meteor, R/V Discovery and R/V Maria S Merian for their excellent technical support as well as T. Heene from IOW and Steffen Oesterle and Paloma Ellitson from NatMIRC Institute, Swakopmund for operating the CTD and water samplers. Ilse Büns is gratefully acknowledged for nutrient analyses of water samples from cruise M76-2. Furthermore, we thank Birgit Gaye and two anonymous reviewers for their constructive feedbacks on this manuscript. Financial support by DFG (SPP511), BMBF (project GENUS) and the Helmholtz-Zentrum Geesthacht are gratefully acknowledged.

SUPPLEMENT

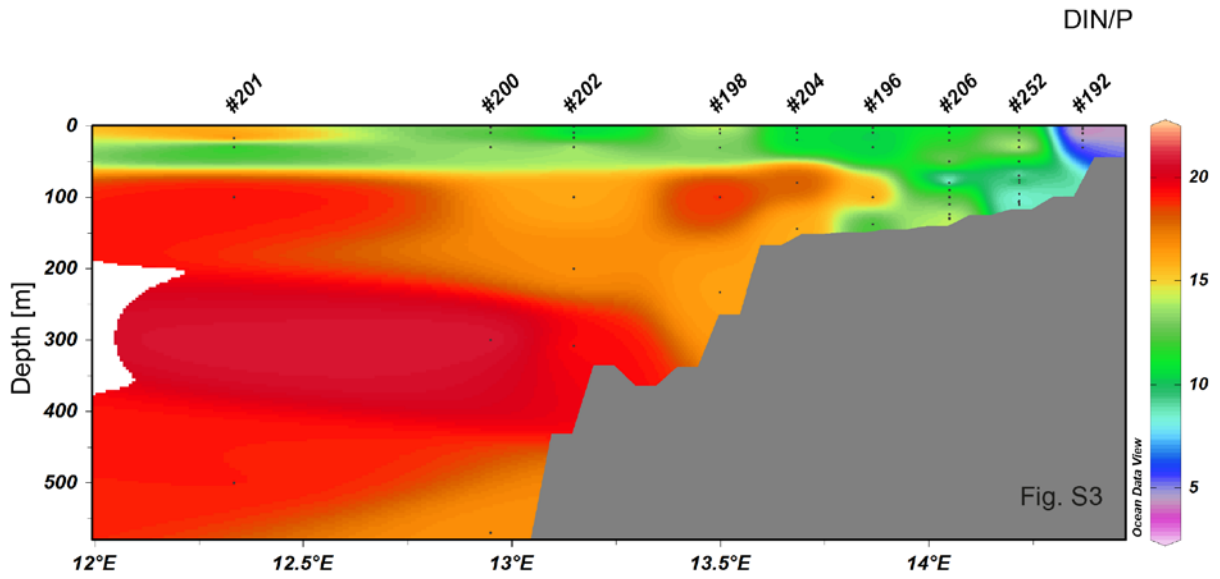
Samples were taken during expedition M76-2 in May/June 2008.



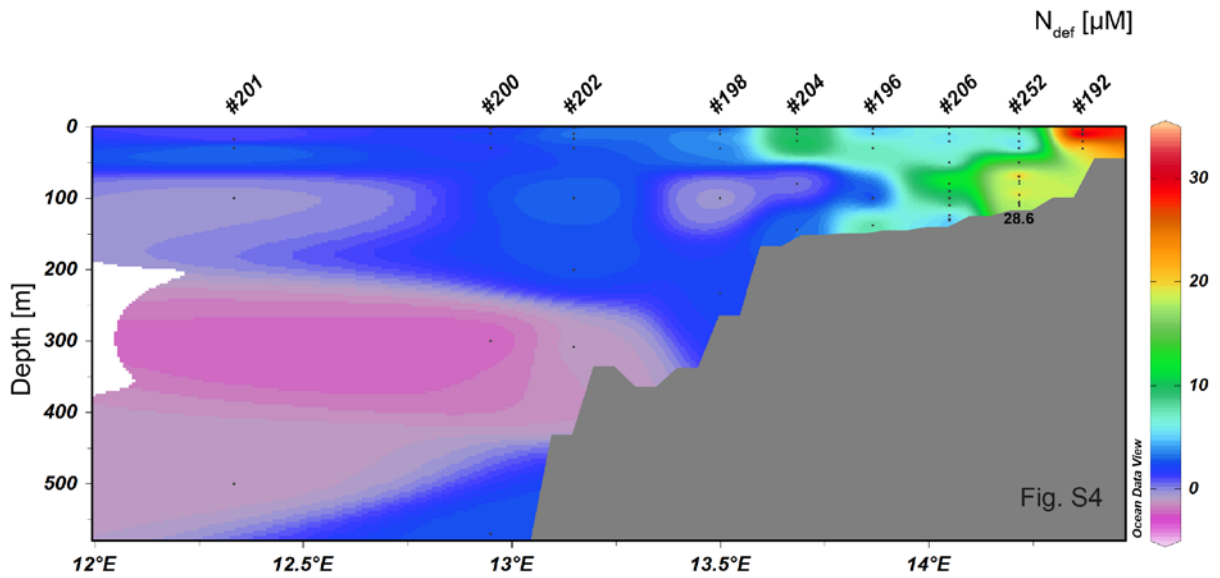
S1: Interpolated suspended matter concentrations (SPM) shown in mg/l.



S2: Interpolated particulate organic matter content (POC) shown in weight-%.



S3: Interpolated molar DIN/P ratio calculated as $(\text{NO}_3^- + \text{NO}_2^- + \text{NH}_4^+) / \text{PO}_4^{3-}$.



S4: Interpolated N-deficit was defined as the difference between the preformed inorganic N/P conditions and the measured inorganic N-pool (NO_3^- , NO_2^- , and NH_4^+).

4 Effects of current regimes and oxygen deficiency on particulate matter preservation on the Namibian shelf: insights from amino acid biogeochemistry

Birgit Nagel, Birgit Gaye, Niko Lahajnar, Ulrich Struck and Kay-Christian Emeis

Submitted to LIMNOLOGY AND OCEANOGRAPHY

ABSTRACT

Many reconstructions of past biogeochemical states rely on proxies such as $\delta^{15}\text{N}$ that reflect the origin and preservation state of particulate organic matter. In this study, we aim to test if sedimentary $\delta^{15}\text{N}$ ratios are a suitable proxy for N-turnover processes in the upwelling system on the Namibian shelf, where lateral particle advection and differential degradation under oxic to anoxic conditions complicate source assignments of proteins in suspended matter and surface sediments. Surface sediments contain more reactive amino acids than the suspended matter pool, and the preservation state of organic matter in surface sediments within the oxygen minimum zone is generally better than on the oxic outer shelf, where organic matter preservation depends on water depth. A principal component analysis of the amino acid composition of suspended matter and sediments suggests that both pools have taken different diagenetic pathways and that there is only limited exchange between them. Amino acid monomer patterns of suspended matter imply significant onshore transport of suspended matter from the mesopelagic ocean across the shelf break, induced by the effects of internal waves and tides. Thus, $\delta^{15}\text{N}$ ratios of sediment cores from the inner shelf are unbiased and depict the N-cycling history of the coastal upwelling system, whereas those from the outer shelf integrate depth-dependent lateral transport from the upper continental slope, progressive

degradation during organic matter spiralling on the shelf, and an admixture of fresh organic matter from the high productivity in the surface created by shelf-break upwelling.

4.1. INTRODUCTION

The Benguela upwelling system is one of the most productive coastal upwelling systems on earth (Carr 2002). Diatomaceous and organic-rich shelf sediments accumulate at high rates in that part of the shelf where oxygen concentrations at the sea floor are low. Remineralisation and degradation of organic matter (OM), vertical and lateral transport of particles, and resuspension of sediments control the amount and preservation state of organic carbon stored in mud belts of the shelf and upper continental slope (Inthorn *et al.*, 2006; Mollenhauer *et al.*, 2003) and affect the $\delta^{15}\text{N}$ signature of sediments (Emeis *et al.*, 2009; Möbius *et al.*, 2011; Pichevin *et al.*, 2005).

Sedimentation on the Namibian and South African shelf is defined by the combination of three effects (Giraudeau *et al.*, 2000; Jahnke and Shimmiel 1995; Monteiro *et al.*, 2005): (1) primary and secondary production rates that are controlled by nutrient supply, (2) hydrological processes (currents and internal waves and tides) that transport, resuspend or deposit particles and thus influence the location of depositional centres, (3) diagenetic processes within the water column, at the sediment-water interface and in the sediment. Of these three aspects, the energy regime is the dominant factor for sedimentation and sediment type on the Namibian shelf and upper continental slope. The interaction between the shelf shape (double shelf break) with the barotropic-baroclinic energy of internal tides and waves determines where resuspension of sediment (high energy regime) and sedimentation (quiescent zones) take place (Mollenhauer *et al.*, 2003; Monteiro *et al.*, 2005).

Deposits of the shelf and the upper slope have been the targets for paleoenvironmental reconstructions from dated sediment cores (Emeis *et al.*, 2009; Pichevin *et al.*, 2005). But the quality of these records is questionable. Lateral advection of resuspended sediments and differential deposition of particulate matter of different grain sizes cause discrepancies between foraminifera-ages and alkenone-ages in surface sediments on the SW African shelf (Mollenhauer *et al.*, 2003). Progressive degradation during repeated cycles of resuspension and deposition causes differences in OM preservation of surface sediments and particulate matter from the benthic boundary layer (BBL; Inthorn *et al.*, 2006). The mode and degree of OM degradation depends on the oxygenation of bottom water and has an impact on the sedimentary $\delta^{15}\text{N}$ record (Möbius *et al.*, 2011). It is still a matter of debate if the spatial

distribution of $\delta^{15}\text{N}$ ratios in surface sediments reflects the isotope signature of the consumed N-source, or is affected by patterns of OM degradation (Emeis *et al.*, 2009; Pichevin *et al.*, 2005).

The degradation state of OM in suspended particulate matter (SPM) and surface sediments is mirrored in amino acid (AA) composition that tracks origin and protein alteration during spiralling of particulate OM (Ingalls *et al.*, 2003; King 1977). Concentrations of reactive AAs such as Tyr, Met, Glu, Phe, Ile, and Leu generally decrease from preferential consumption by microbes during diagenesis. The non-protein AAs β -Ala, γ -Aba and Orn increase in relative abundance, because they are either refractory, or are degradation products of decarboxylation or dehydration of other amino acids, or are newly produced by bacteria (Ingalls *et al.*, 2003; Lee and Cronin 1982).

We here assess the degradation state of OM in surface sediments and in SPM on the shelf and upper continental slope off SW Africa by AA composition. Because they are the building blocks of proteins, the alteration of AA during OM spiralling and diagenesis affects $\delta^{15}\text{N}$ ratios that are key for reconstructions of past environmental conditions in the upwelling area.

4.2 METHODS

Sampling

Sediments were retrieved during cruises of R/V Alexander von Humboldt in 2004 (AHAB4 and AHAB5), R/V Meteor (cruise 76-1 in May/June 2008), and R/V Maria S. Merian (cruise 17/3 in Jan/Feb 2011) using a multicorer and a box corer at stations depicted in Fig. 1A. Both samplers yielded intact sediment/water interfaces, and 0-1 cm slices were processed for the determination of carbon and nitrogen contents, $\delta^{15}\text{N}$, and the AA composition.

Water containing SPM was sampled with a CTD/rosette sampler during M76-2 in May/June 2008 (Fig. 4.1A and 4.1B). Two to twelve litres of water were filtered over pre-combusted (450°C) and pre-weighed Whatman GF/F-Filters onboard and were dried immediately after filtration at 40°C for 48h before storage. The benthic boundary layer at #206 and #252 was sampled using a bottom water sampler. Filtrated volumes from bottom water sampler were between 1 and 2.5 litres.

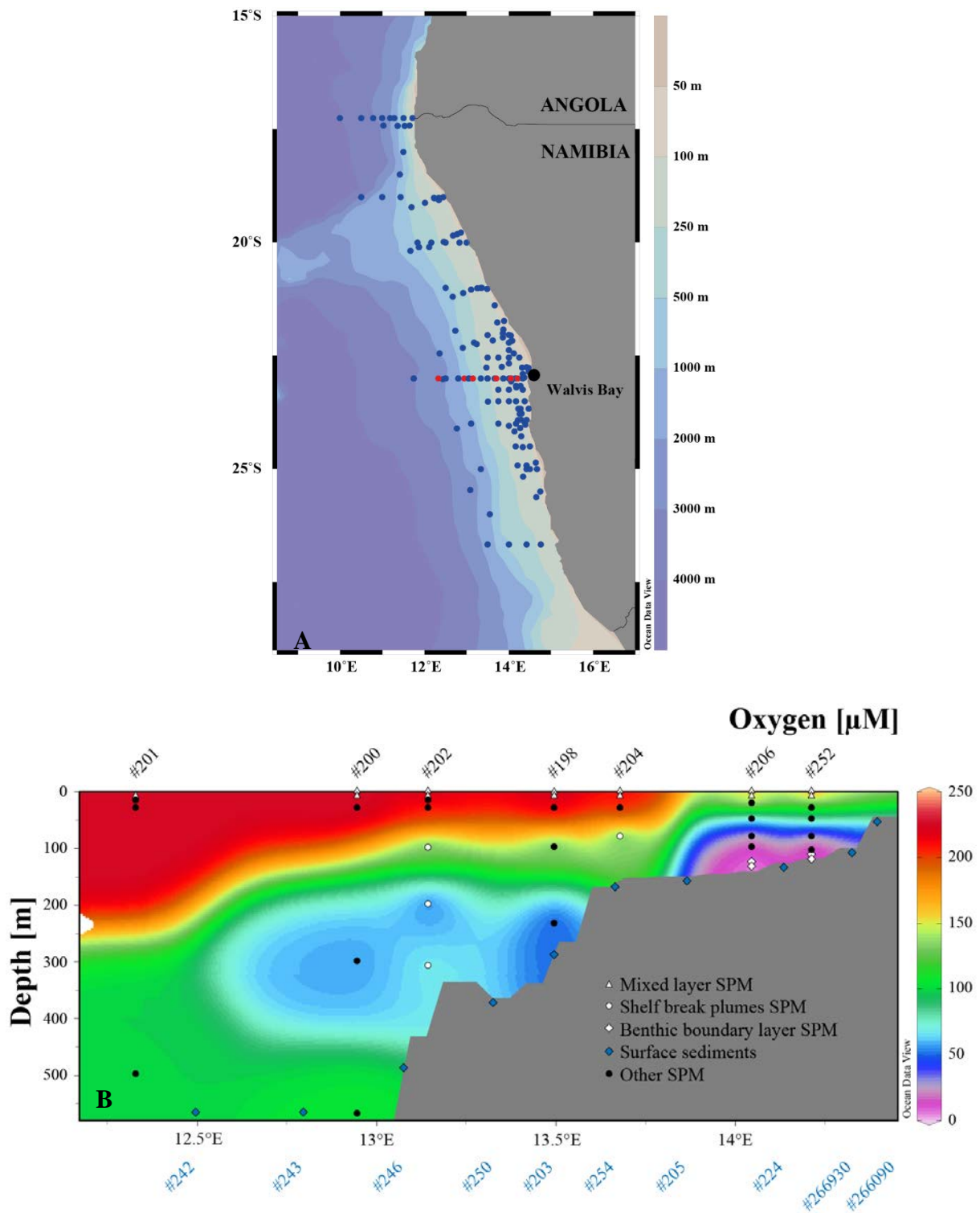


Fig. 4.1: A) Map of sampling locations of SPM and surface sediments on the Namibian shelf and continental slope. Sites of sediment sampling are indicated by blue dots and SPM sampling stations by red dots. B) Interpolated oxygen concentrations on the 23°S transect perpendicular to the coast in May/June 2008 (color code) superimposed with symbols for different sample types at sampled depths. Black and blue station numbers indicate SPM and surface sediment sampling locations, respectively.

Analyses

Particulate organic carbon (POC) and total nitrogen (TN) concentrations (%weight) of sediments and SPM were measured after flash combustion (1020°C) using a Carlo Erba Nitrogen Analyser 1500. For the determination of organic carbon, samples were repeatedly treated with 20 µl of 1 M HCl *suprapur* in order to remove carbonate prior to combustion. The standard deviation of duplicate measurements is 0.05% for carbon and 0.005% for nitrogen.

Total hydrolysable amino acids were analysed after hydrolysis with 6 M HCl *suprapur* for 22 h at 110°C under argon atmosphere using a Biochrom 30 Amino Acid Analyser. Duplicate measurements of individual monomers have a relative error of 0.02 – 1.32% for standards and 0.03 – 2.66% for surface sediments (Table 4.1). Due to inhomogeneous particle coverage of filters, SPM samples can have slightly higher relative errors. For abbreviation of monomers see Table 1.

The stable nitrogen isotope data set of surface sediments combines published data from (Emeis *et al.*, 2009) and new own data from sediments that were retrieved during M76-2 and MSM 17-3. The $\delta^{15}\text{N}$ ratios of surface sediments from M76-2 and MSM17-2 were analysed with a Thermo Delta XP mass spectrometer after combustion in a Thermo Flash EA 1112. IAEA-N1, IAEA-N2 and IVA sediment standards have been measured every eight to ten samples during each sequence run to assure measurement quality and to assess the long-term analytical performance. The standard deviation for IAEA-N1 was less than 0.2‰ and duplicate measurements of surface sediments differ less than 0.2‰. A single-point calibration was performed with IAEA-N1. Oxygen concentrations, POC and TN content from suspended matter have been published elsewhere (Nagel *et al.*, 2013).

Monomer	Abbreviation	relative error [%] for standards	relative error [%] for sediments	relative error [%] for SPM
<i>protein AA</i>				
Aspartic acid	Asp	0.33	0.47	0.02
Threonine	Thr	0.25	0.29	0.12
Serine	Ser	0.97	0.61	0.16
Glutamic acid	Glu	1.32	0.29	0.10
Glycine	Gly	0.74	0.09	0.04
Alanine	Ala	0.38	0.22	0.05
Valine	Val	0.13	0.03	0.30
Methionine	Met	0.07	0.31	1.98
Iso-Leucine	Ile	0.79	0.45	1.12
Leucine	Leu	1.02	0.03	0.08
Tyrosine	Tyr	0.30	0.04	2.05
Phenylalanine	Phe	0.15	0.49	0.10
Histidine	His	0.20	0.91	0.27
Lysine	Lys	0.23	0.48	1.37
Arginine	Arg	0.17	0.33	0.21
<i>non-protein AA</i>				
Ornithine	Orn	0.06	2.66	2.02
β -Alanine	β -Ala	0.29	1.10	1.78
γ -Aminobutyric acid	γ -Aba	0.28	2,01	0.08

Table 4.1: Amino acids analysed in this study, their abbreviations and relative errors.

4.3 RESULTS

Sediments

The different origins, transport and remineralisation histories of particulate matter in the very turbid water column and surface sediments in the system are reflected in distinct sediment types emplaced in bands parallel to the coast and shelf breaks (Bremner 1983). The diatomaceous mud-belt roughly coincides with the extent of the OMZ (Emeis *et al.*, 2004) and is emplaced within a low-energy water depth interval between gravity-wave stresses above 50 m and the baroclinic turbulent energy dissipation zone above the inner shelf break at ~150 m water depth (Monteiro *et al.*, 2005). Bordering the mud belt seaward is an erosional, or non-depositional high energy zone, where sedimentation does apparently not occur (Emeis *et al.*, 2004). Calcareous mud is the dominant sediment facies on the adjacent upper continental slope.

POC concentrations of sediments were highly variable on the shelf off Walvis Bay and ranged between 3.1 and 12.1% (Fig. 4.2). The ranges and patterns agree with previous compilations (Mollenhauer *et al.*, 2003) in that POC contents are low at the shelf breaks and high on the inner shelf. Seaward of the outer shelf break POC concentrations increased again from 900 m to 1640 m water depth. Conspicuous patches of high POC concentrations in SPM of surface water from May/June 2008 (#198 and #206) corresponded with zones of high surface sediment POC content on the shelf. The distribution pattern of TN concentrations in surface sediments corresponded to that of POC concentrations (Fig. 4.2).

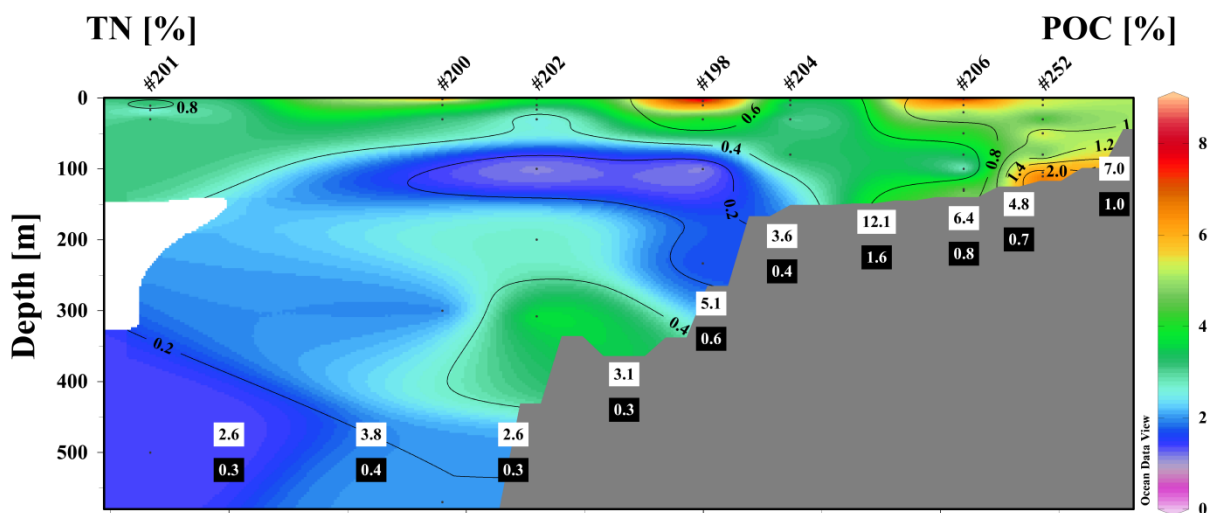


Fig. 4.2: Interpolated POC (color code) and TN content (isolines) of SPM on the 23°S transect in May/June 2008. Numbers in white and black squares represent POC and TN contents of surface sediments.

Spatial distribution of $\delta^{15}\text{N}$ in surface sediments and OM preservation

The banding of different sediment types on the Namibian shelf parallel to the coast is reflected in their $\delta^{15}\text{N}$ ratios (Fig. 4.3A). The diatomaceous mud on the shelf extends from 20°S to 26°S and has $\delta^{15}\text{N}$ ratios $>7.5\text{‰}$ in the central sector and near the coast. Residual sediments from the outer shelf have lower $\delta^{15}\text{N}$ ratios that range between 5.5 and 6.5‰. Slope sediments again have slightly elevated $\delta^{15}\text{N}$ ratios (around 7.0‰) at 23°S. North of 18.5°S, the $\delta^{15}\text{N}$ ratios are low near the coast (4‰) and increase in offshore direction to 5.2‰ on the upper continental slope.

The “Degradation Index” (DI) that describes the OM preservation state in sediments is calculated by a Principal Component Analysis (PCA) in which recalcitrant AAs (Gly, Arg,

Asp, Thr and Val) have negative factor loadings and reactive AAs (Tyr, Leu, His, Ile Met, Phe) have positive factor loadings (Dauwe *et al.*, 1999). High DI values thus indicate good preservation of OM. Surface sediments off SW Africa show high DI values in a band near the coast (Fig. 4.3B). DI values decrease in offshore direction and suggest that OM becomes more degraded.

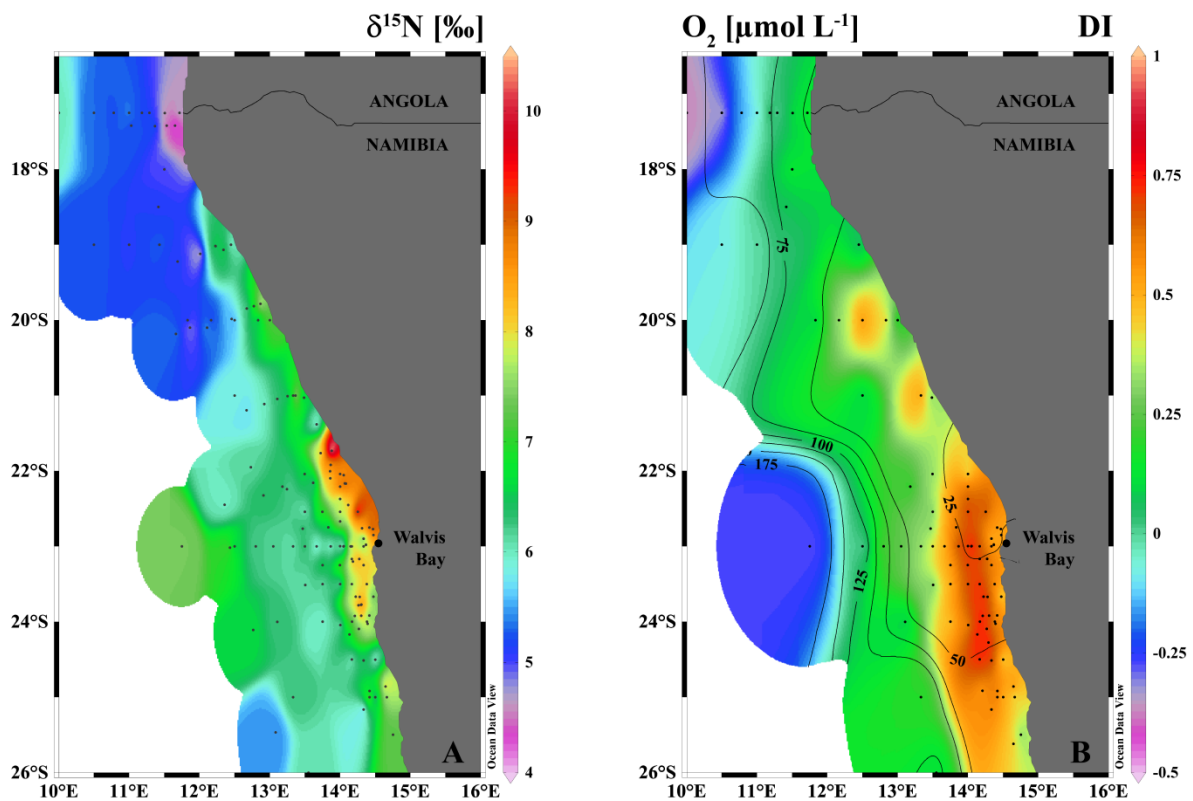


Fig. 4.3: A) Distribution of $\delta^{15}\text{N}$ ratios in surface sediments with high ratios in the diatomaceous mud decreasing in offshore direction. $\delta^{15}\text{N}$ ratios of surface sediments in the northern sector are generally lower than in the southern study area. B) The preservation state of OM is indicated by the DI (color code) that shows good preservation (DI values > 0.25) on the inner shelf. Isolines mark the mean annual bottom water oxygen concentration taken from the Namibian Bottle Collection data set. DI and bottom water oxygen concentration do not co-vary on the inner shelf.

Suspended matter

POC and TN concentrations in SPM ranged between 0.9% and 10.9% and 0.1% and 3.0%, respectively (Fig. 4.2). Patches of high POC and TN concentrations ($> 8\%$ and $> 0.6\%$) were located in the mixed layer at stations #200, #198, and #206. A second POC and TN maximum ($> 7\%$ and $> 1\%$, respectively) was consistently situated within the BBL on the inner shelf. In between these two maximum layers, POC concentrations ranged between 6.1

and 2.2% above the inner shelf and between 5.4 and 0.9% above the outer shelf and upper continental slope.

4.4 DISCUSSION

Our investigations aimed to identify the origin and cycling history of organic matter suspended in the water column and in surface sediments. We expected that SPM essentially was a mixture of fresh phytoplankton material variably admixed with resuspended surface sediments. Interestingly, this is not the case, and a third source of organic matter comes into play.

4.4.1 Indicators for sources of OM and OM degradation

Fresh OM from primary production is best identified on the basis of individual AA monomers. Diatoms – the main primary producer in the Benguela upwelling system – have elevated proportions of Ser, Gly and Thr in proteins of their cell walls (Hecky *et al.*, 1973; King 1977), and we expected that contributions of these monomers to total AA co-varied and dominated amino acids in suspended matter and surface sediments. However, Gly, Thr and Ser proportions in SPM and surface sediments (Fig. 4.4A, 4.4B and 4.4C) did not co-vary and their distribution patterns were not consistent with this expectation. Due to elevated contributions of reactive AAs in SPM, Gly proportions (Fig. 4.4A) were lowest both in the mixed layer and in the BBL over the diatomaceous mud at 23°S. The Thr contribution to total AA was indeed high in mixed-layer SPM and in the BBL over the mud belt (Fig. 4.4B) and indicate good OM preservation (Gaye *et al.*, 2013). Ser proportions of SPM (Fig. 4.4C) increased with water depth in off-shore direction in a similar way to Gly (Fig. 4.4A). In surface sediments, Gly contributions to total AA increased in offshore direction on the 23°S transect (Fig. 4.4A) because of its unreactive behaviour in high-productive environments (Cowie and Hedges 1992). Thr proportions in surface sediments decreased continuously in offshore direction which illustrates that Thr is rather a preservation indicator than an indicator for diatom-derived material. Ser proportions are the best diatom indicators in surface sediments as they decreased abruptly at the offshore zone of the diatomaceous mud from 7.7 mol-% to 6.2 mol-% (Fig. 4.4C). Since the distribution patterns of Gly, Thr and Ser differ in SPM as well as in surface sediments, we suggest that other factors besides diatomaceous primary production determine the AA composition of OM.

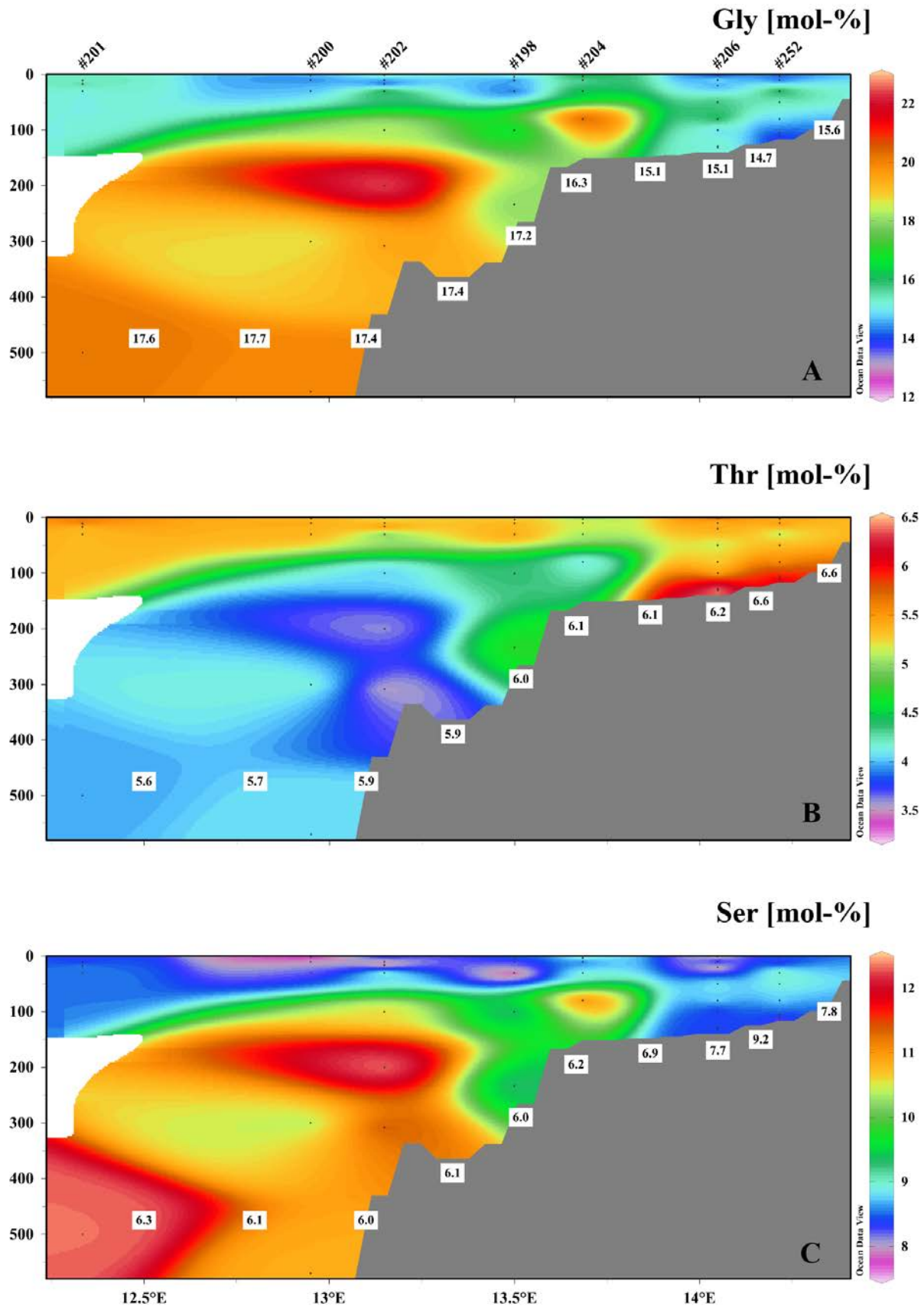


Fig. 4.4: Interpolated distributions of A) Gly, B) Thr and C) Ser on the 23°S transect in May/June 2008. Numbers in white squares represent the respective AA proportions from surface sediments.

High POC and TN concentrations (up to 12.1% and 1.6%, respectively) in sediments from the inner shelf (station #205; Fig. 4.2) are well in the range reported for the diatom mud-belt (POC <15%, e.g. Summerhayes *et al.*, 1995). General trends of decreasing POC and TN concentrations (Fig. 4.2) and DI (Fig. 4.3B) in sediments in offshore direction roughly mirror decreasing primary production and increasing degradation of OM.

4.4.2 Compositional differences between SPM and surface sediments

SPM is generally defined by its diameter (smaller than $10^2 \mu\text{m}$) and originates from disaggregated sinking particles, free-living microbes or self-assembled dissolved material (Burd and Jackson 2009; Chin *et al.*, 1998). Horizontal transport of SPM dominates over vertical transport in the water column (McCave 1984). To examine the AA characteristics of SPM and sediments, and to investigate possible interaction mechanisms, we carried out a PCA. Because the SPM data suggest different AA characteristics of OM in plume-like features (Fig. 4.4A, 4.4B, 4.4C), SPM data were further subdivided into SPM from the mixed layer (0 to 11 m water depth), SPM from the shelf break plumes (station #202-100m, -200m, -308m and station #204-80m), SPM from the BBL, and “other” SPM samples (Fig. 4.1B). AA data for plankton biomass were taken from (Gaye *et al.*, 2013) because the AA composition of phytoplankton is independent of the sampling area (see Ingalls *et al.*, (2003) and references therein). All available surface sediments between 22.5 and 23.5°S were chosen for the comparison between SPM and sediments (Fig. 4.1A).

Factor F1 is defined by high positive loadings on non-protein AAs like β -Ala, γ -Aba and Orn as well as Lys, and high negative loadings on Glu, Leu, and Arg. It explains 45% of the variance in the combined data set (Fig. 4.5) and distinguishes SPM from surface sediments. There is some overlap between the SPM and the sediment pools in particulate matter from the BBL that has slightly lower F1 scores and plots around reactive AAs like Thr, Val, Phe and Asp which are abundant in fresh plankton (Gaye *et al.*, 2007; Ingalls *et al.*, 2003). The AA composition thus indicates that particulate matter in the BBL from the inner shelf is a precursor of or in exchange with surface sediments and principally derives from fresh biomass produced in the euphotic zone.

Factor F2 has positive loadings on Ala, Asp, Val and Thr and negative loadings on Ser and Gly. It explains 18% of the total variance and is related to water depth. Plotted on this factor, SPM from the surface mixed layer is distinct from plankton biomass which is thought to be the precursor for the formation of SPM (Burd and Jackson 2009). Gly and Ser define negative F2 loadings and separate two SPM classes (A and B in Fig. 4.5). SPM from the

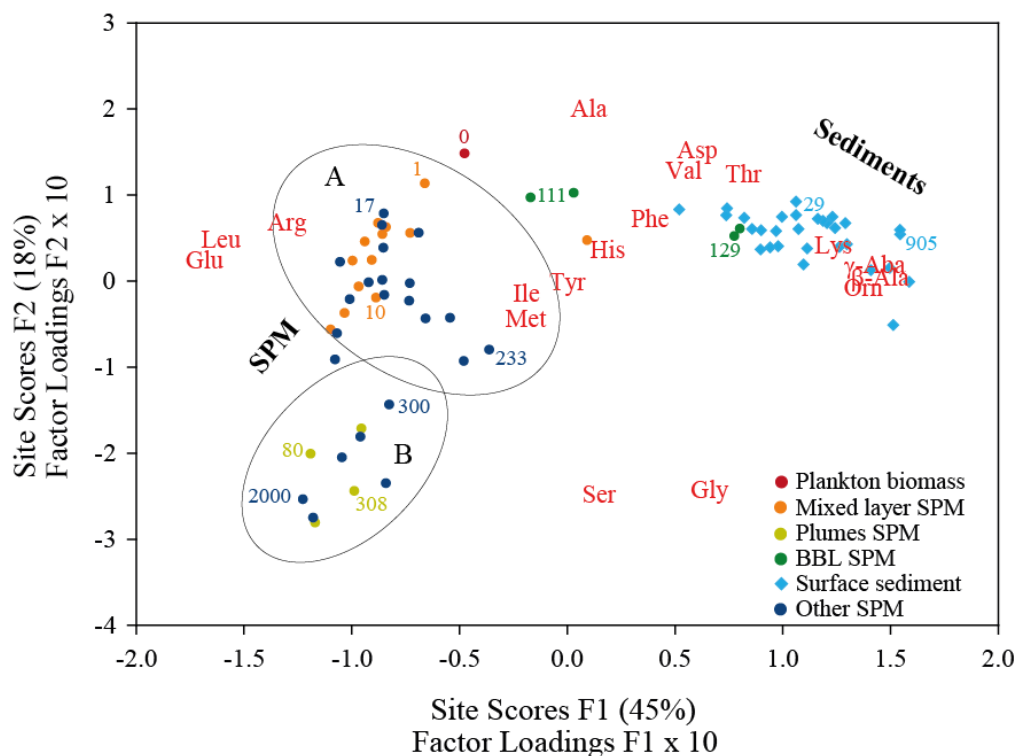


Fig. 4.5: The results of the PCA from different groups of SPM and surface sediments reflect the subdivision into a sediment-type branch and a SPM-branch. Individual AA monomers and their factor loadings multiplied by 10 are given by red abbreviations. Coloured numbers give the water depth range of each sample type and their location within the PCA. The subdivision in two clusters (A and B) on the SPM branch may be due to differences in water mass composition (see text for detailed information).

mixed layer clusters with “other” SPM samples from down to 233 m water depth (Fig. 4.5) and plots between cluster B and fresh phytoplankton. SPM from 500 to 2000 m water depth and SPM from the shelf break plumes (308 to 80 m water depth) form cluster B on the SPM branch that has high negative F2 scores due to the dominance of Gly and Ser.

Three end-members thus emerge from the statistical treatment of AA data: The apex is marked by fresh phytoplankton biomass, from which one branch evolves that is characterized by a successive enrichment of non-protein AA and encompasses SPM from the BBL and surface sediments. The second branch connects fresh phytoplankton biomass and SPM in deep water of the adjacent South Atlantic Ocean; on this branch, we encounter samples from the shelf break plumes, mixed-layer and “other” SPM.

The diverging AA patterns of SPM and sediments in the Benguela upwelling system resembles those of SPM and sinking particles in the Arabian Sea (Gaye *et al.*, 2013). That study attributed differences in AA composition of sinking particles (that we did not analyse

here) and sediments on the one hand, and SPM from the water column on the other hand to different bacterial populations. Marine snow-type sinking particles host a prokaryotic community that differs distinctly from free-living assemblages in the overall SPM pool that consists of buoyant particles (Aristegui *et al.*, 2009; Moeseneder and Herndl 2001). Different degradation pathways and metabolisms for suspended and sinking particles, as well as limited exchange between the two most likely cause the diverging in AA compositions of both sample types: Bacterial degradation shifts the AA composition to classical degradation products like non-protein AAs (Lee and Cronin 1982) so that they accumulate on sinking particles and in sediments rather than on suspended particles (Gaye *et al.*, 2013; Lee and Cronin 1982).

Investigating the AA composition of SPM, we expected to trace the cycling history of OM from the mixed layer to the sediment. Instead, we found that SPM and surface sediments are two distinct particle pools with limited interaction. The presumed source of significant amounts of SPM over the shelf break and in the mixed layer is the deep ocean, and the allochthonous material that defines the SPM compositional path is imported by specific dynamical factors at the transition from the shelf to the upper continental rise offshore SW Africa.

4.4.3 Influence of internal waves and tides on the SPM distribution

As stated in the introduction, the general pattern of sedimentation on the Namibian shelf is strongly influenced by the interaction between the shelf topography and the release of internal wave and tide energy. Energy is dissipated at the two shelf breaks offshore Walvis Bay (in 170 m and 350 m water depth), and imported and resuspended particulate matter is transported into more quiescent zones above and below (Monteiro *et al.*, 2005). The transfer of altered and allochthonous particulate matter to deposition centres causes discrepancies between ages of particulate matter from the BBL and sediments (Inthorn *et al.*, 2006), as well as offsets between ^{14}C ages of biomarkers and foraminifer tests in shelf sediments (Mollenhauer *et al.*, 2003).

The plumes of allochthonous SPM with high concentrations of unreactive AAs Gly and Ser registered in May/June 2008 (Fig. 4.4A and 4.4C) mark the breaking of internal waves and tides, that at the same time injected dissolved nutrients into the base of the euphotic zone (Nagel *et al.*, 2013). The allochthonous OM mainly derives from deep-water SPM with only minor contribution from sediments or from the BBL. The ascending refractory SPM in that plume (Fig. 4.5) implies that particulate matter in the water surging up at the

shelf break originates from at least 500 m water depth and the SPM is similar to that in waters as deep as 2000 m. But observed temperature oscillations of 1 to 2°C in the critical 400 to 450 m water depth interval correspond to a vertical water mass displacement of only 100 to 150 m (Monteiro *et al.*, 2005), so that the injection of SPM from more than 600 m water depth is unrealistic. How then can SPM from the shelf break plumes have a similar AA composition to that from 500 to 2000 m water depth? SPM is colonized by free-living microbial communities that are highly water mass-specific (see Arístegui *et al.*, (2009) and references therein), and we hypothesize that the AA composition of SPM is also specific for prevalent intermediate and deep water masses. Water at the shelf break is a mixture of South Atlantic Central Water (SACW) from the Angola Dome with surface-derived Eastern South Atlantic Central Water (ESACW) (Mohrholz *et al.*, 2008). Underlying Antarctic Intermediate Water (AAIW) is characterized by a salinity minimum (Stramma and England 1999) that is constantly found between 750 and 800 m water depth at 23 °S with an upper limit between 600 and 650 m water depth (V. Mohrholz, pers. comm.). Thus, AAIW is our best candidate source for the degraded OM and dissolved nutrients that are injected at the dynamical shelf break into the shelf environment and into the euphotic zone off Namibia. In this case, the two clusters on the SPM branch of the PCA (Fig. 4.5) represent differences in AA composition of SPM from the SACW/ESACW mixture (cluster A) and from AAIW (cluster B) that is uplifted by the breaking of internal waves and tides.

4.4.4 Implications for $\delta^{15}\text{N}$ zonation in surface sediments and diagenetic impact on $\delta^{15}\text{N}$ ratios

The $\delta^{15}\text{N}$ pattern of surface sediments (Fig. 4.3A) is not significantly correlated with either nitrate concentrations or with $\delta^{15}\text{N}_{\text{NO}_3}$ in surface water (Emeis *et al.*, 2009; Nagel *et al.*, 2013). Nitrate from the inner shelf is indeed enriched in ^{15}N (6.3 to 7.8‰) compared with the oceanic background of ~5‰ (Sigman *et al.*, 2005) due to heterotrophic denitrification (and possibly anammox) in the OMZ (Nagel *et al.*, 2013). A fractionation factor of 5‰ for nitrate assimilation alone (Granger *et al.*, 2004) would result in sedimentary $\delta^{15}\text{N}$ ratios much below 7.5‰. The conspicuous belt of $\delta^{15}\text{N}$ ratios >7.5‰ in the coastal zone between 25°S and 21°S is mirrored in low mean annual bottom water oxygen concentrations (Fig. 4.3B) taken from the Namibian Bottle Collection data set (Fig. 4.3B; (http://ioc.unesco.org/oceanteacher/OceanTeacher2/07_Example/examples.htm) and must thus be caused by processes other than or additional to nitrate assimilation. As yet, we have

not identified the enrichment mechanism and have to resort to speculation. One possible source of ^{15}N -enriched surface sediment is the admixture of sulfide-oxidizing bacterial biomass that has a crucial role in nitrate cycling (Schulz *et al.*, 1999). The second putative source of ^{15}N -enrichment in surface sediments of the mud belt area is phytoplankton assimilation of ammonia enriched in ^{15}N due to branching of this remineralisation product between nitrification and assimilation (Nagel *et al.*, 2013; Wankel *et al.*, 2007)

Biological and physical mechanisms replenish the nitrate pool seawards of this inner shelf $\delta^{15}\text{N}$ maximum and decrease $\delta^{15}\text{N}_{\text{NO}_3}$ on the outer shelf. Ammonification and nitrification mainly occur in the steep oxygen gradient enveloping the OMZ of the outer shelf/upper slope water column. The breaking of internal waves and tides increases turbulent diapycnical mixing and entrains SPM and nutrients from deep water at the double shelf breaks as discussed above. The entrainment of ^{15}N -depleted deep-water nitrate to the base of the euphotic zone and its uptake by assimilating phytoplankton is reflected in a band of decreased ^{15}N ratios of surface sediments on the outer shelf.

Near the Cape Frio upwelling cell between 17 and 18°S, sedimentary $\delta^{15}\text{N}$ ratios are around 4‰. Subsurface water at 17°S consists essentially of SACW that has a $\delta^{15}\text{N}_{\text{NO}_3}$ of 5.5 to 6‰ (Nagel, unpublished data). This value is slightly elevated compared to deep-ocean nitrate due to hypoxic to suboxic conditions on the narrow shelf (15 to 50 μM O_2) which probably promote sporadic water-column denitrification. The increase in $\delta^{15}\text{N}$ ratios of surface sediments in offshore direction at 17°S reflects the progressive increase in $\delta^{15}\text{N}_{\text{NO}_3}$ caused by nitrate assimilation (Nagel, unpublished data from Oct 2009; Pichevin *et al.*, 2005).

The preservation state of OM primarily depends on the sinking velocity and residence time in the water column (Iversen and Ploug 2010; Ploug *et al.*, 2008) and is thus correlated with water depth (Gaye-Haake *et al.*, 2005). Early diagenetic alteration of sedimentary $\delta^{15}\text{N}$ ratios lowers the DI and increases the $\delta^{15}\text{N}$ ratios of the residual particulate matter since the fractionation factor of ammonification is assumed to be 2-3‰ (Möbius 2013; Möbius *et al.*, 2011). But also oxygenation may play a crucial role on OM degradation in the water column (Nguyen and Harvey 1997) and in the sediment (Cowie *et al.*, 1995). High O_2 levels in bottom waters favor early diagenetic degradation of OM and result in elevated proportions of non-protein AAs (Cowie *et al.*, 1995).

Although $\delta^{15}\text{N}$ ratios and DI show a similar distribution pattern in the northern Benguela surface sediments (Fig. 4.3A and 4.3B), they are not significantly correlated in the study area ($r^2 = 0.08$). The quality of sedimentary OM from the OMZ (<140 m water depth) can generally be described as “fresh” (DI > 0.25; Fig. 4.3B), but the DI is neither significantly

correlated with water depth ($r^2 = 0.47$) nor with the mean annual O_2 concentration (Fig. 4.3B). Thus, the introduction of newly produced OM by diverse metabolic pathways like heterotrophic denitrification, nitrification and sulfate reduction and sulfide-oxidizing bacteria has a major influence on the AA composition of OM. Outside the OMZ, the OM is generally more degraded (Fig. 4.3B) and the DI is correlated with water depth ($r^2 = 0.72$) and moderately with mean annual bottom water O_2 concentrations ($r^2 = 0.53$).

We conclude, that degradation of OM in the study area has only a minor effect on $\delta^{15}N$ ratios in sediments. The sedimentary $\delta^{15}N$ ratios on the inner shelf carry the isotopic imprint of N-cycling processes that are bound to the OMZ but the causes of which have to be identified. Thus, $\delta^{15}N$ ratios of sediment cores from the inner shelf can be used for the interpretation of the OMZ intensity and extent. Decreasing $\delta^{15}N$ ratios in offshore direction reflect the renewal of the nitrate pool mainly by nitrification and diapycnical mixing of deep-water nitrate induced by the breaking of internal waves and tides.

ACKNOWLEDGEMENTS

We thank the officers and crews of R/V Meteor and F/S Alexander von Humboldt for their excellent technical support onboard as well as T. Heene from IOW and Steffen Oesterle and Paloma Ellitson from NatMIRC Institute, Namibia for operating the CTD. Astrid Deek and Frauke Langenberg are grateful acknowledged for their help with water and sediment sampling. Volker Mohrholz is thanked for helpful comments on the water mass distribution. We thank Reiner Schlitzer and the ODV group for supplying the Ocean Data View program. Financial support by DFG (SPP511), Project GENUS (BMBF 03F0497A) and the Helmholtz-Zentrum Geesthacht are grateful acknowledged.

5. Conclusions and Outlook

N and O stable isotope ratios of nitrate and nitrite, and stable N isotope ratios of particulate matter are powerful proxies to determine turnover processes in the nitrogen cycle and to identify N sinks and sources. Upwelling systems in combination with OMZs are study areas of preferential interest for investigations on nutrient, N-, and particle cycling due to highly increased and diverse metabolic activity and due to their relevance for global marine nitrogen cycling.

The nutrient, oxygen and stable isotope data sets from the OMZ of the Arabian Sea show that active denitrification is restricted to a zone between 100 and 400 m water depth during the late SW monsoon in 2007. Three aspects of our results illustrate that denitrification is not the only feasible N-turnover process in the denitrification zone: (1) Fractionation factors are much higher than those that were determined in pure cultures of denitrifiers. (2) The differences between stable nitrate and nitrite isotope ratios are higher than for nitrate reduction alone. (3) The decoupling of $\delta^{15}\text{N}_{\text{NO}_3}$ and $\delta^{18}\text{O}_{\text{NO}_3}$ at the upper and lower fringes of the denitrification zones is illustrated by negative $\Delta(15,18)$ values. Together, these three aspects suggest that nitrification plays an important role within two layers around 150 m and 400 m water depth. The box model shows that nutrient concentrations and stable isotope ratios can be reproduced in a 1000 model year run if ~50% of the initial nitrate is either reduced to nitrite or N_2 . To obtain the measured (and calculated) stable isotope ratios of nitrate and nitrite, 25% of the nitrate that was initially reduced to nitrite is reoxidized to nitrate via nitrite oxidation and 40% of the initially reduced nitrate is completely denitrified to N_2 . The remaining 35% of nitrite accumulate in the OMZ or are partly used by anammox. Oxygen concentrations below 400 m water depth are suitable for further denitrification, but stable nitrate isotope ratios indicate only spatial denitrification activity. Possibly, other electron acceptors like iron, manganese and iodate control the remineralisation of organic matter.

Many investigations on N-cycling activity in the Arabian Sea OMZ have been carried out, and recent work mainly focuses on the denitrification vs. anammox activity by using isotope-pairing incubation experiments (Bulow *et al.*, 2010; Jensen *et al.*, 2011; Ward *et al.*, 2009). Nitrification is known to occur in OMZs for longer times (Lipschultz *et al.*, 1990; Ward *et al.*, 1989; Ward and Zafiriou, 1988), but its quantification in the Arabian Sea focuses on ammonia oxidation rates (Lam *et al.*, 2011). Our N-isotope data set and box model results show that investigations on N-cycling should be expanded to the determination of nitrite

oxidation rates. Additionally, research about seasonal variations in N-turnover processes during the SW- and NE-monsoon as well as during the intermonsoon are just as underrepresented as investigations about N-cycling activity below the denitrification zone. Furthermore, it appears promising to study atmospheric nitrogen inputs from the Indian subcontinent vs. the nitrogen input due to upwelling and diapycnial mixing – especially during the NE-monsoon.

In the northern Benguela Upwelling System, N-turnover processes, N-sources and N-sinks were studied in the water column on a transect perpendicular to the coast by the use of stable N isotopes of nitrate and particulate matter in combination with nutrient and oxygen data. Ammonium from benthic remineralisation and ammonification in the water column accumulated in surface water of the coastal upwelling zone. Higher particulate $\delta^{15}\text{N}$ ratios than $\delta^{15}\text{N}_{\text{NO}_3}$ ratios indicate a co-existence of nitrification and ammonium assimilation. Isotope-based estimates reveal that denitrification contributes only 10% to the total nitrogen deficit, created in the OMZ. The N-deficit vanished as upwelled water moves across the shelf. The calculations show that N-gain by N_2 fixation is about 6 times lower than the N-loss due to denitrification. The balancing of the N-deficit mainly results from diapycnial mixing with subsurface waters containing N excess. It is entrained to the base of the mixed layer most likely due to physical mixing induced by internal waves and tides. Since the water mass composition and thus the N/P ratios vary seasonally on the Namibian shelf, the BUS is a system where N-loss and N-supply are temporally and spatially decoupled.

Future work on the N-cycle in the BUS should focus on the seasonality, the spatial distribution, and the quantification of N turnover processes. To date, only a snapshot of N-cycling processes is available with the main focus on the 23°S transect. This two-dimensional picture disregards changes in time and space. Thus, investigations are by far not sufficient for calculating an N budget, since water mass dynamics and thus oxygenation are highly variable on the Namibian shelf. Another interesting point might be the evaluation of nutrient data with respect to N deficits and N excess in relation to the seasonally changing water mass composition. The incidence of ammonium accumulation in the surface water of the coastal upwelling zone seems to be an uncommon feature and its control mechanisms are still unclear. Furthermore, data on atmospheric nitrogen inputs from the African continent are scarce and model results are tainted with great uncertainties.

The third publication of this thesis dealt with the question, whether the N turnover processes identified in the water column are preserved in the $\delta^{15}\text{N}$ ratios of surface sediments. Amino acid data reveal that organic matter in surface sediments from the OMZ sampling sites is generally well preserved. Thus, N isotope shifts during degradation of organic matter are lower in the OMZ than outside where organic matter of surface sediments is more degraded. However, the degradation index from sampling sites within the OMZ does neither correlate with the mean annual bottom water oxygen content nor with water depth, which are both factors that control the degradation state. Thus, I can only state that high sedimentary $\delta^{15}\text{N}$ ratios in the diatomaceous mudbelt are caused by N turnover processes within the OMZ without identifying them explicitly. What I can identify is that lower $\delta^{15}\text{N}$ ratios on the outer shelf and upper slope are caused by the entrainment of deep-water nutrients into the euphotic zone due to the breaking of internal waves and tides. The principal component analysis with the SPM and surface sediment AA data was initially carried out to trace the cycling history of organic matter from the plankton source via the water column into the sediments. Instead, it highlights the differences of particulate matter from the benthic boundary layer and surface sediments on the one hand and SPM on the other hand. Both represent different types of organic matter with distinct origin, fate, and limited exchange between these two pools. The differentiation of several SPM types is poorly traced by the PCA which emphasizes the influence of advective mixing. The overall trend of ascending SPM emerges well from the PCA.

There are still unsolved questions on the origin of suspended matter and the reasons for its distinct AA composition. Differences between AA compositions of suspended matter and sinking particles/sediments are also evident in the Arabian Sea (Gaye *et al.*, 2013) and the Mediterranean Sea (Möbius, pers. comm.) but the reasons for the differences still remain unclear. Does accretion of dissolved organic matter play a crucial role for the differences in AA composition or do free-living microbial communities determine the AA composition of suspended matter? If they do so, what influences do water masses have on them? The spatial aspect of particle and AA distribution is underrepresented in this work and thus influences of different water masses cannot be determined. Another special feature of the Namibian upwelling system is the settlement of the sediment surface with sulphur bacteria within the OMZ in high densities. These sulphur bacteria are able to take up nitrate and to convert it into ammonium. Their metabolism contributes to the phosphorite generation and phosphate efflux from the sediments (Brock & Schulz-Vogt, 2011; Flohr *et al.*, 2013), but to which extent it influences the sedimentary N isotope ratios remains unclear.

Figure captions

Fig. 1.1: Mean annual dissolved O₂ concentrations at 400 m water depth (World Ocean Atlas, 2009). Oxygen minimum zones that are discussed in this thesis are marked on the map (1, Arabian Sea oxygen minimum zone; 2, Benguela Upwelling System off SW-Africa). Note that the cores of different OMZs are located in different water depths and that the core of the Namibian OMZ is situated on the shelf (<300 m).

Fig. 1.2: N* in 400 m water depth (World Ocean Atlas, 2009). Major oceanic OMZs can be identified by N-deficits (negative N* values) that are again situated in different water depths. Excess N relative to phosphate (positive values of N*) is found in areas where particulate N from diazotrophic N₂-fixation is remineralised and adds to the dissolved nitrate pools.

Fig. 1.3: The oceanic N-cycle in OMZs and the adjacent ocean. Decreasing O₂ concentrations are indicated by intensifying colour shading. Anammox and heterotrophic denitrification produce N₂ and cause an N-deficit over phosphorus. Nitrate reduction and DNRA are remineralisation processes that produce NO₂⁻ and NH₄⁺. Nitrification consists of two individual steps: ammonia oxidation seems less tolerant towards low O₂ concentrations than nitrite oxidation.

¹ these assimilatory processes as well as diazotrophic N₂ fixation are mostly carried out by photoautotrophs that are restricted to the euphotic zone.

² Ammonification is not restricted to certain O₂ concentrations. Adapted from Lam and Kuypers, 2011.

Fig. 1.4: Changes in δ¹⁵N of nitrate and phytoplankton biomass during phytoplankton growth in a closed system – the so-called Rayleigh fractionation. Initial nitrate concentration was 20 μM with a δ¹⁵N_{NO₃} of 6‰. Nitrate consumption occurs with a fractionation factor of ¹⁵ε = 5‰. The dashed line gives the initial nitrate isotope signature that the accumulated phytoplankton biomass reaches, when nitrate is consumed completely. The example is calculated after Mariotti *et al.*, 1981; Montoya, 2008.

Fig. 2.1: Processes of nitrogen cycling in the ocean showing oxic and suboxic transformation processes. Nitrate and ammonium assimilation are restricted to photic zones. Ammonia and nitrite oxidation occur in oxic to even anoxic environments. Suboxic processes taking place in oxygen depleted zones (ODZs) are nitrate reduction (the first step of heterotrophic denitrification), denitrification and dissimilatory nitrate reduction to ammonium (DNRA).

Figure captions

Chemolithotrophic bacteria use anaerobic ammonium oxidation (anammox) as an energy source and remove nitrite and ammonium as N_2 in the suboxic environment. The figure is adapted from Lam and Kuypers (2011).

Fig. 2.2: Sampling locations in the Arabian Sea along the coast of Oman and in the open Arabian Sea.

Fig. 2.3: Depth profiles of oxygen, nitrate deficit, nitrite, $\delta^{15}N$ [‰], $\delta^{18}O$ [‰], and $\Delta(15,18)$ at the near shore locations #944-#947 (2.3a), and the offshore locations #949, #950, #953, #955 and #957 (2.3b).

Fig. 2.4: Correlation of nitrate vs. phosphate concentrations. All samples plot above the mean oceanic ratio of $[NO_3^-] = 16 [PO_4^{3-}] + 2.9$ (dashed line; Gruber and Sarmiento, 1997) and most samples above the ratio of $[NO_3^-] = 14.89 ([PO_4^{3-}] - 0.28) * 0.86$ typical for the Arabian Sea (solid line; Codispoti et al., 2001). Colour coding of dots indicates the potential density σ_θ [$kg\ m^{-3}$]. Strongest nitrate deficiencies are observed in PGW, ICW and part of the RSW.

Fig. 2.5: $\delta^{15}N_{NO_3+NO_2}$ [‰] plotted against $\delta^{18}O_{NO_3+NO_2}$ [‰] (a) and $\delta^{15}N_{NO_3}$ [‰] plotted against $\delta^{18}O_{NO_3}$ [‰] (b). Colour coding of dots indicates the potential density σ_θ [$kg\ m^{-3}$]. The 1:1 line corrected for the deep water offset between paired isotopes of 2 ‰ is indicated.

Fig. 2.6: Schematic picture of the processes in the water column using station # 953 as an example. The PNM is at the base of the mixed layer. The oxycline is the zone of sharply decreasing oxygen concentrations and of the upper $\delta^{15}N_{NO_3+NO_2}$ and $\delta^{18}O_{NO_3+NO_2}$ minimum. The zone dominated by denitrification is evident from nitrite accumulation, maxima of $\delta^{15}N_{NO_3+NO_2}$ and $\delta^{18}O_{NO_3+NO_2}$ as well as high $\Delta(15,18)$. Denitrification is coupled to anammox to remove the ammonia released during organic matter oxidation. Above and below this are zones dominated by nitrification indicated by minima of the $\Delta(15,18)$ which may co-occur with denitrification. The bimodal nitrite maxima may be a product of both nitrite accumulation during incomplete denitrification and nitrification. Removal of nitrite by anammox in the core of the denitrification zone could also explain the small nitrite minimum at 250 m.

Fig. 2.7: Box model of N-cycling in the Arabian Sea ODZ (see further explanation in the text and in supplement text02). Unitless numbers are fluxes in 10^{11} moles N yr^{-1} . Nitrogen sources are advection of nitrate and sinking organically bound nitrogen. Nitrogen sinks are heterotrophic denitrification and lateral export of nitrate and nitrite (all in blue). Red colours

indicate concentrations of nitrate and nitrite in the ODZ and their stable isotopic values and correspond with measurements at location #953.

Fig. 2.8: Model run of 1000 years changing the conditions in 200 year steps:

I – accumulation of nitrate concentrations by advective inflow

II – nitrification of settling organic matter so that the remineralised organic nitrogen is added to the nitrate pool is reactive nitrogen

III – denitrification starts; part of the organic nitrogen is oxidised by nitrification and part of it is respired by denitrification; 24 % of the nitrite accumulating is not further denitrified to dinitrogen but accumulates in the water column

IV – the entire organic matter decomposition is carried out by heterotrophic denitrification; nitrite is allowed to accumulate as in step III

V – 40% of the nitrite produced during nitrate reduction is denitrified and released as dinitrogen gas and 40 % of the remaining nitrite is reoxidised to nitrate (i.e. 24 % of initially produced nitrite).

Concentrations of nitrate and nitrite (in μM) are shown in black; their respective stable isotopic ratios are shown in red. The assumed nitrification, denitrification and nitrite oxidation rates are shown in Tg N yr^{-1} .

Fig. fs01: Cross-sections of oxygen (a) nitrate (b), nitrite (c), nitrate deficit (d), $\delta^{15}\text{N}_{\text{NO}_3+\text{NO}_2}$ (e) and $\delta^{18}\text{O}_{\text{NO}_3+\text{NO}_2}$ (f) along the cruise track of Meteor 74/1. The horizontal distance is given in km from station 944. Units in Figs. a-e are μM and units in Figs. e and f are ‰.

Fig. 3.1a: Map of the study area showing nitrate concentrations in surface water (0-5 m, data taken from the Namibia National Collection of Bottle Data, 1906-1990). Red line labels 23°S-transect where detailed sampling was carried out during the three cruises in 2008, 2010 and 2011. Dashed line indicates location of the shelf break and arrows mark the Benguela Coastal Current (BCC) and the Poleward Undercurrent (PU) supplying ESACW (Eastern South Atlantic Central Water) and SACW (South Atlantic Central Water), respectively.

Fig. 3.1b: Water mass distribution (% SACW, colours) and temperature (contours) on the transect at 23°S during expedition M76-2 (May-June 2008).

Fig. 3.2: Interpolated concentrations during M76-2 (May-June 2008) on the 23°S transect normal to the coast. a) oxygen; b) nitrate; c) phosphate; d) nitrite and e) ammonium. Numbers mark individual concentrations that deviate from the colour code due to steep concentration gradients.

Figure captions

Fig. 3.3: Interpolated isotopic compositions in ‰ during M 76-2. a) $\delta^{15}\text{N}_{\text{NO}_3}$; b) $\delta^{15}\text{N}_{\text{PN}}$.

Fig. 3.4: O_2 concentrations on the 23°S transect (3.4a) show enhanced oxygenation during Aug/Sep 2010 that was caused by strong upwelling and cross-shelf currents transporting ESACW with elevated DIN/P ratios (3.4b) onto the shelf. In February/March 2011 the OMZ (3.4c) covered almost the entire shelf and molar DIN/P ratios (3.4d) decreased from 17.5 above the upper slope to 5 in coastal surface water.

Fig. 3.5: Linear correlation between dissolved inorganic nitrogen ($\text{NO}_3^- + \text{NO}_2^- + \text{NH}_4^+$) and phosphate of sampling sites from M76-2 on the 23 °S-transect between 50 and 500 m water depth and $\text{O}_2 > 65 \mu\text{M}$.

Fig. S1: Interpolated suspended matter concentrations (SPM) shown in mg/l.

Fig. S2: Interpolated particulate organic matter content (POC) shown in weight-%.

Fig. S3: Interpolated molar DIN/P ratio calculated as $(\text{NO}_3^- + \text{NO}_2^- + \text{NH}_4^+) / \text{PO}_4^{3-}$.

Fig. S4: Interpolated N-deficit was defined as the difference between the preformed inorganic N/P conditions and the measured inorganic N-pool (NO_3^- , NO_2^- , and NH_4^+).

Fig. 4.1: A) Map of sampling locations of SPM and surface sediments on the Namibian shelf and continental slope. Sites of sediment sampling are indicated by blue dots and SPM sampling stations by red dots. B) Interpolated oxygen concentrations on the 23°S transect perpendicular to the coast in May/June 2008 (color code) superimposed with symbols for different sample types at sampled depths. Black and blue station numbers indicate SPM and surface sediment sampling locations, respectively.

Fig. 4.2: Interpolated POC (color code) and TN content (isolines) of SPM on the 23°S transect in May/June 2008. Numbers in white and black squares represent POC and TN contents of surface sediments.

Fig. 4.3: A) Distribution of $\delta^{15}\text{N}$ ratios in surface sediments with high ratios in the diatomaceous mud decreasing in offshore direction. $\delta^{15}\text{N}$ ratios of surface sediments in the northern sector are generally lower than in the southern study area. B) The preservation state of OM is indicated by the DI (color code) that shows good preservation (DI values > 0.25) on the inner shelf. Isolines mark the mean annual bottom water oxygen concentration taken from the Namibian Bottle Collection data set. DI and bottom water oxygen concentration do not covary on the inner shelf.

Fig. 4.4: Interpolated distributions of A) Gly, B) Thr and C) Ser on the 23°S transect in May/June 2008. Numbers in white squares represent the respective AA proportions from surface sediments.

Fig. 4.5: The results of the PCA from different groups of SPM and surface sediments reflect the subdivision into a sediment-type branch and a SPM-branch. Individual AA monomers and their factor loadings multiplied by 10 are given by red abbreviations. Coloured numbers give the water depth range of each sample type and their location within the PCA. The subdivision in two clusters (A and B) on the SPM branch may be due to differences in water mass composition (see text for detailed information).

Table captions

Table 1.1: List of fractionation factors $^{15}\epsilon$ and $^{18}\epsilon$ for major N-cycling processes. Normal fractionation is expressed as positive values and inverse fractionation as negative values.

Table 2.1: Depth ranges of oxygen concentrations $<4.5 \mu\text{M}$, $<1 \mu\text{M}$, nitrite concentrations $>0.5 \mu\text{M}$, and a nitrate deficit ($\text{NO}_{3\text{def}}$) $>5 \mu\text{M}$. Nitrite and nitrate concentrations, nitrogen deficit ($\text{NO}_{3\text{def}}$) are given in Mol m^{-2} .

Table 2.2: Measured $\delta^{15}\text{N}_{\text{NO}_3+\text{NO}_2}$ and $\delta^{18}\text{O}_{\text{NO}_3+\text{NO}_2}$, $\delta^{15}\text{N}_{\text{NO}_3}$ and $\delta^{18}\text{O}_{\text{NO}_3}$, and calculated $\delta^{15}\text{N}_{\text{NO}_2}$ and $\delta^{18}\text{O}_{\text{NO}_2}$ in ‰, nitrite concentrations in μM . $\Delta\delta^{15}\text{N}$ and $\Delta\delta^{18}\text{O}$ are the differences between stable isotopic values of nitrate and nitrite. $\Delta(15,18)$ is the difference between $\delta^{15}\text{N}_{\text{NO}_3+\text{NO}_2}$ and $\delta^{18}\text{O}_{\text{NO}_3+\text{NO}_2}$ corrected for the offset between both stable isotopic ratios at 1000-1200 m water depth. $\delta^{15}\text{N}_{\text{NO}_3+\text{NO}_2}$, $\delta^{18}\text{O}_{\text{NO}_3+\text{NO}_2}$, $\delta^{15}\text{N}_{\text{NO}_3}$ and $\delta^{18}\text{O}_{\text{NO}_3}$ are shown in italics when $\delta^{15}\text{N}_{\text{NO}_2}$ and $\delta^{18}\text{O}_{\text{NO}_2}$ are not calculated in samples with nitrite $< 1 \mu\text{M}$. Numbers in italics were not included in the average values (Σ) and standard deviations (Stdev).

Table 2.3: Fractionation factors ϵ by the Rayleigh fractionation model derived from the slope of a plot of $\ln(f)$ against $\delta^{15}\text{N}_{\text{NO}_3+\text{NO}_2}$, $\delta^{18}\text{O}_{\text{NO}_3}$ or $\delta^{15}\text{N}_{\text{NO}_3}$, respectively (see text for explanation of the Rayleigh model).

Table 4.1: Amino acids analysed in this study, their abbreviations and relative errors.

List of abbreviations

AA	amino acid
AAIW	Antarctic Intermediate Water
Ala	Alanine
anammox	anaerobic ammonium oxidation
AOB	ammonia-oxidising bacteria
Asp	aspartic acid
Arg	arginine
β -Ala	β -Alanine
BBL	benthic boundary layer
BCC	Benguela Coastal Current
BMBF	Bundesministerium für Bildung und Forschung
BUS	Benguela Upwelling System
C	carbon
CTD	conductivity, temperature, depth
DFG	Deutsche Forschungsgemeinschaft
DNRA	dissimilative nitrate reduction to ammonium
ϵ	fractionation factor (also: isotope effect or discrimination factor)
ESACW	Eastern South Atlantic Central Water
ETSP	eastern tropical South Pacific
γ -Aba	γ -aminobutyric acid
Glu	glutamic acid
Gly	glycine
His	histidine
IAEA	International Atomic Energy Agency
ICW	Indian Central Water
IIW	Indonesian Intermediate Water
Ile	iso-leucine
JGOFS	Joint Global Ocean Flux Study
Leu	leucine
Lys	lysine
Met	methionine
N	nitrogen

Abbreviations

N _{def}	deficit of inorganic nitrogen
O	oxygen
ODZ	oxygen depleted zone
OM	organic matter
OMZ	oxygen minimum zone
Orn	ornithine
P	phosphorus
PCA	principal component analysis
PGW	Persian Gulf Water
Phe	phenylalanine
PN	particulate nitrogen
PNM	primary nitrite maximum
POC	particulate organic carbon
PU	poleward undercurrent
RSW	Red Sea Water
SACW	South Atlantic Central Water
SAMW	Subantarctic Mode Water
Ser	serine
SNM	secondary nitrite maximum
SPM	suspended matter
STOX microsensor	switchable trace amount oxygen microsensor
Thr	threonine
TN	total nitrogen
Tyr	tyrosine
USGS	United States Geological Survey
Val	valine
VSMOW	Vienna Standard Mean Ocean Water

References

- Abramson, L., Lee, C., Liu, Z., Wakeham, S.G., Szlosek, J., 2010. Exchange between suspended and sinking particles in the northwest Mediterranean as inferred from the organic composition of in situ pump and sediment trap samples. *Limnology and Oceanography* 55 (2), 725-739.
- Allredge, A.L., Gotschalk, C.C., 1989. Direct observations of the mass flocculation of diatom blooms: characteristics, settling velocities and formation of diatom aggregates. *Deep Sea Research Part A. Oceanographic Research Papers* 36 (2), 159-171.
- Altabet, M.A., Higginson, M.J., Murray, D.W., 2002. The effect of millennial-scale changes in Arabian Sea denitrification on atmospheric CO₂. *Nature* 415 (6868), 159-162.
- Altabet, M.A., Murray, D.W., Prell, W.L., 1999a. Climatically linked oscillations in Arabian Sea denitrification over the past 1 m.y.: Implications for the marine N cycle. *Paleoceanography* 14 (6), 732-743.
- Altabet, M.A., Pilskaln, C., Thunell, R., Pride, C., Sigman, D., Chavez, F., Francois, R., 1999b. The nitrogen isotope biogeochemistry of sinking particles from the margin of the Eastern North Pacific. *Deep Sea Research Part I: Oceanographic Research Papers* 46 (4), 655-679.
- Andersen, L.A., 1995. On the hydrogen and oxygen content of marine phytoplankton. *Deep-Sea Research I* 42 (9), 1675-1680.
- Anderson, J.J., Okubo, A., Robbins, A.S., Richards, F.A., 1982. A model for nitrate distributions in oceanic oxygen minimum zones. *Deep Sea Research Part A. Oceanographic Research Papers* 29 (9), 1113-1140.
- Arístegui, J., Gasol, J.M., Duarte, C.M., Herndl, G.J., 2009. Microbial oceanography of the dark ocean's pelagic realm. *Limnology and Oceanography* 54 (4), 1501-1529.
- Bahlmann, E., Bernasconi, S.M., Bouillon, S., Houtekamer, M., Korntheuer, M., Langenberg, F., Mayr, C., Metzke, M., Middleburg, J.J., Nagel, B., Struck, U., Voß, M., Emeis, K.C., 2010. Performance evaluation of nitrogen isotope ratio determination in marine and lacustrine sediments: an inter-laboratory comparison. *Organic Geochemistry* 41 (1), 3-12.
- Bailey, G.W., 1991. Organic carbon flux and development of oxygen deficiency on the modern Benguela continental shelf south of 22°S: Spatial and temporal variability. The Geological Society, London.
- Baker, A.R., Kelly, S.D., Biswas, K.F., Witt, M., Jickells, T.D., 2003. Atmospheric deposition of nutrients to the Atlantic Ocean. *Geophysical Research Letters* 30 (24), 1-4.
- Baltar, F., Arístegui, J., Sintès, E., Gasol, J.M., Reinthaler, T., Herndl, G.J., 2010. Significance of non-sinking particulate organic carbon and dark CO₂ fixation to heterotrophic carbon demand in the mesopelagic northeast Atlantic. *Geophysical Research Letters* 37 (9), L09602.
- Banzon, V.F., Evans, R.E., Gordon, H.R., Chomko, R.M., 2004. SeaWiFS observations of the Arabian Sea southwest monsoon bloom for the year 2000. *Deep Sea Research Part II: Topical Studies in Oceanography* 51 (1-3), 189-208.

References

- Barange, M., Pillar, S.C., 1992. Cross-shelf circulation, zonation and maintenance mechanisms of *Nyctiphanes capensis* and *Euphausenia hanseni* (Euphausiacea) in the northern Benguela upwelling system. *Continental Shelf Research* 12 (9), 1027-1042.
- Barford, C.C., Montoya, J.P., Altabet, M., Mitchell, R., 1999. Steady-state nitrogen isotope effects of N₂ and N₂O production in *Paracoccus denitrificans*. *Applied and Environmental Microbiology* 65 (3), 989-994.
- Bartholomae, C.H., van der Plas, A.K., 2007. Towards the development of environmental indices for the Namibian shelf with particular reference to fisheries management. *African Journal of Marine Science* 29 (1), 25-35.
- Bender, M.L., 1990. The $\delta^{18}\text{O}$ of Dissolved O₂ in Seawater: A unique Tracer of Circulation and Respiration in the Deep Sea. *Journal of Geophysical Research* 95 (C12), 22243-22252.
- Benton, M.J., Twitchett, R.J., 2003. How to kill (almost) all life: the end-Permian extinction event. *Trends in Ecology and Evolution* 18 (7), 358-365.
- Bidle, K.D., Azam, F., 1999. Accelerated dissolution of diatom silica by marine bacterial assemblages. *Nature* 397, 508-512.
- Bock, E., 1976. Growth of *Nitrobacter* in the presence of organic matter. *Archives of Microbiology* 108, 306-312.
- Bock, E., Schmidt, I., Stüven, R., Zart, D., 1995. Nitrogen loss caused by denitrifying *Nitrosomonas* cells using ammonium or hydrogen as electron donors and nitrite as electron acceptors. *Archives of Microbiology* 163, 16-20.
- Bock, E., Wilderer, E.A., Freitag, A., 1988. Growth of *Nitrobacter* in the absence of dissolved oxygen. *Water Research* 22, 245-250.
- Böhlke, J.K., Mroczkowski, S.J., Coplen, T.B., 2003. Oxygen isotopes in nitrate: new reference materials for 18O:17O:16O measurements and observations on nitrate-water equilibration. *Rapid Communications in Mass Spectrometry* 17, 1835-1846.
- Böning, P., Bard, E., 2009. Millennial/centennial-scale thermocline ventilation changes in the Indian Ocean as reflected by aragonite preservation and geochemical variations in the Arabian Sea sediments. *Geochimica et Cosmochimica Acta* 73, 6771-6788.
- Bourbonnais, A., Lehmann, M.F., Waniek, J.J., Schulz-Bull, D.E., 2009. Nitrate isotope anomalies reflect N₂ fixation in the Azores Front region (subtropical NE Atlantic). *Journal of Geophysical Research* 114 (C03003), 1-16.
- Brand, T.D., Griffiths, C., 2008. Seasonality in the hydrography and biogeochemistry across the Pakistan margin of the NW Arabian Sea. *Deep-Sea Research* doi:10.1016/j.dsr2.2008.05.036.
- Brandes, J.A., Devol, A.H., 2002. A global marine-fixed nitrogen isotopic budget: Implications for Holocene nitrogen cycling. *Global Biogeochemical Cycles* 16 (4), 1120.
- Brandes, J.A., Devol, A.H., Yoshinari, T., Jayakumar, D.A., Naqvi, S.W.A., 1998. Isotopic composition of nitrate in the central Arabian Sea and eastern tropical North Pacific: A tracer for mixing and nitrogen cycles. *Limnology and Oceanography* 43 (7), 1680-1689.

- Breitbarth, E., Oschlies, A., La Roche, J., 2007. Physiological constraints on the global distribution of *Trichodesmium* - effect of temperature on diazotrophy. *Biogeosciences* 4, 53-61.
- Bremner, J.M., 1983. Biogenic sediments on the SW African (Namibian) continental margin. In: Thiede, J., Suess, E. (Eds.), *Coastal upwelling: its sediment record. Part B: sedimentary records of ancient coastal upwelling*. Plenum Press, New York, p. 610.
- Brock, J., Schulz-Vogt, H.N., 2011. Sulfide induces phosphate release from polyphosphate in cultures of a marine *Beggiatoa* strain. *ISME Journal* 5, 497-506.
- Buchsbaum, R., Valiela, I., Swain, T., Dzierzesky, M., Allen, S., 1991. Available and refractory nitrogen detritus of coastal vascular plants and macroalgae. *Marine Ecology Progress Series* 72, 131-143.
- Buchwald, C., Casciotti, K.L., 2010. Oxygen isotopic fractionation and exchange during bacterial nitrite oxidation. *Limnology and Oceanography* 55 (3), 1064-1074.
- Bulow, S.E., Rich, J.J., Naik, H.S., Pratihary, A.K., Ward, B.B., 2010. Denitrification exceeds anammox as a nitrogen loss pathway in the Arabian Sea oxygen minimum zone. *Deep Sea Research Part I: Oceanographic Research Papers* 57 (3), 384-393.
- Burd, A.B., Jackson, G.A., 2009. Particle aggregation. *Annual Reviews of Marine Science* 1, 65-90.
- Carr, M.-E., 2002. Estimation of potential productivity in Eastern Boundary Currents using remote sensing. *Deep Sea Research II* 49 (1), 59-80.
- Casciotti, K., L., McIlvin, M., Buchwald, C., 2010. Oxygen isotopic exchange and fractionation during bacterial ammonium oxidation. *Limnology and Oceanography* 55 (2), 753-762.
- Casciotti, K.L., 2009. Inverse kinetic isotope fractionation during bacterial nitrite oxidation. *Geochimica et Cosmochimica Acta* 73 (7), 2061-2076.
- Casciotti, K.L., Böhlke, J.K., McIlvin, M.R., Mroczkowski, S.J., Hannon, J.E., 2007. Oxygen Isotopes in Nitrite: Analysis, Calibration, and Equilibration. *Analytical Chemistry* 79 (6), 2427-2436.
- Casciotti, K.L., McIlvin, M.R., 2007. Isotopic analyses of nitrate and nitrite from reference mixtures and application to Eastern Tropical North Pacific waters. *Marine Chemistry* 107 (2), 184-201.
- Casciotti, K.L., Sigman, D.M., Galanter Hastings, M., Böhlke, J.K., Hilkert, A., 2002. Measurement of the Oxygen Isotopic Composition of Nitrate in Seawater and Freshwater Using the Denitrifier Method. *Analytical Chemistry* 74 (19), 4905-4912.
- Casciotti, K.L., Sigman, D.M., Ward, B.B., 2003. Linking Diversity and Stable Isotope Fractionation in Ammonia-Oxidizing Bacteria. *Geomicrobiology Journal* 20, 335-353.
- Casciotti, K.L., Trull, T.W., Glover, D.M., Davies, D., 2008. Constraints on nitrogen cycling at the subtropical North Pacific Station ALOHA from isotopic measurements of nitrate and particulate nitrogen. *Deep Sea Research Part II: Topical Studies in Oceanography* 55 (14-15), 1661-1672.
- Chin, W.-C., Orellana, M.V., Verdugo, P., 1998. Spontaneous assembly of marine dissolved organic matter into polymer gels. *Nature* 391 (6667), 568-572.
- Cline, J.D., Kaplan, I.R., 1975. Isotopic fractionation of dissolved nitrate during denitrification in the eastern tropical North Pacific. *Marine Chemistry* 3, 271-299.

References

- Cline, J.D., Richards, F.A., 1972. Oxygen deficient conditions and nitrate reduction in the eastern tropical North Pacific Ocean. *Limnology and Oceanography* 17 (6), 885-900.
- Codispoti, L.A., 2000. U.S. JGOFS, edited, <http://usjgofs.whoi.edu/jg/dir/jgofs/>.
- Codispoti, L.A., 2007. An oceanic fixed nitrogen sink exceeding 400 Tg N a⁻¹ vs the concept of homeostasis in the fixed-nitrogen inventory. *Biogeosciences* 4, 233-253.
- Codispoti, L.A., Brandes, J.A., Christensen, J.P., Devol, A.H., Naqvi, S.W.A., Paerl, H.W., Yoshinari, T., 2001. The oceanic fixed nitrogen and nitrous oxide budgets: Moving targets as we enter the anthropocene? *Scientia Marina* 65 (Suppl. 2), 85-105.
- Cowie, G.L., Hedges, J.I., 1992. Sources and reactivities of amino acids in a coastal marine environment. *Limnology and Oceanography* 37 (4), 703-724.
- Cowie, G. L., J. I. Hedges, F. G. Prahl, and G. J. De Lange. 1995. Elemental and major biochemical changes across an oxidation front in a relict turbidite: An oxygen effect. *Geochimica et Cosmochimica Acta* 59: 33-46.
- Daims, H., Nielsen, J.L., Nielsen, P.H., Schleifer, K.-H., Wagner, M., 2001. In-situ characterization of Nitrospira-like nitrite-oxidizing bacteria active in wastewater treatment plants. *Applied and Environmental Microbiology* 67, 5273-5284.
- Dauwe, B., J. J. Middelburg, P. M. J. Herman, and C. H. R. Heip. 1999. Linking diagenetic alteration of amino acids and bulk organic matter reactivity. *Limnology and Oceanography* 44: 1809-1814.
- Delwiche, C.C., Steyn, P.L., 1970. Nitrogen isotope fractionation in soils and microbial reactions. *Environmental Science & Technology* 4 (11), 929-935.
- Deutsch, C., Gruber, N., Key, R.M., Sarmiento, J., L., Ganachaud, A., 2001. Denitrification and N₂ fixation in the Pacific Ocean. *Global Biogeochemical Cycles* 15 (2), 483-506.
- Deutsch, C., Sarmiento, J.L., Sigman, D.M., Gruber, N., Dunne, J.P., 2007. Spatial coupling of nitrogen inputs and losses in the ocean. *Nature* 445, 163-167.
- Devol, A.H., 1978. Bacterial oxygen uptake kinetics as related to biological processes in oxygen deficient zones of the oceans. *Deep-Sea Research* 25, 137-146.
- Devol, A.H., 2008. Denitrification including anammox In: Capone, D.G., Bronck, D.A., Mulholland, M.R., Carpenter, E.J. (Eds.), *Nitrogen in the Marine Environment*. Elsevier, Amsterdam, pp. 263-302.
- Devol, A.H., Uhlenhopp, A.G., Naqvi, S.W.A., Brandes, J.A., Jayakumar, D.A., Naik, H., Gaurin, S., Codispoti, L.A., Yoshinari, T., 2006. Denitrification rates and excess nitrogen gas concentrations in the Arabian Sea oxygen deficient zone. *Deep-Sea Research I* 53, 1533-1547.
- Emeis, K.-C., Struck, U., Leipe, T., Ferdelman, T.G., 2009. Variability in upwelling intensity and nutrient regime in the coastal upwelling system offshore Namibia: results from sediment archives. *International Journal of Earth Science* 98, 309-326.
- Emeis, K.C., Brüchert, V., Currie, B., Endler, R., Ferdelman, T., Kiessling, A., Leipe, T., Noli-Pearl, K., Struck, U., Vogt, T., 2004. Shallow gas in shelf sediments of the Namibian coastal upwelling ecosystem. *Continental Shelf Research* 24, 627-642.
- Falkowski, P., 1983. Enzymology of nitrogen assimilation. In: Carpenter, E.J., Capone, D.G. (Eds.), *Nitrogen in the Marine Environment*. Academic Press, New York, pp. 839-868.
- Farrenkopf, A.M., Luther, G.W., 2002. Iodine chemistry reflects productivity and denitrification in the Arabian Sea: evidence for flux of dissolved species from

- sediments of western India into the OMZ. *Deep Sea Research Part II: Topical Studies in Oceanography* 49 (12), 2303-2318.
- Fennel, W., Junker, T., Schmidt, M., Mohrholz, V., 2012. Response of the Benguela upwelling systems to spatial variations in the wind stress. *Continental Shelf Research* 45 (0), 65-77.
- Fennel, W., Lass, H.U., 2007. On the impact of wind curls on coastal currents. *Journal of Marine Systems* 68, 128-142.
- Fernandez, C., Farías, L., Ulloa, O., 2011. Nitrogen fixation in denitrified marine waters. *PLoS One* 6 (6), e20539.
- Fiadeiro, M., Strickland, J.D.H., 1968. Nitrate reduction and the occurrence of a deep nitrite maximum in the ocean off the west coast of South America. *Journal of Marine Research* 26, 187-201.
- Flohr, A., van der Plas, A., Emeis, K.-C., Mohrholz, V., Rixen, T., 2014. Spatio-temporal patterns of C:N:P ratios in the northern Benguela upwelling system. *Biogeosciences* 11, 885-897.
- Fowler, S.W., Knauer, G.A., 1986. Role of large particles in the transport of elements and organic compounds through the oceanic water column. *Progress in Oceanography* 16 (3), 147-194.
- Freitag, A., Rudert, M., Bock, E., 1987. Growth of *Nitrobacter* by dissimilatory nitrate reduction. *FEMS Microbiology Letters* 48, 105-109.
- Froelich, P.N., Klinkhammer, G.P., Bender, M.L., Luedtke, N.A., G.R., H., 1979. Early oxidation of organic matter in pelagic sediments of eastern equatorial Atlantic: suboxic diagenesis. *Geochimica et Cosmochimica Acta* 43 (7), 1075-1090.
- Füssel, J., Lam, P., Lavik, G., Jensen, M.M., Holtappels, M., Günter, M., Kuypers, M.M.M., 2011. Nitrite oxidation in the Namibian oxygen minimum zone. *ISME Journal*.
- Gaye-Haake, B., Lahajnar, N., Emeis, K.C., Unger, D., Rixen, T., Suthhof, A., Ramaswamy, V., Schulz, H., Paropkari, A.L., Guptha, M.V.S., Ittekkot, V., 2005. Stable nitrogen isotopic ratios of sinking particles and sediments from the northern Indian Ocean. *Marine Chemistry* 96 (3-4), 243-255.
- Gaye, B., Fahl, K., Kodina, L.A., Lahajnar, N., Nagel, B., Unger, D., Gebhardt, A.C., 2007. Particulate matter fluxes in the southern and central Kara Sea compared to sediments: Bulk fluxes, amino acids, stable carbon and nitrogen isotopes, sterols and fatty acids. *Continental Shelf Research* 27 (20), 2570-2594.
- Gaye, B., Nagel, B., Dähnke, K., Rixen, T., Lahajnar, N., Emeis, K.-C., 2013. Amino acid composition and $\delta^{15}\text{N}$ of suspended matter sampled during the late SW monsoon in the Arabian Sea. *Biogeosciences Discussion*.
- Geider, R.J., La Roche, J., 2002. Redfield revisited: variability of C:N:P in marine microalgae and its biochemical basis. *European Journal of Phycology* 37, 1-17.
- Giraudeau, J., Bailey, G.W., Pujol, C., 2000. A high-resolution time-series analyses of particle fluxes in the Northern Benguela coastal upwelling system: carbonate record of changes in biogenic production and particle transfer processes. *Deep Sea Research II* 47 (9-11), 1999-2028.
- Goldammer, T., Brunner, B., Bernasconi, S.M., Ferdelman, T.G., Zabel, M., 2011. Phosphate oxygen isotopes: Insights into sedimentary phosphorus cycling from the Benguela upwelling system. *Geochimica et Cosmochimica Acta* 75, 3741-3756.

- Goutx, M., Wakeham, S.G., Lee, C., Duflos, M., Guigue, C., Liu, Z., Moriceau, B., Sempéré, R., Tedetti, M., Xue, J., 2007. Composition and degradation of marine particles with different settling velocities in the northwestern Mediterranean Sea. *Limnology and Oceanography* 52 (4), 1645-1664.
- Granger, J., Prokopenko, M.G., Sigman, D.M., Mordy, C.W., Morse, Z.M., Morales, L.V., Sambrotto, R.N., Plessen, B., 2011. Coupled nitrification-denitrification in sediment of the eastern Bering Sea shelf leads to ^{15}N enrichment of fixed N in shelf waters. *Journal of Geophysical Research* 116 (C11006), 1-18.
- Granger, J., Sigman, D.M., Lehmann, M.F., Tortell, P.D., 2008. Nitrogen and oxygen isotope fractionation during nitrate reduction by denitrifying bacteria. *Limnology and Oceanography* 53 (6), 2533-2545.
- Granger, J., Sigman, D.M., Needoba, J.A., Harrison, P.J., 2004. Coupled nitrogen and oxygen isotope fractionation of nitrate during assimilation by cultures of marine phytoplankton. *Limnology and Oceanography* 49 (5), 1763-1773.
- Granger, J., Sigman, D.M., Prokopenko, M.G., Lehmann, M.F., Tortell, P.D., 2006. A method for nitrite removal in nitrate N and O isotope analyses. *Limnology and Oceanography: Methods* 4, 205-212.
- Großkopf, T., Mohr, W., Baustian, T., Schunck, H., Gill, D., Kuypers, M.M.M., Lavik, G., Schmitz, R.A., Wallace, D.W.R., LaRoche, J., 2012. Doubling of marine dinitrogen-fixation rates based on direct measurements. *Nature* 488 (7411), 361-364.
- Gruber, N., 2008. The marine Nitrogen Cycle: Overview and Challenges. In: Capone, D.G., Bronk, D.A., Mulholland, M.A., Carpenter, E.J. (Eds.), *Nitrogen in the Marine Environment*. Academic Press, Amsterdam and London.
- Gruber, N., Galloway, J.N., 2008. An Earth-system perspective of the global nitrogen cycle. *Nature* 451, 293-296.
- Gruber, N., Sarmiento, J.L., 1997. Global patterns of marine nitrogen fixation and denitrification. *Global Biogeochemical Cycles* 11 (2), 235-266.
- Hansen, L.S., Blackburn, T.H., 1992. Effect of algal bloom deposition on sediment respiration rates and fluxes. *Marine Biology* 112, 147-152.
- Hecky, R.E., Mopper, K., Kilham, P., Degens, E.T., 1973. The Amino Acid and Sugar Composition of Diatom Cell Walls. *Marine Biology* 19, 323-331.
- Herbert, R.H., 1999. Nitrogen cycling in coastal marine ecosystems. *FEMS Microbiology Reviews* 23 (5), 563-590.
- Hoch, M.P., Fogel, M.L., Kirchman, D.L., 1992. Isotope fractionation associated with ammonium uptake by a marine bacterium. *Limnology and Oceanography* 37, 1447-1459.
- Hoering, T.C., Ford, H.T., 1960. The Isotope Effect in the Fixation of Nitrogen by *Azotobacter*. *Journal of the American Chemical Society* 82 (2), 376-378.
- Ingalls, A.E., Lee, C., Wakeham, S.G., Hedges, J.I., 2003. The role of biominerals in the sinking flux and preservation of amino acids in the Southern Ocean along 170°W. *Deep Sea Research Part II: Topical Studies in Oceanography* 50 (3-4), 713-738.
- Inthorn, M., Wagner, T., Scheeder, G., Zabel, M., 2006. Lateral transport controls distribution, quality, and burial of organic matter along slopes in high-productivity areas. *Geology* 34, 205-208.

- Iversen, M. H., and H. Ploug. 2010. Ballast minerals and the sinking carbon flux in the ocean: carbon-specific respiration rates and sinking velocity of marine snow aggregates. *Biogeosciences* 7: 2613-2624.
- Jahnke, R.A., Shimmield, G.B., 1995. Particle flux and its conversion to the sediment record: coastal ocean upwelling systems. In: al., S.e. (Ed.), *Upwelling in the Ocean: Modern Processes and Ancient Records*. Wiley, New York, pp. 83-100.
- Jennerjahn, T., Ittekkot, V., 1997. Organic matter in sediments in the mangrove areas and adjacent continental margins of Brazil: I. Amino Acids and Hexosamines. *Oceanologica Acta* 20 (2), 359-369.
- Jensen, H.M., Lomstein, E., Sorensen, J., 1990. Benthic NH_4^+ and NO_3^- flux following sedimentation of a spring phytoplankton bloom in Aarhus Bight, Denmark *Marine Ecology Progress Series* 61, 87-96.
- Jensen, M.M., Kuypers, M.M.M., Lavik, G., Thamdrup, B., 2008. Rates and regulations of anaerobic ammonium oxidation and denitrification in the Black Sea. *Limnology and Oceanography* 53 (1), 23-36.
- Jensen, M.M., Lam, P., Revsbech, N.P., Nagel, B., Gaye, B., Jetten, M.S.M., Kuypers, M.M.M., 2011. Intensive nitrogen loss over the Omani shelf due to anammox coupled with dissimilatory nitrite reduction to ammonium. *The International Society for Microbial Ecology Journal*, 5, 1660-1670.
- Jones, C.E., Jenkyns, H.C., 2001. Seawater strontium isotopes, oceanic anoxic events, and seafloor hydrothermal activity in the Jurassic and Cretaceous. *American Journal of Science* 301 (2), 112-149.
- Jones, S.E., Lennon, J.T., 2010. Dormancy contributes to the maintenance of microbial diversity. *Proceedings of the National Academy of Sciences of the United States of America* 107, 5881-5886.
- Joubert, W., 2006. Seasonal Variability of Sediment Oxygen Demand and Biogeochemistry on the Namibian Inner Shelf. Master Thesis, University of Cape Town, Cape Town.
- Kahlil, M.A.K., Rasmussen, R.A., 1992. The global source of nitrous oxide. *Journal of Geophysical Research* 97, 14651-14660.
- Kalvelage, T., Jensen, M.M., Contreras, S., Revsbech, N.P., Lam, P., Günter, M., LaRoche, J., Lavik, G., Kuypers, M.M.M., 2011. Oxygen Sensitivity of Anammox and Coupled N-Cycle Processes in Oxygen Minimum Zones. *PLoS ONE* 6 (12), e29299.
- Kalvelage, T., Lavik, G., Lam, P., Contreras, S., Arteaga, L., Loscher, C.R., Oschlies, A., Paulmier, A., Stramma, L., Kuypers, M.M.M., 2013. Nitrogen cycling driven by organic matter export in the South Pacific oxygen minimum zone. *Nature Geosci* 6 (3), 228-234.
- Karl, D., Letelier, R., Hebel, D.V., Bird, D.F., Winn, C.D., 1992. Trichodesmium blooms and new nitrogen in the north Pacific gyre. In: Carpenter, E.J., Capone, D.G., Rueter, J.G. (Eds.), *Marine Pelagic Cyanobacteria: Trichodesmium and other Diazotrophs*. Kluwer Academic, Dordrecht, pp. 219-237.
- Karl, D., Michaels, A., Bergman, B., Capone, D.G., Carpenter, E., Letelier, R., Lipschultz, F., Paerl, H., Sigman, D.M., Stal, L., 2002. Dinitrogen fixation in the world's oceans. *Biogeochemistry* 57/58, 47-98.
- Karstensen, J., Stramma, L., Visbeck, M., 2008. Oxygen minimum zones in the eastern tropical Atlantic and Pacific oceans. *Progress in Oceanography* 77, 331-350.

- Keil, R.G., Tsamakis, E., Hedges, J.I., 2000. Early diagenesis of particulate amino acids in marine systems. In: Goodfriend, G.A., Collins, M.J., Fogel, M.L., Macko, S.A., Wehmiller, J.F. (Eds.), *Perspectives in Amino Acid and Protein Geochemistry*. Oxford University Press, Oxford, pp. 69-82.
- King, K.J., 1977. Amino acid survey of Recent calcareous and siliceous deep-sea microfossils. *Micropaleontology* 23 (2), 180-193.
- Knapp, A.N., DiFiore, P.J., Deutsch, C., Sigman, D.M., Lipschultz, F., 2008. Nitrate isotopic composition between Bermuda and Puerto Rico: Implications for N₂ fixation in the Atlantic Ocean. *Global Biogeochemical Cycles* 22 (doi:10.1029/2007/GB003107,2008).
- Knauer, G.A., Martin, J.H., Bruland, K.W., 1979. Fluxes of particulate carbon, nitrogen, and phosphorus in the upper water column of the northeast Pacific. *Deep Sea Research Part A. Oceanographic Research Papers* 26 (1), 97-108.
- Konovalov, S.K., Fuchsman, C.A., Belokopitov, V., Murray, J.W., 2008. Modeling the distribution of nitrogen species and isotopes in the water column of the Black Sea. *Marine Chemistry* 111, 106-124.
- Kool, D.M., Wrage, N., Oenema, O., Dolfing, J., Van Groenigen, J.W., 2007. Oxygen exchange between (de)nitrification intermediates and H₂O and its implications for source determination of NO₃⁻ and N₂O: a review. *Rapid Communications in Mass Spectrometry* 21 (22), 3569-3578.
- Kuypers, M.M.M., Lavik, G., Woebken, D., Schmid, M., Fuchs, B., M., Amann, R., Jørgensen, B.B., Jetten, M.S.M., 2005. Massive nitrogen loss from the Benguela upwelling system through anaerobic ammonium oxidation. *Proceedings of National Academy of Sciences of the United States of America* 102 (18), 6478-6483.
- Kuypers, M.M.M., Sliemers, A.O., Lavik, G., Schmid, M., Jørgensen, B.B., Kuenen, J.G., Sinninghe Damste, J.S., Strous, M., Jetten, M.S.M., 2003. Anaerobic ammonium oxidation by anammox bacteria in the Black Sea. *Nature* 422 (6932), 608-611.
- Lam, P., Jensen, M.M., Kock, A., Lettmann, K.A., Plancherel, Y., Lavik, G., Bange, H.W., Kuypers, M.M.M., 2011. Origin and fate of the secondary nitrite maximum in the Arabian Sea. *Biogeosciences* 8, 1565-1577.
- Lam, P., Kuypers, M.M.M., 2011. Microbial Nitrogen Cycling Processes in Oxygen Minimum Zones. *Annual Review of Marine Science* 3, 317-345.
- Lam, P., Lavik, G., Jensen, M.M., van de Vossenberg, J., Schmid, M., Woebken, D., Gutierrez, D., Amann, R., Jetten, M.S.M., Kuypers, M.M.M., 2009. Revising the nitrogen cycle in the Peruvian oxygen minimum zone. *Proceedings of the National Academy of Sciences of the United States of America* 106 (12), 4752-4757.
- Lee, C., Cronin, C., 1982. The vertical flux of particulate organic nitrogen in the sea: decomposition of amino acids in the Peru upwelling area and the equatorial Atlantic. *Journal of Marine Research* 40, 227-251.
- Lee, C., Wakeham, S.G., 1988. Organic matter in seawater: biogeochemical processes. In: Riley, J.P. (Ed.), *Chemical Oceanography*. Academic Press, New York, pp. 1-51.
- Letelier, R., Karl, D., 1996. Role of *Trichodesmium* spp. in the productivity of the subtropical North Pacific Ocean. *Marine Ecology Progress Series* 133, 263-273.

- Letelier, R., Karl, D., 1998. *Trichodesmium* spp. physiology and nutrient fluxes in the North Pacific subtropical gyre. *Aquatic Microbial Ecology* 15, 265-276.
- Levine, N.M., Bender, M.L., Doney, S.C., 2009. The $\delta^{18}\text{O}$ of dissolved O_2 as a tracer of mixing and respiration in the mesopelagic ocean. *Global Biogeochemical Cycles* 23 (GB1006), 1-12.
- Lewis, B.L., Luther, G.W., 2000. Processes controlling the distribution and cycling of manganese in the oxygen minimum zone of the Arabian Sea. *Deep Sea Research Part II: Topical Studies in Oceanography* 47 (7-8), 1541-1561.
- Lipschultz, F., Wofsy, S.C., Ward, B.B., Codispoti, L.A., Friedrich, G., Elkins, J.W., 1990. Bacterial transformations of inorganic nitrogen in the oxygen-deficient waters of the eastern tropical south Pacific Ocean. *Deep Sea Research* 37, 1513-1541.
- Lomas, M.W., Lipschultz, F., 2006. Forming the primary nitrite maximum: Nitrifiers or phytoplankton. *Limnology and Oceanography* 51, 2453-2467.
- Mantoura, C., Fauzi, R., Law, C.S., J.P. Owens, N., Burkill, P.H., Malcolm S. Woodward, E., J.M. Howland, R., Llewellyn, C.A., 1993. Nitrogen biogeochemical cycling in the northwestern Indian Ocean. *Deep Sea Research Part II: Topical Studies in Oceanography* 40 (3), 651-671.
- Mariotti, A., Germon, J.C., Hubert, P., Kaiser, P., Letolle, R., Tardieux, A., Tardieux, P., 1981. Experimental determination of nitrogen kinetic isotope fractionation: Some principles; Illustration for the denitrification and nitrification processes. *Plant and Soil* 62, 413-430.
- Mariotti, A., Landreau, A., Simon, B., 1988. ^{15}N isotope biogeochemistry and natural denitrification process in groundwater: Application to the chalk aquifer of northern France. *Geochimica et Cosmochimica Acta* 52, 1869-1878.
- Marra, J., Barber, R.T., 2005. Primary productivity in the Arabian Sea: A synthesis of JGOFS data. *Progress in Oceanography* 65 (2-4), 159-175.
- McCalley, C., K., Sparks, J., P., 2008. Controls over nitric oxide and ammonia emissions from Mojave Desert soils. *Ecosystem Ecology* 156, 871-881.
- McCarthy, J.J., Carpenter, E.J., 1979. *Oscillatoria (Trichodesmium) thiebautii* (Cyanophyta) in the central north Atlantic Ocean. *Journal of Phycology* 15, 75-82.
- McCarthy, J.J., Carpenter, E.J., 1983. Nitrogen cycling in near-surface waters of the open ocean. In: Carpenter, E.J., Capone, D.G. (Eds.), *Nitrogen in the Marine Environment*. Academic Press, New York, pp. 487-512.
- McCave, I.N., 1984. Size spectra and aggregation of suspended particles in the deep ocean. *Deep Sea Research Part A. Oceanographic Research Papers* 31 (4), 329-352.
- Meador, T.B., Aluwihare, L.I., C., M., 2007. Isotopic heterogeneity and cycling of organic nitrogen in the oligotrophic ocean. *Limnology and Oceanography* 52 (3), 935-947.
- Menzel, P., Gaye, B., Wiesner, M.G., Prasad, S., Stebich, M., Das, B.K., Anoop, A., Riedel, N., Basavaiah, N., 2013. Influence of bottom water anoxia on nitrogen isotopic ratios and amino acid contributions of recent sediments from small eutrophic Lonar Lake, central India. *Limnology and Oceanography* 58 (3), 1061-1074.
- Möbius, J., 2013. Isotope fractionation during nitrogen remineralization (ammonification): Implications for nitrogen isotope biogeochemistry. *Geochimica et Cosmochimica Acta* 105 (0), 422-432.

References

- Möbius, J., Gaye, B., Lahajnar, N., Bahlmann, E., Emeis, K.-C., 2011. Influence of diagenesis on sedimentary $\delta^{15}\text{N}$ in the Arabian Sea over the last 130kyr. *Marine Geology* 284 (1–4), 127-138.
- Moeseneder, M.M., Herndl, G.J., 2001. Horizontal and vertical complexity of attached and free-living bacteria of the eastern Mediterranean Sea, determined by 16S rDNA and 16S rRNA fingerprints. *Limnology and Oceanography* 46 (1), 95-10.
- Moffett, J.W., Goepfert, T.J., Naqvi, S.W.A., 2007. Reduced iron associated with secondary nitrite maxima in the Arabian Sea. *Deep Sea Research Part I: Oceanographic Research Papers* 54 (8), 1341-1349.
- Mohrholz, V., Bartholomae, C.H., van der Plas, A.K., Lass, H.U., 2008. The seasonal variability of the northern Benguela undercurrent and its relation to the oxygen budget on the shelf. *Continental Shelf Research* 28, 424-441.
- Mohrholz, V., Heene, T., 2011. Observations of nonlinear internal waves at the Namibian shelf. 3rd Annual Science Forum of Benguela Current Commission, Swakopmund, Namibia.
- Mohrholz, V., Schmidt, M., Lutjeharms, J.R.E., 2001. The hydrography and dynamics of the Angola-Benguela frontal zone and environment in April 1999. *South African Journal of Marine Science* 97, 199-208.
- Mollenhauer, G., Eglinton, T.I., Ohkouchi, N., Schneider, R.R., Müller, P.J., Grootes, P.M., Rullkötter, J., 2003. Asynchronous alkenone and foraminifera records from the Benguela Upwelling System. *Geochimica et Cosmochimica Acta* 67 (12), 2157-2171.
- Monteiro, P.M.S., Nelson, G., van der Plas, A., Mabilhe, E., Bailey, G.W., Klingelhoeffer, E., 2005. Internal tide—shelf topography interactions as a forcing factor governing the large-scale distribution and burial fluxes of particulate organic matter (POM) in the Benguela upwelling system. *Continental Shelf Research* 25 (15), 1864-1876.
- Monteiro, P.M.S., van der Plas, A., Mohrholz, V., Mabilhe, E., Pascall, A., Joubert, W., 2006. Variability of natural hypoxia and methane in a coastal upwelling system: Oceanic physics or shelf biology? *Geophysical Research Letters* 33 (L16614), 1-5.
- Monteiro, P.M.S., Van der Plas, A.K., 2006. Low Oxygen Water (LOW) Variability in the Benguela System: Key Processes and Forcing Scales Relevant to Forecasting. In: Shannon, V., Hempel, G., Malanotte-Rizzoli, P., Moloney, C., Woods, J. (Eds.), *Large Marine Ecosystems*. Elsevier.
- Monteiro, P.M.S., van der Plas, A.K., Mélice, J.-L., Florenchie, P., 2008. Interannual hypoxia variability in a coastal upwelling system: Ocean-shelf exchange, climate and ecosystem-state implications. *Deep Sea Research I* 55, 435-450.
- Montoya, J.P., 2008. Nitrogen Stable Isotopes in Marine Environments. In: Capone, D.G., Bronk, D.A., Mulholland, M.A., Carpenter, E.J. (Eds.), *Nitrogen in the Marine Environment*, Amsterdam and London, pp. 1277-1302.
- Morrison, J.M., 1997. Inter-monsoonal changes in the T-S properties of the near-surface waters of the northern Arabian Sea. *Geophysical Research Letters* 24 (21), 2553-2556.
- Morrison, J.M., Codispoti, L.A., Gaurin, S., Jones, B., Manghnani, V., Zheng, Z., 1998. Seasonal variation of hydrographic and nutrient fields during the US JGOFS Arabian Sea Progress Study. *Deep-Sea Research II* 45, 2053-2101.

- Morrison, J.M., Codispoti, L.A., Smith, S.L., Wishner, K., Flagg, C., Gardner, W.D., Gaurin, S., Naqvi, S.W.A., Manghnani, V., Prosperie, L., Gundersen, J.S., 1999. The oxygen minimum zone in the Arabian Sea during 1995. *Deep-Sea Research II* 46, 1903-1931.
- Müller, P.J., Suess, E., 1979. Productivity, sedimentation rate, and sedimentary organic matter in the oceans—I. Organic carbon preservation. *Deep Sea Research Part A. Oceanographic Research Papers* 26 (12), 1347-1362.
- Nagel, B., Emeis, K.-C., Flohr, A., Rixen, T., Schlarbaum, T., Mohrholz, V., van der Plas, A., 2013. N-cycling and balancing of the N-deficit generated in the oxygen minimum zone over the Namibian shelf—An isotope-based approach. *Journal of Geophysical Research: Biogeosciences* 118 (1), 361-371.
- Naqvi, S.W.A., 1987. Some aspects of the oxygen-deficient conditions and denitrification in the Arabian Sea. *Journal of Marine Research* 45 (4), 1049-1072.
- Naqvi, S.W.A., 1991. Geographical extent of denitrification in the Arabian Sea in relation to some physical processes. *Oceanologica Acta* 14, 281-290.
- Naqvi, S.W.A., Voss, M., Montoya, J.P., 2008. Recent advances in the biogeochemistry of nitrogen in the ocean. *Biogeosciences* 5, 1033-1041.
- Naqvi, S.W.A., Yoshinari, T., Jayakumar, D.A., Altabet, M.A., Narvekar, P.V., Devol, A.H., Brandes, J.A., Codispoti, L.A., 1998. Budgetary and biogeochemical implications of N₂O isotope signatures in the Arabian Sea. *Nature* 394, 462-464.
- Nathan, Y., Bremner, J.M., Loewenthal, R.E., Monteiro, P.M.S., 1993. Role of Bacteria in Phosphorite Genesis. *Geomicrobiology Journal* 11, 69-76.
- Needoba, J.A., Harrison, P.J., 2004. Influence of low-light and a light: dark cycle on NO₃-uptake, intracellular NO₃-, and nitrogen isotope fractionation by marine phytoplankton. *Journal of Phycology* 40 (3), 505-516.
- Neumann, A., 2012. Elimination of reactive nitrogen in continental shelf sediments measured by membrane inlet mass spectrometry. PhD thesis, University of Hamburg, Hamburg.
- Nguyen, R.T., Harvey, H.R., 1997. Protein and amino acid cycling during phytoplankton decomposition in oxic and anoxic waters. *Organic Geochemistry* 27 (3-4), 115-128.
- Niemi, A., 1979. Blue-green algal blooms and N:P ratios in the Baltic Sea. *Acta Botanica Fennica* 110, 57-61.
- Nier, A.O., 1950. A Redetermination of the Relative Abundances of the Isotopes of Carbon, Nitrogen, Oxygen, Argon, and Potassium. *Physical Review* 77 (6), 789-793.
- Olson, D.B., Hitchcock, G.L., Fine, R.A., Warren, B.A., 1993. Maintenance of the low-oxygen layer in the central Arabian Sea. *Deep Sea Research Part II: Topical Studies in Oceanography* 40 (3), 673-685.
- Oschlies, A., Schulz, K.G., Riebesell, U., Schmittner, A., 2008. Simulated 21st century's increase in oceanic suboxia by CO₂-enhanced biotic carbon export. *Global Biogeochemical Cycles* 22, GB4008.
- Paulmier, A., Ruiz-Pino, D., 2009. Oxygen minimum zones (OMZs) in the modern ocean. *Progress in Oceanography* 80, 113-128.
- Pichevin, L., Martinez, P., Philippe, B., Schneider, R., Giraudeau, J., 2005. Nitrogen cycling on the Namibian shelf and slope over the last two climatic cycles: Local and global forcings. *Paleoceanography* 20, PA2006, 2001-2013.

References

- Ploug, H., M. H. Iversen, M. Koski, and E. T. Buitenhuis. 2008. Production, oxygen respiration rates, and sinking velocity of copepodal fecal pellets: Direct measurements of ballastin by opal and calcite. *Limnology and Oceanography* **53**: 469-476.
- Poole, R., Tomczak, M., 1999. Optimum multiparameter analysis of the water mass structure in the Atlantic Ocean thermocline. *Deep Sea Research I* **46**, 1895-1921.
- Prasad, T.G., Ikeda, M., Prasanna Kumar, S., 2001. Seasonal spreading of Persian Gulf Water mass in the Arabian Sea. *Journal of Geophysical Research* **106** (C8), 17059-17071.
- Prokopenko, M.G., Hammond, D.E., Berelson, W.M., Bernhard, J.M., Stott, L., Douglas, R., 2006. Nitrogen cycling in the sediments of Santa Barbara basin and Eastern Subtropical North Pacific: Nitrogen isotopes, diagenesis and possible chemosymbiosis between two lithotrophs (*Thioploca* and *Anammox*)—"riding on a glider". *Earth and Planetary Science Letters* **242** (1-2), 186-204.
- Redfield, A.C., 1934. On the proportions of organic derivations in sea water and their relation to the composition of plankton. In: Daniel, R.J. (Ed.), *James Johnstone Memorial Volume*. University Press of Liverpool, Liverpool, pp. 177-192.
- Repeta, D.J., Gagosian, R.B., 1984. Transformation reactions and recycling of carotenoids and chlorins in the Peru upwelling region (15°S, 75°W). *Geochimica et Cosmochimica Acta* **48** (6), 1265-1277.
- Revsbech, N.P., Larsen, L.H., Gundersen, J.S., Dalsgaard, T., Ulloa, O., Thamdrup, B., 2009. Determination of ultra-low oxygen minimum zones by the STOX sensor. *Limnology and Oceanography Methods* **7**, 371-381.
- Richards, F.A., 1965. Anoxic basins and fjords. In: Ripley, J.P., Skirrow, G. (Eds.), *Chemical Oceanography*. Academic Press, London and New York, pp. 611-645.
- Rixen, T., Gupta, M.V.S., Ittekkot, V., 2002. Sedimentation. In: Watts, L. (Ed.), *Report of the Indian Ocean Synthesis Group on the Arabian Sea Process Study*. JGOFS International Project Office, Bergen, pp. 65-73.
- Rixen, T., M.V.S., G., Ittekkot, V., 2005. Deep ocean fluxes and their link to surface ocean processes and the biological pump. *Progress in Oceanography* **65**, 240-259.
- Rixen, T., Ramaswamy, V., Gaye, B., Herunadi, B., Maier-Reimer, E., Bange, H.W., Ittekkot, V., 2009. Monsoonal and ENSO Impacts on Particle Fluxes and the Biological Pump in the Indian Ocean. American Geophysical Union, Washington D.C.
- Rontani, J.-F., Zabeti, N., Wakeham, S.G., 2011. Degradation of particulate organic matter in the equatorial Pacific Ocean: Biotic or abiotic? *Limnology and Oceanography* **56** (1), 333-349.
- Rueter, J.G., 1988. Iron stimulation of photosynthesis and nitrogen fixation in *Anabaena* 7120 and *Trichodesmium* (Cyanophyceae). *Journal of Phycology* **24**, 249-254.
- Sanudo-Wilhelmy, S.A., Kustka, A.B., Gobler, C.J., Hutchins, D.A., Yang, M., Lwiza, K., Burns, J., Capone, D.G., Raven, J.A., Carpenter, E.J., 2001. Phosphorus limitation of nitrogen fixation by *Trichodesmium* in the central Atlantic Ocean. *Nature* **411** (6833), 66-69.
- Schulz, H.N., Jørgensen, B.B., 2001. BIG BACTERIA. *Annual Review of Microbiology* **55** (1), 105-137.

- Schulz, H. N., T. Brinkhoff, T. G. Ferdelman, M. Hernández Mariné, A. Teske, and B. B. Joergensen. 1999. Dense Populations of a Giant Sulfur Bacterium in Namibian Shelf Sediments. *Science* **284**: 493-495.
- Shaffer, G., Olsen, S.M., Pedersen, J.O.P., 2009. Long-term ocean oxygen depletion in response to carbon dioxide emissions from fossil fuels. *Nature Geoscience* 2, 105-109.
- Shailaja, M.S., Narvekar, P.V., Alagarsamy, R., Naqvi, S.W.A., 2006. Nitrogen transformations as inferred from the activities of key enzymes in the Arabian Sea oxygen minimum zone. *Deep Sea Research II* 53, 960-970.
- Shannon, L.V., Nelson, G., 1996. *The Benguela: Large-scale features and processes and system variability*. Springer, Berlin.
- Sheridan, C.C., Lee, C., KWakeham, S.G., Bishop, J.K.B., 2002. Suspended particle organic composition and cycling in surface and midwaters of the equatorial Pacific Ocean. *Deep Sea Research I* 49, 1983-2008.
- Sigman, D., Granger, J., DiFiore, P.J., Lehmann, M.F., Ho, R., Cane, G., van Green, A., 2005. Coupled nitrogen and oxygen isotope measurements of nitrate along the eastern North Pacific margin. *Global Biogeochemical Cycles* 19 (GB4022).
- Sigman, D.M., Casciotti, K.L., Andreani, M., Barford, C., Galanter, M., Böhlke, J.K., 2001a. A Bacterial Method for the Nitrogen Isotopic Analysis of Nitrate in Seawater and Freshwater. *Analytical Chemistry* 73 (17), 4145-4153.
- Sigman, D.M., Casciotti, K.L., John, H.S., 2001b. Nitrogen Isotopes in the Ocean. *Encyclopedia of Ocean Sciences*. Academic Press, Oxford, pp. 1884-1894.
- Sigman, D.M., DiFiore, P.J., Hain, M.P., Deutsch, C., Wang, Y., Karl, D.M., Knapp, A.N., Lehmann, M.F., Pantoja, S., 2009a. The dual isotopes of deep nitrate as a constraint on the cycle and budget of oceanic fixed nitrogen. *Deep Sea Research Part I: Oceanographic Research Papers* 56, 1419-1439.
- Sigman, D.M., Karsh, K.L., Casciotti, K.L., John, H.S., Karl, K.T., Steve, A.T., 2009b. Ocean Process Tracers: Nitrogen Isotopes in the Ocean. *Encyclopedia of Ocean Sciences*. Academic Press, Oxford, pp. 4138-4153.
- Smethie, W.M., 1987. Nutrient regeneration and denitrification in low oxygen fjords. *Deep-Sea Research* 34, 983-1006.
- Snider, D.M., Spoelstra, J., Schiff, S.L., Venkiteswaran, J.J., 2010. Stable oxygen isotope ratios on nitrate produced from nitrification: ^{18}O -labeled water incubations of agricultural and temperate forest soils. *Environmental Science and Technology* 44, 5358-5364.
- Sohm, J.A., Hilton, J.A., Noble, A.E., Zehr, J.P., Saito, M.A., Webb, E.A., 2011. Nitrogen fixation in the South Atlantic Gyre and the Benguela Upwelling System. *Geophysical Research Letters* 38 (L16608).
- Stramma, L., England, M., 1999. On the water masses and mean circulation of the South Atlantic Ocean. *Journal of Geophysical Research: Oceans* 104 (C9), 20863-20883.
- Stramma, L., Johnson, G.C., Sprintall, J., Mohrholz, V., 2008. Expanding Oxygen-Minimum Zones in the Tropical Oceans. *Science* 320, 655-658.
- Strohm, T.O., Griffin, B., Zumft, W.G., Schink, B., 2007. Growth Yields in Bacterial Denitrification and Nitrate Ammonification. *Applied and Environmental Microbiology* 73 (5), 1420-1424.

References

- Summerhayes, C.P., Kroon, D., Rosell-Melé, A., Jordan, R.W., Schrader, H.J., Hearn, R., Villanueva, J., Grimalt, J.O., Eglinton, G., 1995. Variability in the Benguela Current upwelling system over the past 70,000 years. *Progress in Oceanography* 35 (3), 207-251.
- Suthhof, A., Ittekkot, V., Gaye-Haake, B., 2001. Seasonal biogeochemical fluxes of ^{234}Th and ^{210}Po in the Upper Sargasso Sea: Influence from atmospheric iron deposition. *Global Biogeochem. Cycles* 15 (3), 637-649.
- Thamdrup, B., Dalsgaard, T., Jensen, M.M., Ulloa, O., Farias, L., Escribano, R., 2006. Anaerobic ammonium oxidation in the oxygen-deficient waters off Chile. *Limnology and Oceanography* 51 (5), 2145-2156.
- Tyrrell, T., 1999. The relative influences of nitrogen and phosphorus on oceanic primary production. *Nature* 400, 525-531.
- Tyrrell, T., Lucas, M.I., 2002. Geochemical evidence of denitrification in the Benguela upwelling system. *Continental Shelf Research* 22, 2497-2511.
- van der Plas, A.K., Monteiro, P.M.S., Pascall, A., 2007. Cross-shelf biogeochemical characteristics of sediments in the central Benguela and their relationship to overlying water column hypoxia. *African Journal of Marine Science* 29 (1), 37-47.
- Van Mooy, B.A.S., Keil, R.G., Devol, A.H., 2002. Impact of suboxia on sinking particulate organic carbon: Enhanced carbon flux and preferential degradation of amino acids via denitrification. *Geochimica et Cosmochimica Acta* 66 (3), 457-465.
- Voss, M., Dippner, J.W., Montoya, J.P., 2001. Nitrogen isotope patterns in the oxygen-deficient waters of the Eastern Tropical North Pacific Ocean. *Deep Sea Research II* 48, 1905-1921.
- Wakeham, S.G., Canuel, E.A., 1988. Organic geochemistry of particulate matter in the eastern tropical North Pacific Ocean: Implications for particle dynamics. *Journal of Marine Research* 46 (1), 183-213.
- Wakeham, S.G., Lee, C., 1989. Organic geochemistry of particulate matter in the ocean: The role of particles in oceanic sedimentary cycles. *Organic Geochemistry* 14 (1), 83-96.
- Wakeham, S.G., Lee, C., Farrington, J.W., Gagosian, R.B., 1984. Biogeochemistry of particulate organic matter in the oceans: results from sediment trap experiments. *Deep Sea Research Part A. Oceanographic Research Papers* 31 (5), 509-528.
- Wankel, S.D., Kendall, C., Pennington, J.T., Chavez, F.P., Paytan, A., 2007. Nitrification in the euphotic zone as evidenced by nitrate dual isotopic composition: Observations from Monterey Bay, California. *Global Biogeochem. Cycles* 21.
- Ward, B.B., 2008. Nitrification in Marine Systems. In: Capone, D.G., Bronk, D.A., Mulholland, M.R., Carpenter, E.J. (Eds.), *Nitrogen in the marine environment*. Elsevier, London, pp. 199-262.
- Ward, B.B., Devol, A.H., Rich, J.J., Chang, B.X., Bulow, S.E., Naik, H., Pratihary, A., Jayakumar, A., 2009. Denitrification as the dominant nitrogen loss process in the Arabian Sea. *Nature* 461, 78-82.
- Ward, B.B., Glover, H.E., Lipschultz, F., 1989. Chemoautotrophic activity and nitrification in the oxygen minimum zone off Peru. *Deep Sea Research* 36, 1031-1051.
- Ward, B.B., Zafiriou, O.C., 1988. Nitrification and nitric oxide in the oxygen minimum zone of the eastern tropical north Pacific. *Deep Sea Research* 35, 1127-1142.

-
- Waser, N.A.D., Harrison, P.J., Nielsen, B., Calvert, S.E., Turpin, D.H., 1998a. Nitrogen Isotope Fractionation During the Uptake and Assimilation of Nitrate, Nitrite, Ammonium, and Urea by a Marine Diatom. *Limnology and Oceanography* 43 (2), 215-224.
- Waser, N.A.D., Harrison, P.J., Nielsen, B., Calvert, S.E., Turpin, D.H., 1998b. Nitrogen Isotope Fractionation During the Uptake and Assimilation of Nitrate, Nitrite, Ammonium, and Urea by a Marine Diatom. *Limnology and Oceanography* 43 (2), 215-224.
- Wasmund, N., Lass, H.U., Nausch, G., 2005. Distribution of nutrients, chlorophyll and phytoplankton primary production in relation to hydrographic structures bordering the Benguela-Angolan front region. *African Journal of Marine Science* 27 (1), 177-190.
- Watson, A.J., 1995. Are upwelling areas sources or sinks of CO₂? John Wiley and Sons, Chichester.
- Weber, T.S., Deutsch, C., 2010. Ocean nutrient ratios governed by plankton biogeography. *Nature* 467, 550-554.
- Wetzel, P., Winguth, A., Maier-Reimer, E., 2005. Sea-to-air CO₂ flux from 1948 to 2003: A model study. *Global Biogeochemical Cycles* 19, GB2005. 2010.1029/2004gb002339.
- Wyrski, K., 1962. The oxygen minima in relation to ocean circulation. *Deep Sea Research and Oceanographic Abstracts* 9 (1-2), 11-23.
- Yoshida, N., 1988. ¹⁵N-depleted N₂O as a product of nitrification. *Nature* 335 (6190), 528-529.
- Zehr, J.P., Ward, B.B., 2002. Nitrogen cycling in the ocean: New perspectives on processes and paradigms. *Applied and Environmental Microbiology* 68 (3), 1015-1024.
- Zumft, W., 1997. Cell biology and molecular basis of denitrification. *Microbiology and Molecular Biology Reviews* 61 (4), 533-616.

Author contributions

Chapter 2 is an article that was published in 2013:

Gaye, B., Nagel, B., Dähnke, K., Rixen, T., Emeis, K.-C. (2013): Evidence of parallel denitrification and nitrite oxidation in the ODZ of the Arabian Sea from paired stable isotopes of nitrate and nitrite. *Global Biogeochemical Cycles*. (doi:10.1002/2011GB004115).

Birgit Gaye and Birgit Nagel designed the study. Birgit Nagel and Kirstin Dähnke conducted the N and O isotope analyses. Tim Rixen provided nutrient data and designed the box model. Birgit Gaye, Birgit Nagel and Kay-Christian Emeis wrote the manuscript with input and critical discussion from Kirstin Dähnke and Tim Rixen.

Chapter 3 is an article that was published in 2013:

Nagel, B., Emeis, K.-C., Flohr, A., Rixen, T., Schlarbaum, T., Mohrholz, V., van der Plas, A. (2013). N-cycling and balancing of the N-deficit generated in the oxygen minimum zone over the Namibian shelf - an isotope-based approach. *Journal of Geophysical Research: Biogeosciences* **118**(1): 361-371.

Birgit Nagel and Kay-Christian Emeis designed the study. Birgit Nagel and Tim Schlarbaum carried out the nitrate isotope analyses. Birgit Nagel conducted ^{15}N and POC analyses on suspended matter. Anita Flohr and Tim Rixen provided nutrient data from Aug/Sep 2010 and from Feb/March 2011. Anja van der Plas contributed time-series of intensity, extent and thickness of the oxygen minimum zone. Volker Mohrholz provided information about water mass composition and oxygen data. Birgit Nagel wrote the manuscript with important advices from Kay-Christian Emeis and critical discussion from Anita Flohr, Tim Rixen, Volker Mohrholz and Anja van der Plas.

Chapter 4 is an article that is submitted to LIMNOLOGY AND OCEANOGRAPHY. Birgit Nagel and Kay-Christian Emeis designed the study. Niko Lahajnar carried out all amino acid analyses and POC and TN analyses of samples from cruise MSM17-3. Birgit Nagel analysed POC and TN from suspended matter and surface sediment retrieved during M76-2. Birgit Nagel and Ulrich Struck analysed the $\delta^{15}\text{N}$ ratios of surface sediments. Birgit Gaye carried out the principal component analysis. Birgit Nagel wrote the manuscript with advices from Kay-Christian Emeis and input and critical discussion from Birgit Gaye, Niko Lahajnar and Ulrich Struck.

Curriculum Vitae

Contact information

Birgit Nagel
Bahnhofstraße 3
21441 Garstedt

Personal information

Date of birth: 16.03. 1977
Place of birth: Esslingen/Neckar
Nationality: German

Education

1996 Abitur at Helfenstein-Gymnasium Geislingen/Steige

1996 - 1998 Voluntary work in the social sector, Heim für Mehrfachbehinderte
 Haslachmühle

1998 - 2001 Studies of Geology and Paleontology, Eberhard-Karls-Universität Tübingen
 (Vordiplom)

2001 - 2006 Studies of Geology and Paleontology, University of Hamburg
 Diploma thesis:
 „Kartierung der neogenen Schichtenfolge zwischen Sedini und Laerru, NW-
 Sardinien“ (Part A)
 „Isotopengeochemische Untersuchungen an Suspensionsproben,
 Oberflächensedimenten und Schwerelotkernen in der Karasee:
 Zusammenhänge zwischen $\delta^{13}\text{C}_{\text{org}}$ und (Paläo-)Salinität“ (Part B).

2007-2008 ph.D. scholarship from the University of Hamburg: „Auswirkungen des
 Abbaus organischen Materials auf die Verhältnisse stabiler Stickstoffisotopen
 in Schwebstoffen und Sedimenten“

Since

Sep 2008 Doctorate at the Helmholtz Zentrum Geesthacht, Institute of Coastal Research
 in cooperation with the University of Hamburg.

Dec 2009 - Nov 2010 parental leave

May 2012 - April 2013 parental leave

List of Publications

- Gaye, B., Fahl, K., Kodina, L.A., Lahajnar, N., **Nagel, B.**, Unger, D., Gebhardt, A.C. (2007). Particulate matter fluxes in the southern and central Kara Sea compared to sediments: Bulk fluxes, amino acids, stable carbon and nitrogen isotopes, sterols and fatty acids. *Continental Shelf Research* **27**(20): 2570-2594.
- Nagel, B.**, Gaye, B., Kodina, L.A., Lahajnar, N. (2009). Stable carbon and nitrogen isotopes as indicators for organic matter sources in the Kara Sea. *Marine Geology* **266**: 42-51.
- Bahlmann, E., Bernasconi, S.M., Bouillon S., Houtekamer, M., Korntheuer, M., Langenberg, F., Mayr, C., Metzke, M., Middelburg, J.J., **Nagel, B.**, Struck, U., Voß, M., Emeis, K.-C. (2010). Performance evaluation of nitrogen isotope ratio determination in marine and lacustrine sediments: an inter-laboratory comparison. *Organic Geochemistry* **41**(1): 3-12.
- Dähnke, K., Emeis, K.-C., Johannsen, A., **Nagel, B.** (2010). "Stable isotopic composition and turnover of nitrate in the German Bight." *Marine Ecology Progress Series* **408**: 7-18.
- Jensen, M. M., Lam, P., Revsbech, N. P., **Nagel, B.**, Gaye, B., Jetten, M. S. M. and Kuypers, M. M. M. (2011). Intensive nitrogen loss over the Omani Shelf due to anammox coupled with dissimilatory nitrite reduction to ammonium. *ISME Journal* **5**: 1660-1670.
- Nagel, B.**, Emeis, K.-C., Flohr, A., Rixen, T., Schlarbaum, T., Mohrholz, V., van der Plas, A. (2013). N-cycling and balancing of the N-deficit generated in the oxygen minimum zone over the Namibian shelf - an isotope-based approach. *Journal of Geophysical Research: Biogeosciences* **118**(1): 361-371.
- Gaye, B., **Nagel, B.**, Dähnke, K., Rixen, T., Emeis, K.-C. (2013): Evidence of parallel denitrification and nitrite oxidation in the ODZ of the Arabian Sea from paired stable isotopes of nitrate and nitrite. *Global Biogeochemical Cycles*: 2011GB004115.
- Gaye, B., **Nagel, B.**, Dähnke, K., Rixen, T., Lahajnar, N., Emeis, K.-C. (2013): Amino acid composition and $\delta^{15}\text{N}$ of suspended matter in the Arabian Sea: implications for organic matter sources and degradation. *Biogeosciences* **10**: 7689-7702.
- Rixen, T., Baum, A., Gaye, B., **Nagel, B.** (2013): Seasonal and interannual variations of the nitrogen cycle in the Arabian Sea. *Biogeosciences Discussions* **10**: 19541-19570.
- Nagel, B.**, Gaye, B., Lahajnar, N., Struck, U., Emeis, K.-C.: Effects of current regimes and oxygenation on particulate matter preservation on the Namibian shelf: insights from amino acid biogeochemistry. Submitted to *Limnology and Oceanography*.

Acknowledgements/Danksagung

An allererster Stelle möchte ich Prof. Emeis für die Betreuung dieser Arbeit danken, für wertvolle Diskussionen, für die fachgerechten Kürzungen meiner Manuskripte, für die immerwährende Unterstützung trotz knapper Zeitressourcen und dafür, dass ich sehr selbständig arbeiten konnte.

Birgit Gaye bin ich sehr dankbar für die fachliche Unterstützung und Betreuung dieser Arbeit, für den jahrelangen offenen und vertrauensvollen Umgang und für die vielen Diskussionen, die neue Ideen befeuerten und mich sehr oft auf den richtigen Weg führten.

Beiden Betreuern danke ich für die zu keinem Zeitpunkt zur Debatte stehende (aber leider nicht selbstverständliche) Akzeptanz meines privaten Lebensentwurfs, die meine Motivation zusätzlich erhöhte.

Dem Helmholtz-Zentrum Geesthacht danke ich für die Chance, unter hervorragenden Forschungsbedingungen arbeiten zu können, den Mitarbeitern der Abteilungen KBI, KB und KBC für die gute Arbeitsatmosphäre und die geselligen Mittagsrunden. Speziell Kirstin Dähnke, Carsten Frank, Astrid Deek und Angela Nawrocki danke ich für die fachlichen, seelischen und moralischen Unterstützungen während der Doktorandenzeit.

Herzlicher Dank geht an Frauke Langenberg und Niko Lahajnar vom Institut für Biogeochemie und Meereschemie der Uni Hamburg, die mich nicht nur bei der Laborarbeit unterstützten, sondern mit denen ich etliche gute Zeit auf diversen Forschungsschiffen verbracht habe.

Zu guter Letzt möchte ich mich herzlich bei meiner engeren und weiteren Familie bedanken: Für all die Unterstützung, vor allem während des Publikationsprozesses in der Elternzeit, für euer Lachen, das Chaos, meine grauen Haare, den Ausgleich zur Arbeit und was ihr sonst noch so anstellt!

Eidesstattliche Erklärung

Hiermit versichere ich, Birgit Nagel, geboren am 16. März 1977 in Esslingen /Neckar, an Eides statt, dass ich die vorgelegte Dissertation mit dem Titel:

Insights into Nitrogen and Particle Cycling in Marine Oxygen Minimum Zones

abgesehen durch die Beratung meiner Betreuer selbständig ausgearbeitet und verfasst habe und keine anderen Quellen und Hilfsmittel als die angegebenen verwendet habe bzw. die benutzten Quellen als solche kenntlich gemacht habe. Ich habe die vorliegende Arbeit weder gänzlich noch in Teilen einem anderen Fachbereich im In- oder Ausland im Rahmen eines Prüfungsverfahrens vorgelegt.

Hamburg, den

Birgit Nagel